

LIDAR-BASED POTATO CROP SUITABILITY MAPPING ALONG THE UPPER  
SAINT JOHN RIVER VALLEY IN NEW BRUNSWICK

by

Kamille Eve Lemieux

Bachelor of Science in Biology, University of New Brunswick, 2020

A Thesis Submitted in Partial Fulfillment  
of the Requirements for the Degree of

Master of Science in Forestry

in the Graduate Academic Unit of Forestry and Environmental Management

**Supervisor:** Paul Arp, PhD, Forestry and Environmental Management

**Examining Board:** Graham Forbes, PhD, Forestry and Environmental Management,  
Chair  
Charles Bourque, PhD, Forestry and Environmental Management  
Dirk Jaeger, PhD, Forest Sciences and Forest Ecology, University  
of Göttingen

This thesis is accepted by the  
Dean of Graduate Studies

THE UNIVERSITY OF NEW BRUNSWICK

December, 2022

©Kamille Lemieux, 2022

## **ABSTRACT**

This thesis reports on potato crop suitability mapping along the Upper Saint John River Valley in New Brunswick based on province-wide available high-resolution light detection and ranging (LiDAR) derived digital elevation model (DEM). Potato crop suitability rating was done by way of multi-criteria evaluation accounting for (i) topsoil and subsoil texture, (ii) soil calcareousness, (iii) soil coarse fragment content, (iv) depth-to-compaction of soil, (v) soil drainage (depth-to-water table (DTW)), and (vi) elevation (slope percent). It was found that:

1. the tax assessment values of farmlands and farm and woodland combinations reflect the soil suitability for potato cropping across the Saint John River Valley, as mapped;
2. some of the field-surveyed soil property and associated tuber yield variations can be quantified and mapped using the LiDAR-DEM derived flow channels and associated DTW layers; this verification was done based on three published field-survey reports that deal with potato cropping near Saint-André, Florenceville, and Hartland, NB.

## **ACKNOWLEDGEMENTS**

I would like to thank my supervisor, Dr. Paul Arp, for his patience, guidance, and expertise. Specifically, I would like to thank Dr. Arp for sharing his deep knowledge of forestry, particularly on forest soils and hydrology, with me and guiding me through the process of producing results and articulating them; I could not have done it without him. I would like to thank M. Ogilvie for making time in his busy schedule to help me with GIS and LiDAR related matters. Furthermore, I am appreciative of his engaging teaching style. I am also appreciative of the inputs of my examining board members, Dr. Bourque and Dr. Jaeger. I would also like to acknowledge Dr. Shane Furze (J.D. Irving) for sharing his digital soil mapping work with me. I am also grateful for the attention and financial support received from the New Brunswick Department of Agriculture, as facilitated by Pat Toner and his colleagues. This support allowed the research of this thesis to take shape over a number of years, all based on the province-wide 1-meter resolution LiDAR-DEM as foundational element. Finally, I would like to thank my family and friends for their encouragement and support.

# TABLE OF CONTENTS

ABSTRACT.....	ii
ACKNOWLEDGEMENTS.....	iii
TABLE OF CONTENTS.....	iv
LIST OF TABLES.....	vii
LIST OF FIGURES.....	viii
Chapter 1: GENERAL INTRODUCTION.....	1
1.1. Problem Statement.....	1
1.2. Crop Suitability Rating Schemes.....	4
1.3. Literature on Potato Crop Suitability Rating.....	6
1.4. Research Objective.....	9
1.5. Thesis Structure.....	10
1.6. Literature Cited.....	12
Chapter 2: POTATO CROP SUITABILITY MAPPING.....	14
2.1. Introduction.....	14
2.2. Methods.....	15
2.2.1. Study Area.....	15
2.2.2. Data.....	16
2.2.3. Crop Suitability Mapping by Soil Association.....	21
2.2.4. Crop Suitability Mapping by Soil Drainage and Slope.....	27
2.2.5. Crop Suitability Mapping by Growing Degree Days and Frost-Free Days.....	29
2.2.6. Crop Suitability Mapping by Socioeconomic Factors.....	32
2.3. Results.....	33
2.4. Discussion and Conclusion.....	33
2.5. Literature Cited.....	36
Chapter 3: MAPPING RESULTS, QUALITATIVE EVALUATIONS.....	38
3.1. Introduction.....	38
3.2. Methods.....	39
3.2.1. Qualitative Assessments.....	39
3.2.2. Quantitative Assessment.....	40
3.3. Results.....	41

3.3.1.	Qualitative Assessment: Woodstock Area.....	41
3.3.2.	Qualitative Assessment: Hartland-Florenceville Area.....	47
3.3.3.	Qualitative Assessment: Northwestern NB .....	52
3.3.4.	Qualitative Assessment: LiDAR-DEM versus Coarse-Grained Crop Suitability Mapping .....	59
3.3.5.	Quantitative Assessment.....	66
3.5.	Conclusion.....	67
3.6.	Literature Cited .....	69
Chapter 4:	PARCEL ACCOUNT NUMBER GENERATED RESULTS.....	70
4.1.	Introduction .....	70
4.2.	Methods.....	70
4.2.1.	Study Area and Data .....	70
4.2.2.	Geoprocessing.....	73
4.2.3.	Statistical Analyses .....	75
4.3.	Results .....	76
4.4.	Conclusion.....	83
4.5.	Literature Cited .....	85
Chapter 5:	COMPARISONS OF PUBLISHED FIELD-GENERATED CROP AND SOIL DATA WITH DSM- AND GIS-GENERATED DATA LAYERS .....	86
5.1.	Introduction .....	86
5.2.	Methods.....	86
5.2.1.	Study Area .....	86
5.2.3.	Geoprocessing and Statistical Analyses.....	90
5.3.	Results and Discussion.....	92
5.3.1.	Saint-André Field.....	92
5.3.2.	Centreville Field.....	98
5.5.	Conclusion.....	102
5.6.	Literature Cited .....	105
Chapter 6:	RE-EXAMINING SOIL VARIATIONS ACROSS A HUMMOCKY FIELD UNDER INTENSIVE POTATO PRODUCTION USING A CARTOGRAPHIC DEPTH- TO-WATER MAPPING PROTOCOL.....	106
6.1.	Abstract .....	106
6.2.	Introduction .....	107

6.3. Methods .....	107
6.3.1. Study Area .....	107
6.3.2. Soil Analysis .....	108
6.3.3. GIS Analysis .....	109
6.3.4. Statistical Analysis .....	110
6.4. Results and Discussion .....	110
6.4.1. Field-Surveyed Versus LiDAR-Registered Elevation .....	112
6.4.2. Regression Analysis: Sand, Silt, Clay, and Coarse Fragment .....	113
6.4.3. Influences of Topography and Other Factors on the Surveyed Soil- Chemical Properties .....	117
6.5. Conclusion .....	123
6.6. Acknowledgments .....	125
6.7. Literature Cited .....	126
Chapter 7: SUMMARIES, CONCLUSIONS, AND RECOMMENDATIONS FOR FUTURE WORK .....	128
7.1. Summary .....	128
7.2. Suggestions for Further Work .....	129
7.3. Practical Applications .....	130
7.4. Literature Cited .....	132
Curriculum Vitae	

## LIST OF TABLES

Table 1.1. Recent literature criteria and methods used in making potato crop land suitability analysis.....	7
Table 2.1. Potato crop suitability rating by topsoil texture, subsoil texture, depth-to compaction of soil, CF content, and calcareousness.....	23
Table 2.2. Forest soil units with soil rating, total hectare province-wide, and primary lithology of parent materials. Forest soil units within the study area (Figure 2.2) are bolded.....	23
Table 2.3. Potato crop suitability rating by soil association across NB.....	26
Table 3.1. Statistics (mean and/or sum) of PANs area (ha), soil quality rating (%), assessment values (\$), and PANs; split by section and land class.....	66
Table 4.1. Statistics (numbers, means, sums) for PAN areas (ha), PAN building footprints (m <sup>2</sup> ), PAN crop suitability ratings (%), PAN taxation assessment values (\$), all split by study area (POC versus AOI), and PAN type.....	77
Table 4.2. PAN numbers (n), together with the best fitted R <sup>2</sup> and RMSE values for the PAN-based POC and AOI tax assessment analyses. ....	79
Table 4.3. Intercept and regression coefficient with errors and significance levels for the PAN-based POC and AOI tax assessment analyses. ....	80
Table 5.1. Best-fitted trend results with equations for average tuber yield, SM (%), EC (mS/m), Mehlich-3 extracted P, and clay (%), per modified DTW class (0-1, 1-2, 2-3 m, etc.).....	95
Table 6.1. Statistical summary of the field-surveyed variables. Units, mean, standard deviation, and maximum and minimum values of these variables are listed. [AP = plough water depth; CF = coarse fragment; C = carbon; Ca = calcium; Mg = magnesium; K = potassium; P = phosphorus; S = sulfur; Fe = iron; Mn = manganese; Zn = zinc; Cu = copper; Na = sodium; Cs <sup>137</sup> = caesium <sup>137</sup> ; NO <sub>3</sub> -N = nitrate nitrogen; NH <sub>4</sub> -N = ammonium nitrate; pH-H <sub>2</sub> O = pH (1:1 water); SM = soil moisture content; DTW > 4 ha = depth-to-water > 4 ha; DEM = digital elevation model].....	111
Table 6.2. Correlation matrix for the variables listed in Table 6.1. Significant regression coefficients (> -0.300 or < 0.300) are highlighted in gray.....	112
Table 6.3. Multivariable regressions (A, B, and C) regarding field-surveyed elevation with point-centered LiDAR-DEM, silt %, and DTW > ha as predictor variables.....	113
Table 6.4. Multivariate regression results for the variables listed in Table 6.1.....	123

## LIST OF FIGURES

Figure 1.1. Southwestern excerpt of NB-wide apple crop suitability mapping: areas deemed too wet (black), unsuitable (red), fair (yellow), suitable (green), and open waters (white). Source: Government of New Brunswick (2018). .....	2
Figure 1.2. Apple (top image) and potato (bottom image) crop suitability mapping details centered on Pocologan, NB (red box in Figure 1.1), with the 1 meter (m) hillshaded light detection and ranging (LiDAR)-derived digital elevation (DEM) as background. Areas are seen to be (i) fair to suitable when located on flat to slightly sloping uplands (yellow to green), (ii) unsuitable when slopes are too steep (red), or lead into depressions, wetlands, and open waters (transparent to grey). Note the wider suggested uplands suitability conditions for potato than for apple cropping. Source: Government of New Brunswick (2018). .....	3
Figure 1.3. Percentage distribution of land suitability rating techniques among 101 literature-based articles (1993-2019; left), including the extend of combining these techniques (right) as reviewed by Mugiyo et al. (2021). In all of this, there has been a transition from simple schemes to increasingly complex rating computations, from local to region-wide applications. ....	5
Figure 1.4. A mapped potato crop suitability rating example, located in southern Peru (Luya Province), as reported by Trigoso et al. (2020), with details in Table 1.1 above. In this example, climate and soil factors were determined to be the most crop suitability restrictive, while the factors relating to slope as well as crop processing and marketing were less so. ....	9
Figure 2.1. Workflow for addressing rating factors and criteria in the development of potato crop suitability mapping by addressing soil type, drainage, slope, and climate conditions. ....	15
Figure 2.2. NB basemap with study area (yellow boundary) used for LiDAR-based potato crop suitability mapping and evaluation. Basemap source: GeoNB. ....	16
Figure 2.3. LiDAR-generated 1 m resolution DEM for NB (left) and property parcel PID map for NB (right). Source: GeoNB. ....	17
Figure 2.4. Cartographic DTW map for NB (left) and slope map for NB (right). Both are derived from the 1 m DEM. Source: Forest Watershed Centre, UNB (unpublished). ....	18
Figure 2.5. Topsoil (left) and subsoil (right) rating for potato crop suitability mapping across NB, by soil association polygons. Sources: GeoNB; Colpitts et al. (1995). ....	18
Figure 2.6. Soil depth (m, left) and soil CF (% , right) rating for potato crop suitability mapping across NB, by soil association polygons. Sources: GeoNB; Colpitts et al. (1995). .....	19
Figure 2.7. Soil weatherability (m, left) for crop suitability mapping and overall distribution of glacial ablation versus basal till (right) across NB. Sources: GeoNB; Colpitts et al. (1995). ....	19

Figure 2.8. Mapping the distribution of crownlands, and of non-forested areas across NB, also showing water bodies and lakes (left), and roads overlaid on NB’s counties (right). Source: GeoNB. ....	20
Figure 2.9. GDDs (left) and FFDs (right) across NB, generated from geospatially interpolating weather-station recorded air temperature data, extrapolated by elevation. Sources: UNB Forest Watershed Centre; Furze (2018). ....	20
Figure 2.10. Potato crop rating specific to variations in DEM-derived DTW and slope %. ....	29
Figure 2.11. Percent extent of potato shoot, foliage, and tuber development by days after emergence. Source: Rosen & Bierman (2008). ....	30
Figure 2.12. Russet potato tuber numbers and length in relation to the number of stems and increasing GDDs > 5 °C. Source: Goeser et al. (2012). ....	31
Figure 2.13. Increasing the rating for FFD and GDD as generated with Eq. 2.5, 2.6, and 2.7 marks the time available for potato cropping number of days within and across regions depending on local climate conditions. ....	32
Figure 2.14 LiDAR-based potato crop suitability mapping results within the AOI (black boundary). Basemap source: GeoNB. ....	33
Figure 3.1. NB topographic map overlaid on the potato crop suitability (%) map within the study area within the AOI (black boundaries), with the locations of the field-based map examples for the Woodstock, Florenceville and northern NB sectors overlaid. Basemap source: GeoNB. ....	39
Figure 3.2. Close-up of an area within the AOI. World imagery with GeoNB-retrieved property outlines (“PIDs”, white borders) and their agricultural field components (red borders) overlaid. Basemap source: GeoNB. ....	41
Figure 3.3. Locations of the crop suitability examples (PIDs 10283562, 10048296, 10270999, 10175354) within the Woodstock area, overlaid on the forest soil units for the area and roads (yellow lines). Source: Colpitts et al. (1995). ....	42
Figure 3.4. Images of PID 10048296 close-ups. From left to right, and from up to down: hillshaded DEM, hillshaded DEM with potato crop suitability (%) overlaid (layer transparency set to 50 %), satellite imagery, satellite imagery with potato crop suitability overlaid (layer transparency set to 50 %). All images also showing streams (4 ha), PIDs, roads, waterbodies, and wetland. Forest soil unit: CR. Basemap source: GeoNB. Potato crop suitability varies from 0 to 100 %, coloured from red through yellow to green, respectively. ....	43
Figure 3.5. Images of PID 10270999 close-ups. From left to right, and from up to down: hillshaded DEM, hillshaded DEM with potato crop suitability (%) overlaid (layer transparency set to 50 %), satellite imagery, satellite imagery with potato crop suitability overlaid (layer transparency set to 50 %). All images also showing streams (4 ha), PIDs, roads, waterbodies, and wetland. Forest soil unit: CR. Basemap source: GeoNB. Potato	

crop suitability varies from 0 to 100 %, coloured from red through yellow to green, respectively. ....	44
Figure 3.6. Images of PID 10175354 close-ups. From left to right, and from up to down: hillshaded DEM, hillshaded DEM with potato crop suitability (%) overlaid (layer transparency set to 50 %), satellite imagery, satellite imagery with potato crop suitability overlaid (layer transparency set to 50 %). All images also showing streams (4 ha), PIDs, roads, waterbodies, and wetland. Forest soil units: CR and TH. Basemap source: GeoNB. Potato crop suitability varies from 0 to 100 %, coloured from red through yellow to green, respectively. ....	45
Figure 3.7. Images of PID 10283562 close-ups. From left to right, and from up to down: hillshaded DEM, hillshaded DEM with potato crop suitability (%) overlaid (layer transparency set to 50 %), satellite imagery, satellite imagery with potato crop suitability overlaid (layer transparency set to 50 %). All images also showing streams (4 ha), PIDs, roads, waterbodies, and wetland. Forest soil units: CA and SE. Basemap source: GeoNB. Potato crop suitability varies from 0 to 100 %, coloured from red through yellow to green, respectively. ....	46
Figure 3.8. Locations of the crop suitability examples within the Hartland-Florenceville area, overlaid on the forest soil units for the area. Source: Colpitts et al. (1995). Yellow lines: roads. ....	47
Figure 3.9 Images of PID 10227098 close-ups. From left to right, and from up to down: hillshaded DEM, hillshaded DEM with potato crop suitability (%) overlaid (layer transparency set to 50 %), satellite imagery, satellite imagery with potato crop suitability overlaid (layer transparency set to 50 %). All images also show streams with > 4 ha upslope flow accumulation areas, PIDs, roads, waterbodies, and wetland. Forest soil unit: CR. Basemap source: GeoNB. Potato crop suitability varies from 0 to 100 %, coloured from red through yellow to green, respectively. ....	48
Figure 3.10. Images of PID 10263366 close-ups. From left to right, and from up to down: hillshaded DEM, hillshaded DEM with potato crop suitability (%) overlaid (layer transparency set to 50 %), satellite imagery, satellite imagery with potato crop suitability overlaid (layer transparency set to 50 %). All images also show streams with > 4 ha upslope flow accumulation areas, PIDs, roads, waterbodies, and wetland. Forest soil unit: CA. Basemap source: GeoNB. Potato crop suitability varies from 0 to 100 %, coloured from red through yellow to green, respectively. ....	49
Figure 3.11. Images of PID 10151512 close-ups. From left to right, and from up to down: hillshaded DEM, hillshaded DEM with potato crop suitability (%) overlaid (layer transparency set to 50 %), satellite imagery, satellite imagery with potato crop suitability overlaid (layer transparency set to 50 %). All images also show streams with > 4 ha upslope flow accumulation areas, PIDs, roads, waterbodies, and wetland. Forest soil unit: CA. Basemap source: GeoNB. Potato crop suitability varies from 0 to 100 %, coloured from red through yellow to green, respectively. ....	51
Figure 3.12. Images of PID 10201267 close-ups. From left to right, and from up to down: hillshaded DEM, hillshaded DEM with potato crop suitability (%) overlaid (layer	

transparency set to 50 %), satellite imagery, satellite imagery with potato crop suitability overlaid (layer transparency set to 50 %). All images also show streams with > 4 ha upslope flow accumulation areas, PIDs, roads, waterbodies, and wetland. Forest soil unit: TH. Basemap source: GeoNB. Potato crop suitability varies from 0 to 100 %, coloured from red through yellow to green, respectively. .... 52

Figure 3.13. Locations of the crop suitability examples within the Grand Falls area, overlaid on the forest soil units for the area. Source: Colpitts et al. (1995). Yellow lines: roads. .... 53

Figure 3.14. Images of PID 65084410 close-ups. From left to right, and from up to down: hillshaded DEM, hillshaded DEM with potato crop suitability (%) overlaid (layer transparency set to 50 %), satellite imagery, satellite imagery with potato crop suitability overlaid (layer transparency set to 50 %). All images also show streams with > 4 ha upslope flow accumulation areas, PIDs, roads, waterbodies, and wetland. Forest soil units: SE and CA. Basemap source: GeoNB. Potato crop suitability varies from 0 to 100 %, coloured from red through yellow to green, respectively. .... 54

Figure 3.15. Images of PID 65085268 close-ups. From left to right, and from up to down: hillshaded DEM, hillshaded DEM with potato crop suitability (%) overlaid (layer transparency set to 50 %), satellite imagery, satellite imagery with potato crop suitability overlaid (layer transparency set to 50 %). All images also show streams with > 4 ha upslope flow accumulation areas, PIDs, roads, waterbodies, and wetland. Forest soil units: CA and SE. Basemap source: GeoNB. Potato crop suitability varies from 0 to 100 %, coloured from red through yellow to green, respectively. .... 55

Figure 3.16. Images of PID 135106236 close-ups. From left to right, and from up to down: hillshaded DEM, hillshaded DEM with potato crop suitability (%) overlaid (layer transparency set to 50 %), satellite imagery, satellite imagery with potato crop suitability overlaid (layer transparency set to 50 %). All images also show streams with > 4 ha upslope flow accumulation areas, PIDs, roads, waterbodies, and wetland. Forest soil unit: SE. Basemap source: GeoNB. Potato crop suitability varies from 0 to 100 %, coloured from red through yellow to green, respectively. .... 56

Figure 3.17. Images of PID 35337989 close-ups. From left to right, and from up to down: hillshaded DEM, hillshaded DEM with potato crop suitability (%) overlaid (layer transparency set to 50 %), satellite imagery, satellite imagery with potato crop suitability overlaid (layer transparency set to 50 %). All images also show streams with > 4 ha upslope flow accumulation areas, PIDs, roads, waterbodies, and wetland. Forest soil units: HM and MG. Basemap source: GeoNB. Potato crop suitability varies from 0 to 100 %, coloured from red through yellow to green, respectively. .... 57

Figure 3.18. Images of PID 35204858 close-ups. From left to right, and from up to down: hillshaded DEM, hillshaded DEM with potato crop suitability (%) overlaid (layer transparency set to 50 %), satellite imagery, satellite imagery with potato crop suitability overlaid (layer transparency set to 50 %). All images also show streams with > 4 ha upslope flow accumulation areas, PIDs, roads, waterbodies, and wetland. Forest soil unit:

HM. Basemap source: GeoNB. Potato crop suitability varies from 0 to 100 %, coloured from red through yellow to green, respectively. ....	58
Figure 3.19. Images of PID 50012996 close-ups. From left to right, and from up to down: hillshaded DEM, hillshaded DEM with potato crop suitability (%) overlaid (layer transparency set to 50 %), satellite imagery, satellite imagery with potato crop suitability overlaid (layer transparency set to 50 %). All images also show streams with > 4 ha upslope flow accumulation areas, PIDs, roads, waterbodies, and wetland. Forest soil unit: TH. Basemap source: GeoNB. Potato crop suitability varies from 0 to 100 %, coloured from red through yellow to green, respectively. ....	59
Figure 3.20. Comparison of potato crop suitability rating from LiDAR-based results (left) and provincial results (right) for PIDs 10283562, 10048296, 10270999, and 10175354.	61
Figure 3.21. Comparison of potato crop suitability rating from LiDAR-based results (left) and provincial results (right) for PIDs 10263366, 10201267, 10151512, 10227098. ....	62
Figure 3.22. Comparison of potato crop suitability rating from LiDAR-based results (left) and provincial results (right) for PIDs 35337989, 50012996, and 35204858. ....	63
Figure 3.23. Comparison of potato crop suitability rating from LiDAR-based results (left) and provincial results (right) for PIDs 35106236, 65085268, and 65084410. ....	64
Figure 4.1. Evaluating the extent of soil-based potato crop rating on property tax assessment: POC (red outline), a portion of Carleton County; AOI (yellow outline), the Upper Saint John River Valley in NB.....	71
Figure 4.2. Maps of layers used to investigate the extent to which farmlands reflect soil quality with respect to potato production. a) potato crop suitability rating map (%), b) building footprint, and c) farmlands, woodlands, and farm and wood land combinations PANs. The layers are “zoomed in” the POC area. Basemap source: GeoNB. ....	72
Figure 4.3. Boxplots of PANs a) assessment values (\$), b) suitability (%), c) area (ha), and d) building area (m <sup>2</sup> ); split by land class (farmlands, woodlands, farm and wood land combinations).....	78
Figure 4.4. Actual versus best-fitted tax assessment scatterplots for \$ and \$/ha for each POC and AOI PAN, using PAN area, building area, and property type (farmlands versus farm and wood land combinations) as PAN-specific predictor variables.....	82
Figure 5.1. Air photos of the Saint-André field (47°06'58.6"N 67°47'54.2"W) on A. 9/16/2013, B. 8/24/2015, C. 9/26/2016, and D. 10/11/2020. Source: Google Earth Pro.	87
Figure 5.2. Air photos of the Centreville field (46°26'22.0"N 67°42'43.2"W) on A. 9/1/2014, B. 8/22/2016, C. 7/8/2019, and D. 5/9/2021. Source: Google Earth Pro. ....	88
Figure 5.3. LiDAR DEMs for the Saint-André field (left; elevations 228.3 to 243.0 m) and the Centreville field (right, elevations 138.7 to 156.9 m). Source: GeoNB.....	89
Figure 5.4. Potato crop suitability rating in % for the Saint-André and Centreville fields, with crop suitability coloured red (poor) through yellow (fair) to green (good).....	89

Figure 5.5. To the right: Kriging maps of the apparent soil EC measured (a)  $EC_{a0-0.3m}$  and (b)  $EC_{a0-1m}$ ; tuber yield (c) 2013, (d) 2014, and (e) 2016; and (f) clay, (g) SM, and (h) Mehlich-3 extracted P of the Saint-André field. To the left: kriging maps of the apparent soil EC (a)  $EC_{a0-0.3m}$  and (b)  $EC_{a0-1m}$ ; tuber yield (c) 2014 and (d) 2016; and Mehlich-3 extracted (e) Ca and (f) P for the Centreville field. Source: Perron et al. (2018). ..... 90

Figure 5.6. LiDAR-DEM generated DTW with > 4 ha upslope flow accumulations centered on the Saint-André field before (left) and after (right) DTW = 0 flow-channel adjustments. .... 92

Figure 5.7. Results generated from Perron et al. (2018) for the Saint-André field (47°06'58.6"N 67°47'54.2"W). ..... 93

Figure 5.8. Fishnet-extracted data on gravimetric SM, EC ( $EC_{a0-0.3m}$  and  $EC_{a0-1m}$ ), Clay content, Mehlich-3 extracted P, and 2013, 2014, and 2015 tuber yields (Mg/ha) from Perron et al. (2018), with best-fitted drainage-adjusted DTW projections for the Saint-André field. .... 94

Figure 5.9. Averaged 2013, 2014 and 2015 tuber yields (Mg/ha) per 1 m modified DTW classes on the Saint-André field..... 95

Figure 5.10. Overlays of the fishnet-extracted data on the drainage-adjusted DTW projections for tuber yield (2016), SM, clay, Mehlich-3 extracted P, and EC for the Saint-André field. .... 97

Figure 5.11. Results generated from Perron et al. (2018) for the Centreville field (46°26'22.0"N 67°42'43.2"W). ..... 99

Figure 5.12. Fishnet extract values for 2014 and 2015 tuber yields, EC ( $EC_{a0-0.3m}$  and  $EC_{a0-1m}$ ), and Mehlich-3 extracted Ca and P for the Centreville field. Also shown are the best-fitted trend lines with their regression equations. .... 100

Figure 5.13. Depth-to-water patterns (DTW) along flow channels with > 2 and > 4 ha upslope flow accumulation for the Centreville field (left), compared with the DTW > 2 ha evaluated tuber yield pattern (top right) overlaid with fishnet-extracted tuber yield points (bottom right). ..... 101

Figure 5.14. Mean 2014 and 2016 tuber yields per 1- m DTW > 2 ha classes from DTW > 2ha = 0.5 m upwards. Also shown are their best-fitted regression lines and equations. The 2014 versus 2016 differences are likely due to year-by-year variations in seasonal weather and field-specific crop management patterns. .... 102

Figure 6.1. To the left: NB basemap with AOI (yellow boundary) used for LiDAR-based potato crop suitability mapping and evaluation. To the right: this chapter’s study area, an agricultural field located approximately 1 km east of Harland, NB (46°18'23"N 67°30'41"W). Basemap source: GeoNB. .... 108

Figure 6.2. Survey grid and cartographic DTW associated from A to D, with the LiDAR and DEM derived flow channels with > 4 ha, 0.25, and 0.1 ha upslope flow accumulation

areas overlaid on the hillshaded study area DEM, respectively. DTW grades from < 10 cm (dark blue) to 1 m (light blue) deep. .... 110

Figure 6.3. Sand, silt, and clay % (left) and very coarse, coarse and medium sand % versus DTW<sub>4ha</sub> along the LiDAR-DEM-derived flow channels with > 4 ha upslope flow accumulation areas..... 114

Figure 6.4. Left: surveyed CF % overlaid on the hillshaded LIDAR DEM. Right: surveyed CF % overlaid on the cartographic DTW. Grid colour: red (low CF %) to green (high CF %). .... 115

Figure 6.5. Left: decreasing trend from very coarse (vc) to coarse (c) and fine medium (m) sand % fractions versus DTW > 4 ha upslope flow accumulation, with regression equations. Right: silt % versus DTW (m) along the LiDAR-DEM-derived flow channels with DTW > 4 ha, > 1 ha, > 0.25 ha and > 0.1 ha upslope flow accumulation areas, with regression equations..... 116

Figure 6.6. Factor analysis: Factor 2 (top) and Factor 3 (bottom) versus Factor 1 plots, with the Factor 2 (Ca, Mg, K, P, S, NO<sub>3</sub>-N) and Factor 3 (Cs<sup>137</sup>, Cu, Fe, Zn, C, Ap) entries polygonised. .... 118

Figure 6.7. Factor 3 versus Factor 2 plot, with the Factor 1 (silt, DTW > 4 ha, SM, sand, Na), Factor 2 (Ca, Mg, K, P, S, NO<sub>3</sub>-N), and Factor 3 (Cs<sup>137</sup>, Cu, Fe, Zn, C, Ap) defining entries polygonised. .... 120

## LIST OF SYMBOLS, NOMENCLATURES OR ABBREVIATIONS

### Units

°C – Celsius degree, unit of temperature

cm<sup>3</sup> – Cubic centimetre, unit of volume

g – Gram, unit of mass

ha – Hectare, unit of area

kg – Kilogram, unit of mass

km – Kilometre, unit of length

km<sup>2</sup> – Square kilometre, unit of area

m – Meter, unit of length

M – Molarity (moles/litre), quantitative unit of concentration

Mg – Megagram, unit of mass

mg – Milligram, unit of mass

mm – Millimetres, unit of length

### Chemical Formulas

Al – Aluminum

B – Boron

C – Carbon

Ca – Calcium

CaCl<sub>2</sub> – Calcium chloride

CaO – Calcium oxide

CaSO<sub>4</sub> – Gypsum

CH<sub>3</sub>COOH – Acetic acid

Cl – Chloride

Cs<sup>137</sup> – Caesium<sup>137</sup>

Cu – Copper

EDTA – Ethylenediaminetetraacetic acid

Fe – Iron

Fe(OH)<sub>2</sub><sup>+</sup> – Iron(II) hydroxide

HNO<sub>3</sub> – Nitric acid

K – Potassium

K<sub>2</sub>O – Potassium oxide

Mg – Magnesium

Mn – Manganese

Mo – Molybdenum

N – Nitrogen

NH<sub>4</sub>F – Ammonium fluoride

NH<sub>4</sub>-N – Ammonium nitrogen

NH<sub>4</sub>NO<sub>3</sub> – Ammonium nitrate

NO<sub>3</sub>-N – Nitrate nitrogen

P – Phosphorus

Zn – Zinc

## **Geospatial Data**

DEM – Digital Elevation Model

DSM – Digital Soil Mapping

GIS – Geographic Information System

LiDAR – Light Detection and Ranging

## **Soils**

Ap – Plough water layer depth

CEC – Cation exchange capacity

CF – Coarse fragment

Db – Bulk density

DTW – Depth-to-water

EC – Electrical conductivity

FC – Field capacity

OM – Organic matter

PWP – permanent wilting point

SM – Soil moisture

SOC – Soil organic carbon

## **Statistic**

AHP – Analytical Hierarchy Processes

CSM – Crop Simulation Model

ML – Machine Learning

TM – Traditional Method

**Other Abbreviations**

AOI – Area of Interest

DAAF – Department of Agriculture, Aquaculture and Fisheries

FFD – Frost-Free Day

GDD – Growing-Degree Day

LSRS – Land Suitability Rating System

NB – New Brunswick

PA – Precision Agriculture

PAN – Parcel Account Number

PID – Parcel Identifier

POC – Proof of Concept

# CHAPTER 1: GENERAL INTRODUCTION

## 1.1. Problem Statement

In New Brunswick (NB), potatoes are seeded and harvested approximately 20,000 hectares (ha) annually, thereby making them the main crop grown in the province (Government of Canada, 2020). In Canada, the five main producing provinces are Prince Edward Island, Manitoba, Alberta, with NB in fourth place (Government of Canada, 2020). This crop produced 1.19 billion dollars for the Canadian economy in 2017 (Government of Canada, 2020). NB produced 687,601 megagram (Mg) of potatoes in 2017 which are intended to be either processed (63 %, approximate yield of 22 Mg/ha), for seed (19 %, approximate yield of 7 Mg/ha), or for fresh market (18 %, approximate yield of 6 Mg/ha; Government of Canada, 2020). The top five registered seed potatoes varieties in the province are Russet Burbank, Atlantic, Shepody, Goldrush, and Innovator (Government of Canada, 2020). Together, primary, secondary, and other crop-processing activities including trading and selling have become an important revenue source for the province.

Currently, there is an interest in further expanding potato crop production in NB, especially across forested lands deemed most accessible and suitable for farming. Expanding potato production would in part:

1. enhance NB's food security;
2. create new farming opportunities for existing and prospective agricultural producers;
3. generate employment opportunities by way of crop processing and marketing (Government of New Brunswick, 2018).

To this extent, there are methods that can be used to locate additional arable lands across forested and non-forested lands, as reviewed below. In this regard, NB's Department of Agriculture, Aquaculture and Fisheries (DAAF) launched a site in 2018 for locating suitable areas for growing apples, corn, soybeans, grapes, hemp, potatoes, and small grains. However, the maps so produced do not account for cross-province variations in soil type, with slope and soil drainage impacts on cropping remaining poorly resolved, as illustrated in Figure 1.1 and Figure 1.2 (Government of New Brunswick, 2018).

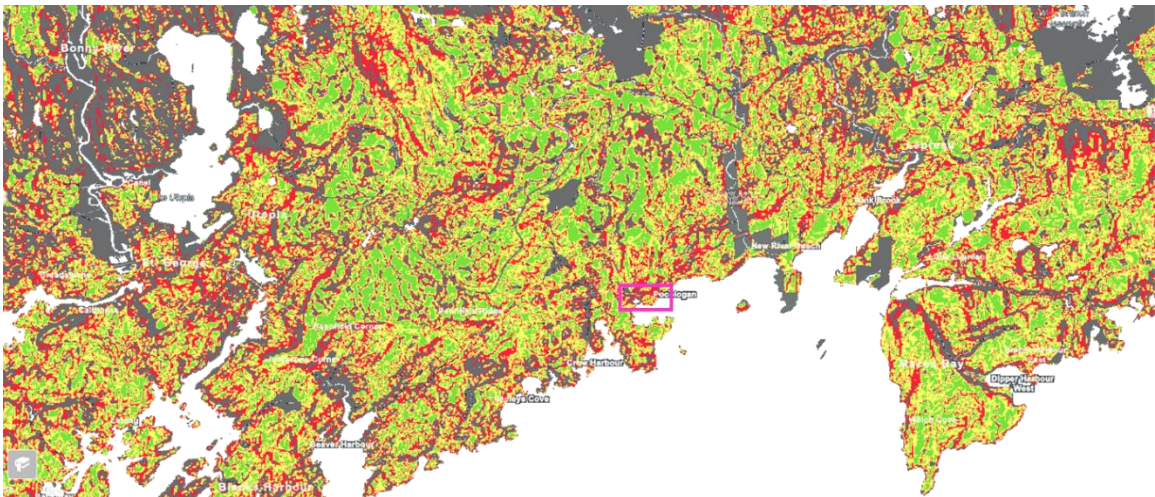


Figure 1.1. Southwestern excerpt of NB-wide apple crop suitability mapping: areas deemed too wet (black), unsuitable (red), fair (yellow), suitable (green), and open waters (white). Source: Government of New Brunswick (2018).

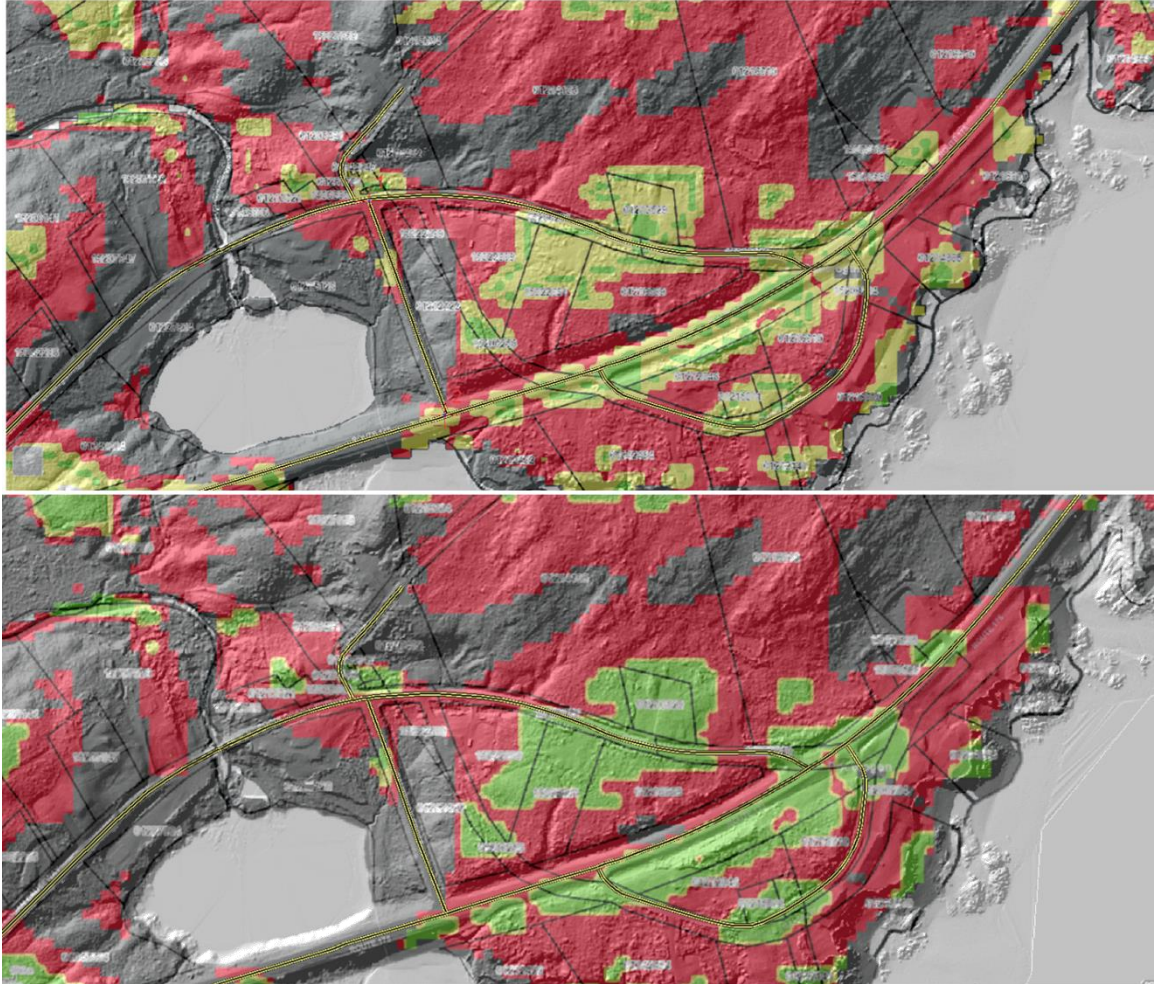


Figure 1.2. Apple (top image) and potato (bottom image) crop suitability mapping details centered on Pocologan, NB (red box in Figure 1.1), with the 1 meter (m) hillshaded light detection and ranging (LiDAR)-derived digital elevation (DEM) as background. Areas are seen to be (i) fair to suitable when located on flat to slightly sloping uplands (yellow to green), (ii) unsuitable when slopes are too steep (red), or lead into depressions, wetlands, and open waters (transparent to grey). Note the wider suggested uplands suitability conditions for potato than for apple cropping. Source: Government of New Brunswick (2018).

## 1.2. Crop Suitability Rating Schemes

Practices pertaining to crop suitability ratings by soil, land and climate have been reviewed recently by, e.g., Akpoti et al. (2019), Moloudi & Mahabadi, (2019) and Mugiyo et al. (2021) as represented in Figure 1.3.

Traditional methods (TMs) use biophysical crop, soil, and climate characteristics to perform - by hand or by computer - qualitatively and quantitatively simple land suitability assessments for individual land parcels from suitable to fair and unsuitable for local to region-wide. Typically, TM-based crop suitabilities are at first rated individually by each growth-affecting factor. The ratings so assigned involve additions, subtractions, multiplications, and/or result-affecting transformations as deemed appropriate. An example of this is the *Land Suitability Rating System* (LRSL) developed by Agri-Food and Agriculture Canada (Agronomic Interpretations Working Group, 1995). Its cross-Canada data layer requirements refer to:

1. Climate: mean annual/seasonal temperatures, precipitation amounts, and frost conditions.
2. Soils: water-holding capacity, texture, structure, organic matter (OM), uncompacted soil depth, pH, salinity, sodicity, soil temperature soil parent material, drainage, and slope.
3. Landscape surface expressions, surface deposits, waterbodies, wetlands, and bedrock formations.
4. Vegetation cover: forests, grasslands, and deserts.

Another widely known TM example using similar information is the Storie Index method for rating soils for land use and productivity across California in original and

revised form (Storie, 1932; O'Green et al., 2008). The crop suitability rating and mapping scheme as it currently exists for NB also represents a TM example, using topographic positioning as the dominant factor.

Apart from TM, modern crop rating schemes also involve (Mugiyo et al., 2021;

Figure 1.3):

1. Analytical hierarchy processes (AHPs).
2. Fuzzy logic.
3. Machine learning (ML).
4. Crop simulation methods (CSMs).

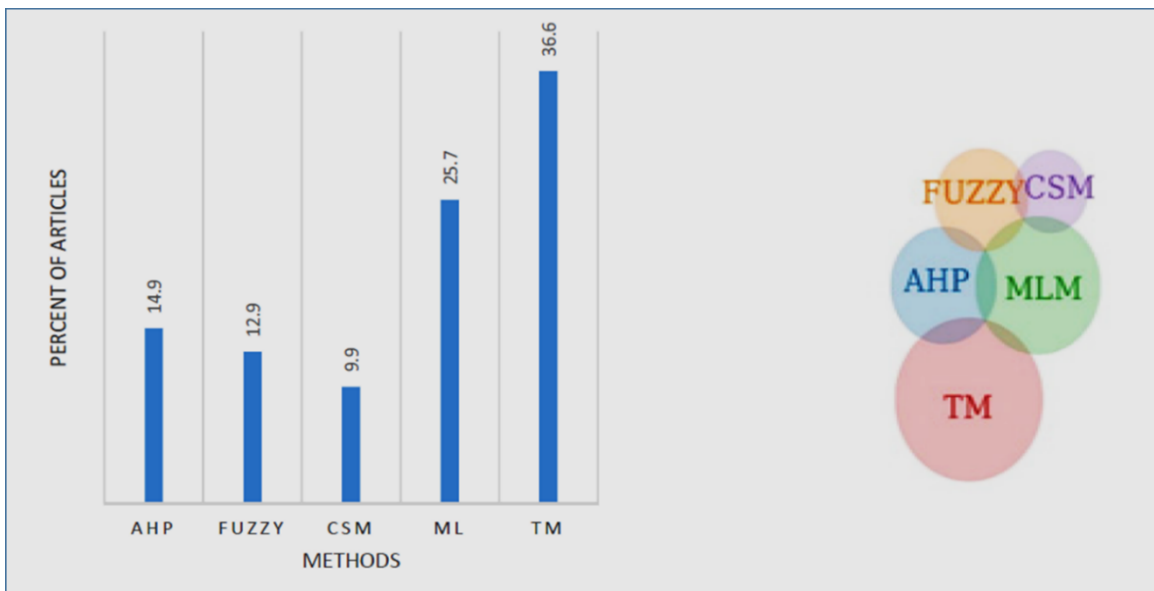


Figure 1.3. Percentage distribution of land suitability rating techniques among 101 literature-based articles (1993-2019; left), including the extend of combining these techniques (right) as reviewed by Mugiyo et al. (2021). In all of this, there has been a transition from simple schemes to increasingly complex rating computations, from local to region-wide applications.

### **1.3. Literature on Potato Crop Suitability Rating**

Table 1.1 provides a brief literature review of criteria and methods used specifically for potato crop suitability mapping. These also differ by local to regional extent, with climate-specific rating factors dominating across large regions (Zhao et al., 2018; Wang et al., 2021). In this, topography, climate and soil property factors are important for local evaluations. Among these, the rating scheme employed by Trigo et al. (2020) is the most complex by also considering (i) soil nutrient status, (ii) socio-economical transportation, and (iii) crop processing factors in relation to distance to roads and rivers. Climatic factors pertaining to precipitation, air temperature, and evapotranspiration are used to assess the extent to which moist soil conditions are naturally maintained across well-aerated potato-growing fields. According to Zhao et al. (2018), wind speed and relative humidity also matter, and especially in dry regions that are subject to desiccating winds.

The extent to which soil moisture conditions vary locally can best be revealed through high-resolution GIS-based slope and soil drainage mapping. To do so, Trigo et al. (2020) used a slope-determining DEM at 12.5 m spatial resolution. Asfaw et al. (2017) used DEM data at 30 m resolution (resampled to 20 m) and Daccache et al. (2012) used DEM data at 25 m resolution. Wang et al. (2021) and Zhao et al. (2018) only used GIS to infer region-wide climate differences from existing weather station information. Thus far, best GIS-determined soil drainage assessment across fields and regions are obtained through DEMs at a 1 m spatial resolution, especially when done in connection with DEM-determined flow directions, flow accumulations, and raster-to-shapefile stream flow-channel delineations (D8; Tarboton, 1997; Murphy et al., 2009).

In brief, AHP refers to complex multi-criteria evaluation by weighing each crop suitability criterion through pairwise land parcel comparisons. Fuzzy logic provides plausible rating ranges rather than single values for each land parcel. CSMs deal with crop growth simulations by crop type, soil type, and daily weather. Among the ML methods, random forest classification is a technique that can be used to expand crop suitability ratings as determined for specific land parcels across entire regions based on GIS-layered crop type, topography, and climate factors (GIS: geographic information system). Further ML developments toward precision agriculture (PA) and forestry currently focus on enhancing the digitized resolution of GIS-layered information for crop-affecting soil properties such as soil texture, depth, density, OM content, coarse fragment (CF) content, and topographic position, as available from existing data coupled with digital soil mapping (DSM; Furze, 2018).

Table 1.1. Recent literature criteria and methods used in making potato crop land suitability analysis.

Authors and Location	Criteria	Method
Trigoso et al. (2020) Amazonas, Peru	<ul style="list-style-type: none"> <li>- Mean annual temperature</li> <li>- Mean annual precipitation</li> <li>- Elevation</li> <li>- Terrain slope</li> <li>- Terrain aspect</li> <li>- Land use</li> <li>- Distance to rivers</li> <li>- Distance to roads</li> <li>- Soil texture</li> <li>- Soil pH</li> <li>- Organic matter</li> <li>- Nitrogen</li> <li>- Phosphorus</li> <li>- Potassium</li> <li>- Cation exchange capacity</li> <li>- Electrical conductivity</li> </ul>	AHP with remote sensing and GIS DEM evaluation

Asfaw et al. (2017) Amhara Region, Ethiopia	<ul style="list-style-type: none"> <li>- Elevation</li> <li>- Slope</li> <li>- Soil type</li> <li>- Mean annual rainfall</li> <li>- Temperature variation</li> <li>- Poor crop management</li> </ul>	Combination of modern multi-criteria decision making and with GIS DEM evaluations
Daccache et al. (2012) England, Wales	<ul style="list-style-type: none"> <li>- Root depth</li> <li>- Growing season</li> <li>- Texture</li> <li>- Organic matter</li> <li>- Structure</li> <li>- Slope</li> <li>- Stoniness</li> <li>- Rainfall</li> <li>- Evapotranspiration</li> <li>- Temperature</li> </ul>	Modelling using pedo-climatic functions and GIS DEM evaluations
Yusianto et al. (2020) Wonosobo, Indonesia	<ul style="list-style-type: none"> <li>- Altitude</li> <li>- Soil texture</li> <li>- Slope percentage</li> <li>- Rainfall</li> <li>- Temperature</li> </ul>	Multi criteria evaluation, with GIS DEM evaluations
Wang et al. (2021) Across China	<ul style="list-style-type: none"> <li>- Annual precipitation</li> <li>- Annual average minimal temperature</li> <li>- Average temperature in the coldest month</li> <li>- Sunshine duration</li> </ul>	Maximum entropy model (machine learning), with GIS based weather station interpolations
Zhao et al. (2018) Across Northern China	<ul style="list-style-type: none"> <li>- Maximal and minimal air temperature</li> <li>- Average air temperature</li> <li>- Precipitation</li> <li>- Solar radiation</li> <li>- Relative humidity</li> <li>- Wind speed</li> </ul>	Fuzzy mathematics with GIS based weather station interpolations

Figure 1.4 provides a 278 square kilometres (km<sup>2</sup>) potato crop suitability mapping example (Trigoso et al., 2020). This example is centered on the Jucusbama and Tincas watersheds within the Luya Province in southern Peru and is based on the AHP rating

criteria summarized in Table 1.1. As shown, climate, soils and topography influenced this rating scheme equally, followed by transportation proximity to roads and rivers.

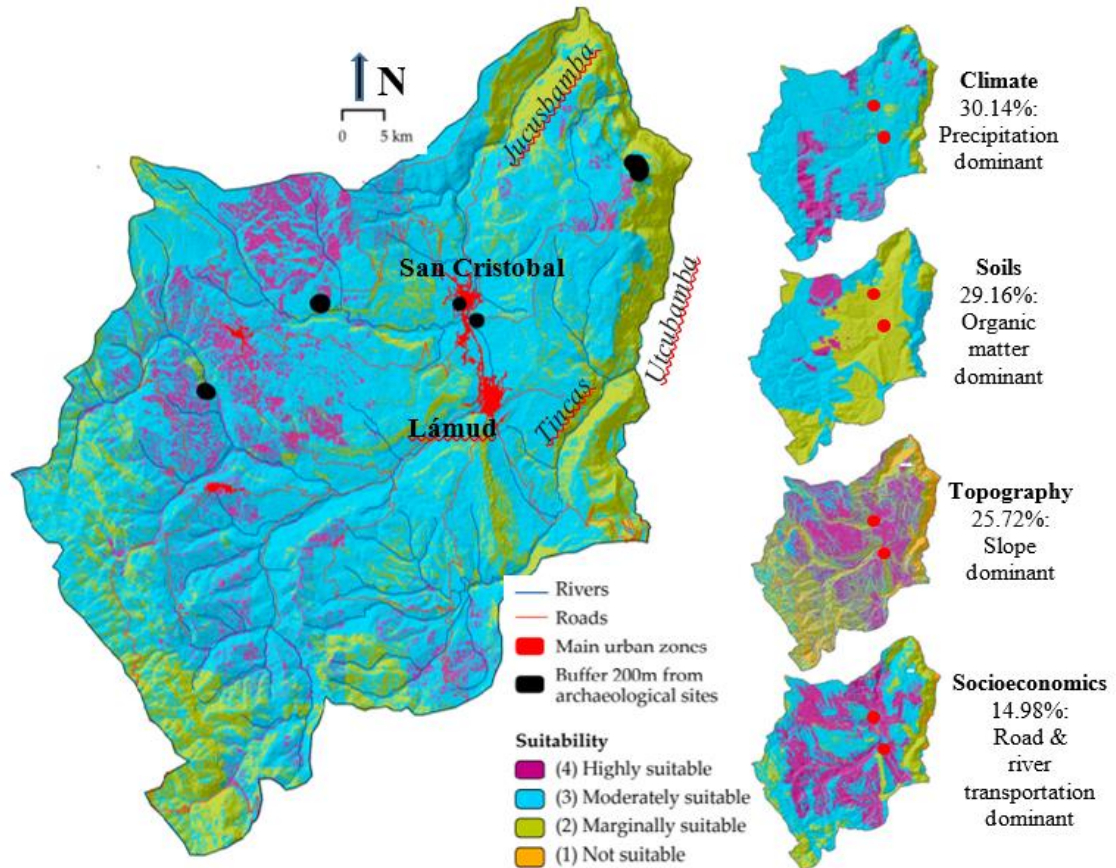


Figure 1.4. A mapped potato crop suitability rating example, located in southern Peru (Luya Province), as reported by Trigoso et al. (2020), with details in Table 1.1 above. In this example, climate and soil factors were determined to be the most crop suitability restrictive, while the factors relating to slope as well as crop processing and marketing were less so.

#### 1.4. Research Objective

The objective of this thesis is to address the issue of potato crop suitability rating by taking advantage of the following province-wide available data layers:

1. The LiDAR-DEM coverage at 1 m resolution raster format.
2. The forest soils map, available as a shapefile.

3. Shapefiles delineating the open water bodies, wetlands, flow channels, and individually held properties across the province.

The objectives and technical aspects for this research refer to:

1. Producing a LiDAR-based potato crop suitability map along the Upper Saint John River Valley at a high 1 m spatial resolution using multi-criteria evaluation.
2. Validating the produced LiDAR-based potato crop suitability map by addressing the extent to which soil factors (potassium content, calcium (Ca) content, phosphorus content, potato tuber yield, electrical conductivity (EC), clay content, and soil moisture (SM) reflect soil quality by way of published records (Perron et al., 2018).
3. Addressing the extent to which the assessed market value of farmlands and woodlands increase with increased crop suitability.
4. Validating the produced LiDAR-based potato crop suitability map by comparing results with DSM- and GIS- derived data layers.

## **1.5. Thesis Structure**

This thesis has seven chapters:

1. Chapter 1: *General Introduction*.
2. Chapter 2: *Potato Crop Suitability Mapping*. This chapter deals with the specific formulations by soil property as per the NB forest soil map, and NB-wide LiDAR DEM derived depth to water (DTW) and slope coverage.
3. Chapter 3: *Mapping Results, Qualitative Evaluations*. Presented in this chapter are example collages for specific areas of interest, each collage done in four parts:
  - a. Hillshaded DEM.

- b. Hillshaded DEM with crop suitability layer overlaid.
- c. Satellite image(s).
- d. Satellite image(s) with crop suitability layer overlaid.

The crop suitability components of these collages are also compared with the current coarse-gridded NB crop suitability rating results, with parcel identifiers (PIDs) flow channels with > 4 ha upslope flow accumulations, wetlands, water bodies, and roads overlaid where and as applicable.

- 4. Chapter 4: *Parcel Account Number Generated Results*. This chapter deals with farmlands and woodlands parcel account numbers (PANs) assessment values in relation with the thesis-derived potato crop suitability mapping results.
- 5. Chapter 5: *Comparisons of Published Field-Generated Crop and Soil Data with DSM- and GIS-Generated Data Layers*. This chapter relates published on-site field data pertaining to electrical conductivity, tuber yield, soil moisture, and mineral contents to the crop suitability informing GIS data layers, at a 1 m resolution (Perron et al., 2018).
- 6. Chapter 6: *Re-Examining Soil Variations Across a Hummocky Field Under Intensive Potato Production Using a Cartographic Depth-to-Water Mapping Protocol*.
- 7. Chapter 7: *Summaries, Conclusions, and Suggestions for Future Work*.

## 1.6. Literature Cited

- Agronomic Interpretations Working Group. 1995. Land Suitability Rating System for Agricultural Crops: 1. Spring-seeded small grains. Edited by W.W. Pettapiece. Tech. Bull. 1995-6E. Centre for Land and Biological Resources Research, Agriculture and Agri-Food Canada, Ottawa. 90 pages, 2 maps.
- Akpoti, K., Kabo-bah, A. T., & Zwart, S. J. 2019. Agricultural land suitability analysis: State-of-the-art and outlooks for integration of climate change analysis. *Agricultural Systems*, 173, 172–208.
- Asfaw, M. 2017. Agricultural Land Suitability Analysis for Potato Crop by Using GIS and Remote Sensing Technology, in the Case of Amhara Region, Ethiopia. *Journal of Biology, Agriculture and Healthcare*, 7, 5-16.
- Daccache, A., Keay, C., Jones, R. J. A., Weatherhead, E. K., Stalham, M. A., & Knox, J. W. 2012. Climate change and land suitability for potato production in England and Wales: Impacts and adaptation. *The Journal of Agricultural Science*, 150(2), 161-177.
- Furze, S. 2018. *A high-resolution digital soil mapping framework for New Brunswick, Canada* [PhD Thesis, University of New Brunswick].
- Government of Canada. 2020. Potato mark information review, 2020-2021. Retrieved from: <https://agriculture.canada.ca/en/agriculture-and-agri-food-canada/canadas-agriculture-sectors/horticulture/horticulture-sector-reports/potato-market-information-review-2020-2021>
- Government of New Brunswick. 2018. Agriculture Site Suitability. Retrieved from: <https://www2.gnb.ca/content/gnb/en/departments/10/agriculture/content/agriculture-suitability.html>.
- Moloudi, A., & Mahabadi, N. Y. 2019. Quantitative and qualitative land suitability assessment for rice cultivation, North of Iran. *Polish Journal of Soil Science*, 52(2), 195–210.
- Mugiyo, H., Chimonyo, V. G. P., Sibanda, M., Kunz, R., Masemola, C. R., Modi, A. T., & Mabhaudhi, T. 2021. Evaluation of land suitability methods with reference to neglected and underutilised crop species: A scoping review. *Land*, 10(2), 1–24.
- Murphy, P. N. C., Ogilvie, J., & Arp, P. A. 2009. Topographic modelling of soil moisture conditions: A comparison and verification of two models. *European Journal of Soil Science*, 60(1), 94–109.
- O’Geen, A. T., Southard, S. B., Southard, R. J. 2008. A Revised Storie Index for Use with Digital Soils Information. ANR Publication 8335.
- Perron, I., Cambouris, A. N., Chokmani, K., Gutierrez, M. F. V., Zebarth, B. J., Moreau, G., Biswas, A., & Adamchuk, V. 2018. Delineating soil management zones using a proximal soil sensing system in two commercial potato fields in New Brunswick, Canada. *Canadian Journal of Soil Science*, 98, 724–737.

- Storie, R. 1978. Storie index soil rating. *Oakland: University of California Division of Agricultural Sciences*. Special Publication 3203.
- Tarboton, D. G. 1997. A new method for the determination of flow directions and upslope areas in grid digital elevation models. *Water Resources Research*, 33, 309-319.
- Trigoso, D. I., López, R. S., Briceño N. B. R., López, J. O. S., Fernández, D.G., Oliva, M., Huatangari, L. Q., Murga, R. E. T., Castillo, E. B., & Gurbillón, M. Á. B. 2020. Land Suitability Analysis for Potato Crop in the Jucusbamba and Tincas Microwatersheds (Amazonas, NW Peru): AHP and RS-GIS Approach. *Agronomy*, 10(12), 1898.
- Wang, C., Shi, X., Liu, J., Zhao, J., Bo, X., Chen, F., & Chu, Q. 2021. Interdecadal variation of potato climate suitability in China. *Agriculture, Ecosystems and Environment*, 310, 107293.
- Yusianto, R., Dian, U., Semarang, N., Marimin, M., Suprihatin, S., & Hardjomidjojo, H. H. 2020. Spatial Analysis for Crop Land Suitability Evaluation: A Case Study of Potatoes Cultivation in Wonosobo, Indonesia. *South China University of Technology*. 313-319.
- Zhao, J., Zhan, X., Jiang, Y., & Xu, J. 2018. Variations in climatic suitability and planting regionalization for potato in northern China under climate change. *PLoS ONE* 13, 1–19.

## CHAPTER 2: POTATO CROP SUITABILITY MAPPING

### 2.1. Introduction

To expand potato (*Solanum tuberosum*) cropping further in NB while sustaining existing cropping areas, it is important to determine which other areas would also be suitable for this production. To this effect, there are already several province-wide crop suitability maps in place (Government of New Brunswick, 2018). However, these maps – derived from a 70 m resolution DEM – are quite coarse, thereby remaining poorly resolved in terms of field-specific slope and drainage conditions, and as yet do not address local to regional variations in soil type and climate (Government of New Brunswick, 2018). The procedures described in this chapter are centered on improving this for the Upper Saint John River Valley in NB (Figure 2.1). Doing so was facilitated by:

1. The province-wide 1 m spatial resolution LiDAR-DEM coverage, to portray flow channels, slope, and soil drainage.
2. The forest soils map for NB to characterize the overall soil conditions within and across field and forest properties (Colpitts et al., 1995).
3. Province-wide data layers for growing degree days (GDDs), frost-free days (FFDs), waterbodies, wetlands, roads; farm and wood lands properties, forested and non-forested areas, and building footprint. These layers provide contextual information about local variations in climate, transportation, and socioeconomic conditions.

The workflow that was needed to track, evaluate, combine, and map the rating factors, criteria, and evaluations is presented in Table 2.1. The overall objective is to produce potato crop suitability maps that can be used for assessing in-field and farm-to-farm variations by crop type, soil type, slope, and drainage in an effort to expand doing so across NB.

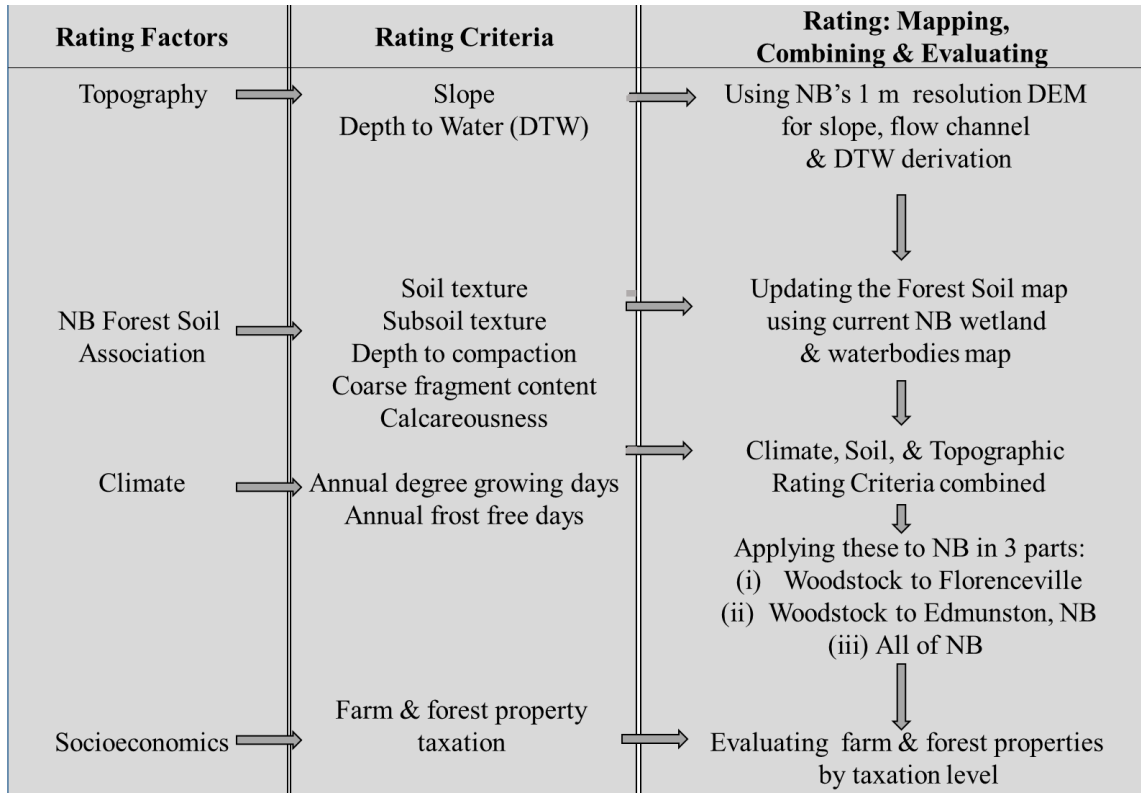


Figure 2.1. Workflow for addressing rating factors and criteria in the development of potato crop suitability mapping by addressing soil type, drainage, slope, and climate conditions.

## 2.2. Methods

### 2.2.1. Study Area

The study area stretches from Edmundston (northwestern boundary) and Saint-Quentin (northeastern boundary) southwards to Canterbury (southern boundary; Figure 2.2). This area is comprising most of the potato cropping activities in NB. This being so, this area enables direct comparisons between crop suitability mapping with actual field layouts and current property-by-property taxation levels.

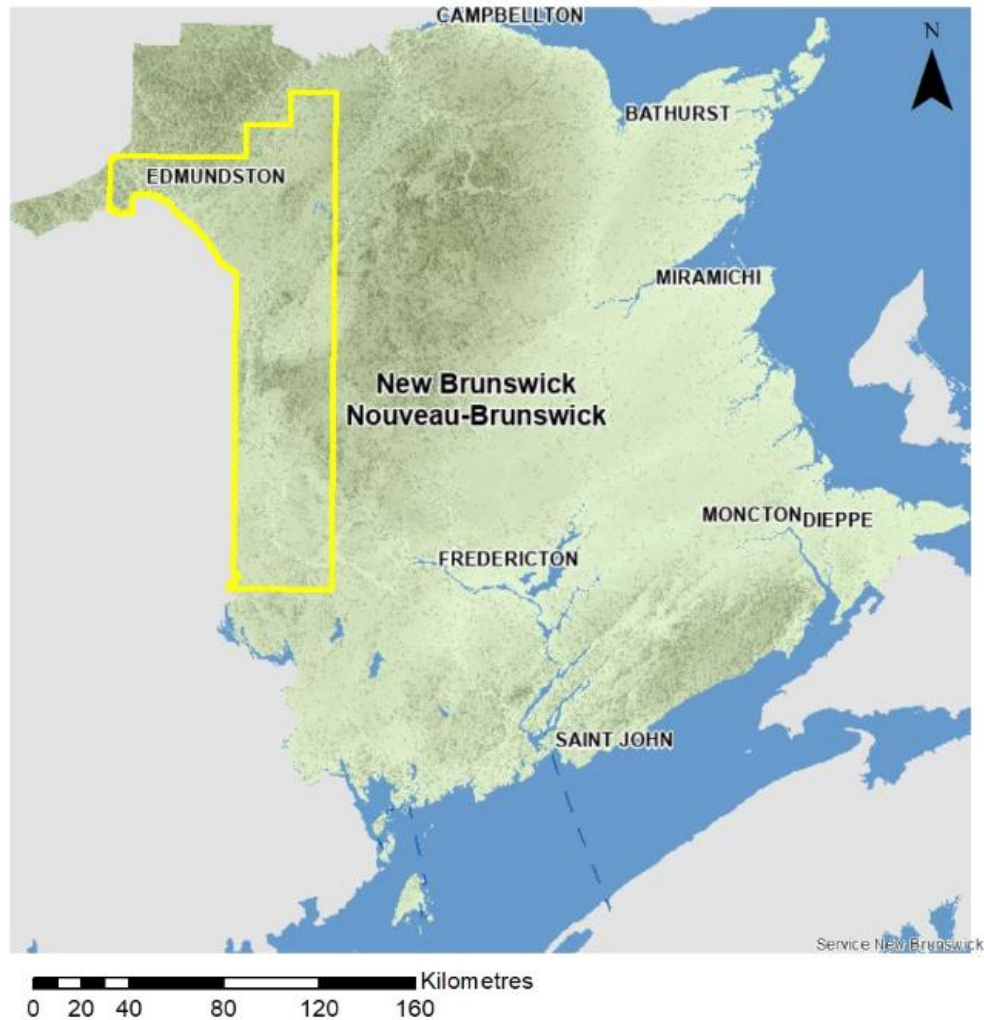


Figure 2.2. NB basemap with study area (yellow boundary) used for LiDAR-based potato crop suitability mapping and evaluation. Basemap source: GeoNB.

### 2.2.2. Data

The 1 m resolution LiDAR-generated DEM raster for NB (Figure 2.3, left) and all the layers outlined below were acquired from NB’s GeoNB website (GeoNB, n.d.). The DEM layer was used to generate province-wide raster layers for slope (%) and cartographic DTW (Figure 2.4), as described by Murphy et al. (2009). The forest soil shapefile presented in part by Figure 2.5, 2.6, and 2.7 provided generalized data information on topsoil and subsoil texture, depth-to-compaction, CF content, and degree of calcareousness by soil

association. Also retrieved from GeoNB were the shapefiles for private properties (Figure 2.3, right), roads, wetlands, water bodies, crownlands, and non-forested areas (Figure 2.8). Non-forested areas include agricultural fields, other fields, roads and built-up areas for residential, institutional, and industrial use. Finally, elevation-interpolated weather station records for air temperature were used to produce province-wide rasters for growing degree days (GDDs  $> 5^{\circ}\text{C}$ ) and frost-free days (FFDs) at 10 m resolution (Figure 2.9). The results so presented at LiDAR-DEM-derived 10 m resolution correspond closely with GDDs and growing days (equivalent to FFDs) maps in Jong et al. (2013) and Pedlar et al. (2015), respectively.

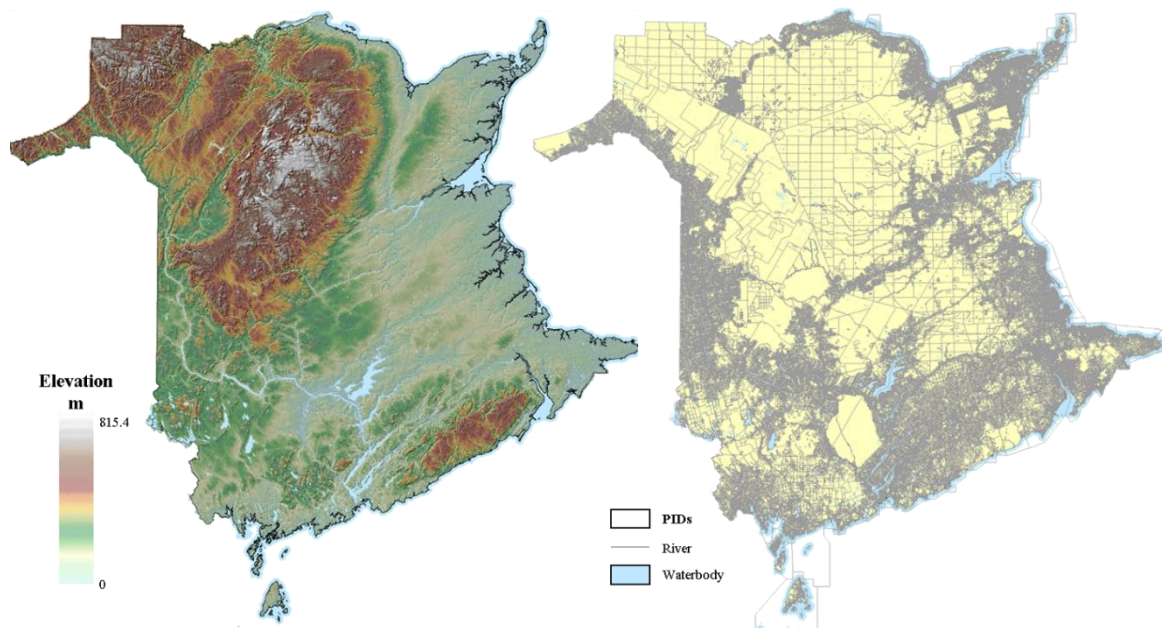


Figure 2.3. LiDAR-generated 1 m resolution DEM for NB (left) and property parcel PID map for NB (right). Source: GeoNB.

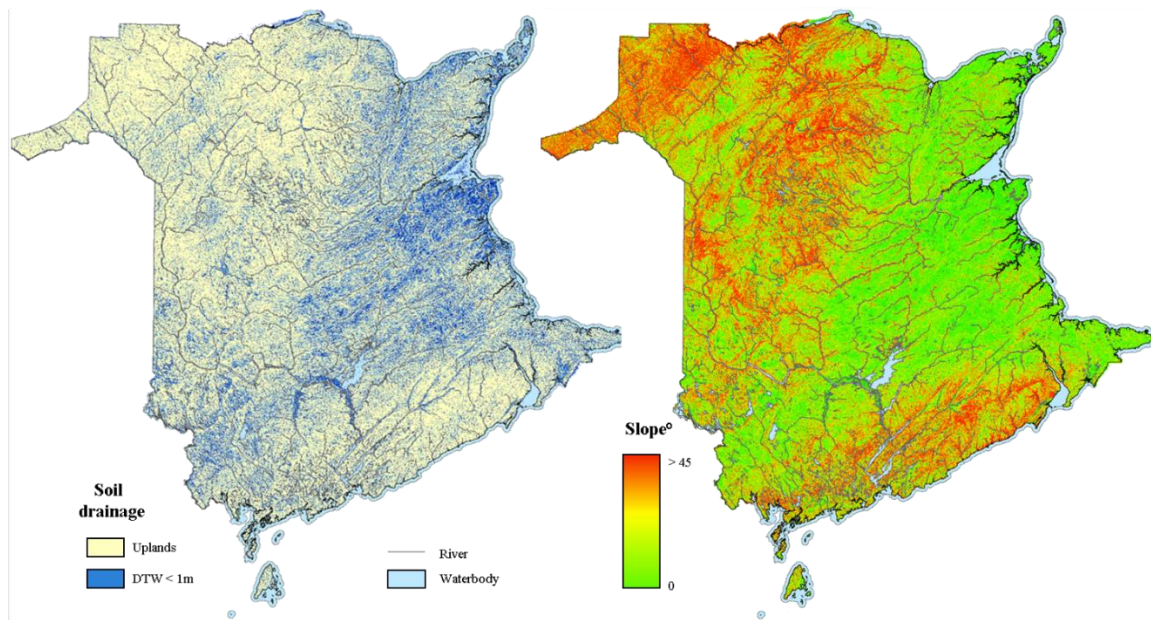


Figure 2.4. Cartographic DTW map for NB (left) and slope map for NB (right). Both are derived from the 1 m DEM. Source: Forest Watershed Centre, UNB (unpublished).

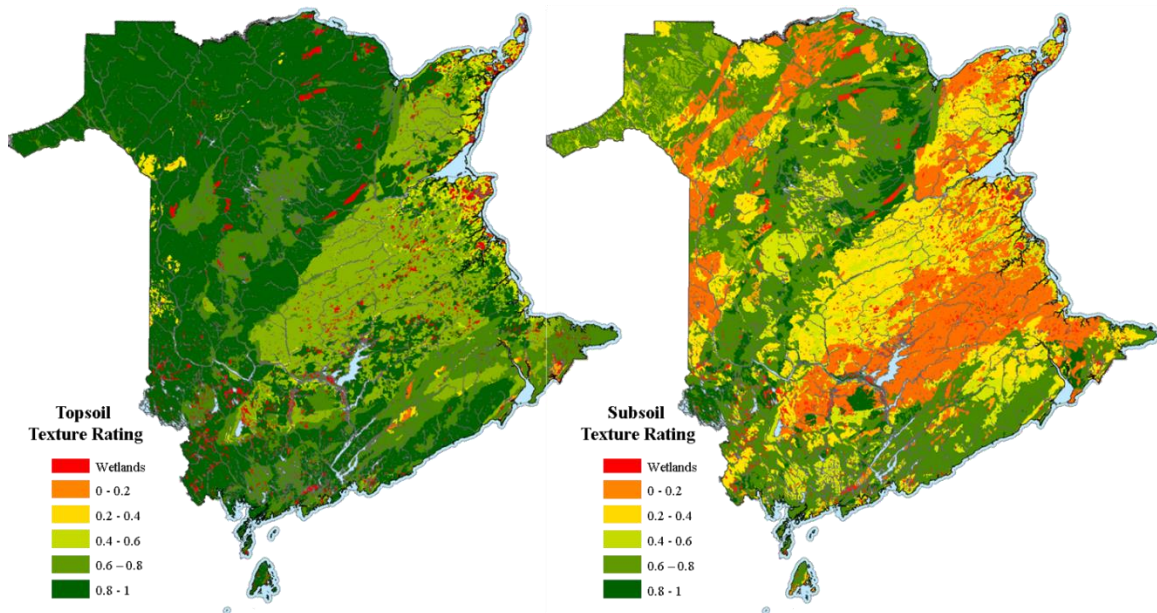


Figure 2.5. Topsoil (left) and subsoil (right) rating for potato crop suitability mapping across NB, by soil association polygons. Sources: GeoNB; Colpitts et al. (1995).

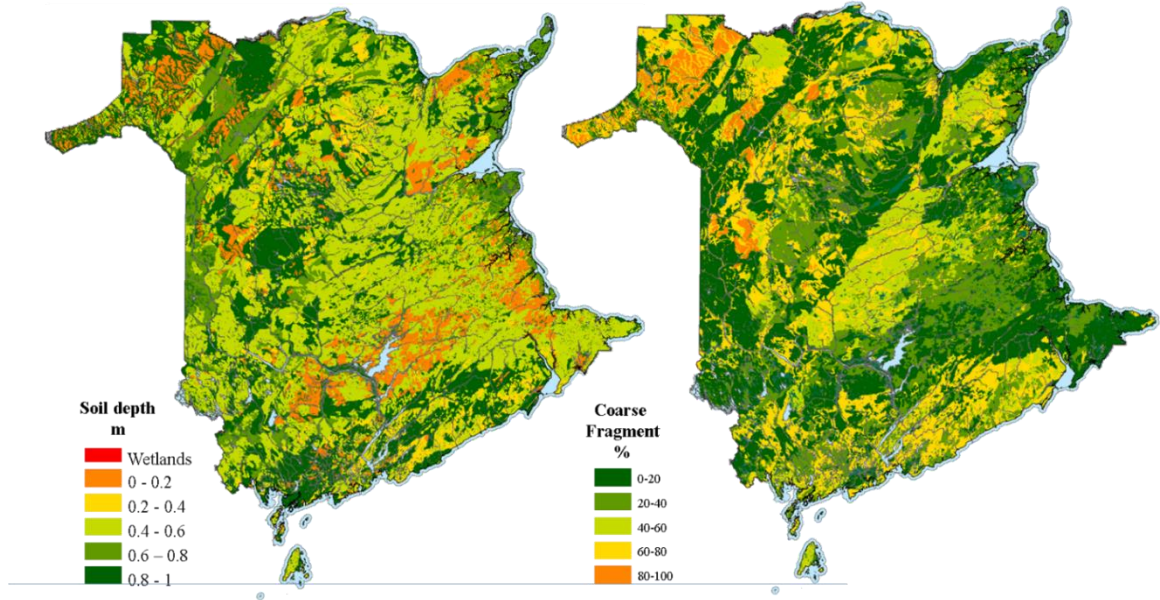


Figure 2.6. Soil depth (m, left) and soil CF (% , right) rating for potato crop suitability mapping across NB, by soil association polygons. Sources: GeoNB; Colpitts et al. (1995).

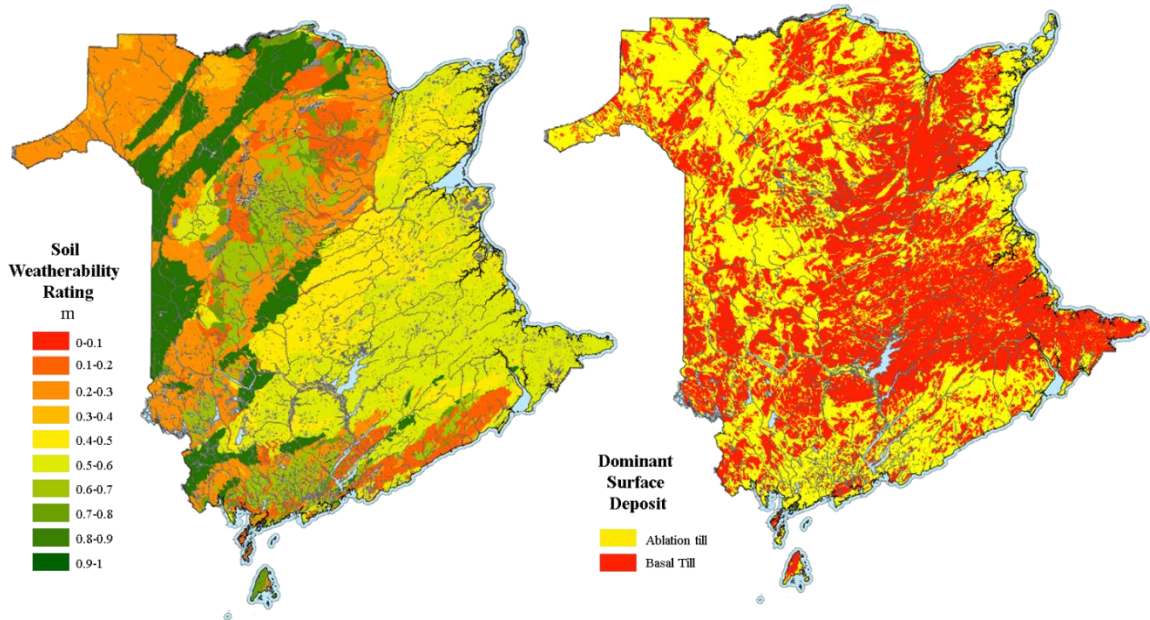


Figure 2.7. Soil weatherability (m, left) for crop suitability mapping and overall distribution of glacial ablation versus basal till (right) across NB. Sources: GeoNB; Colpitts et al. (1995).

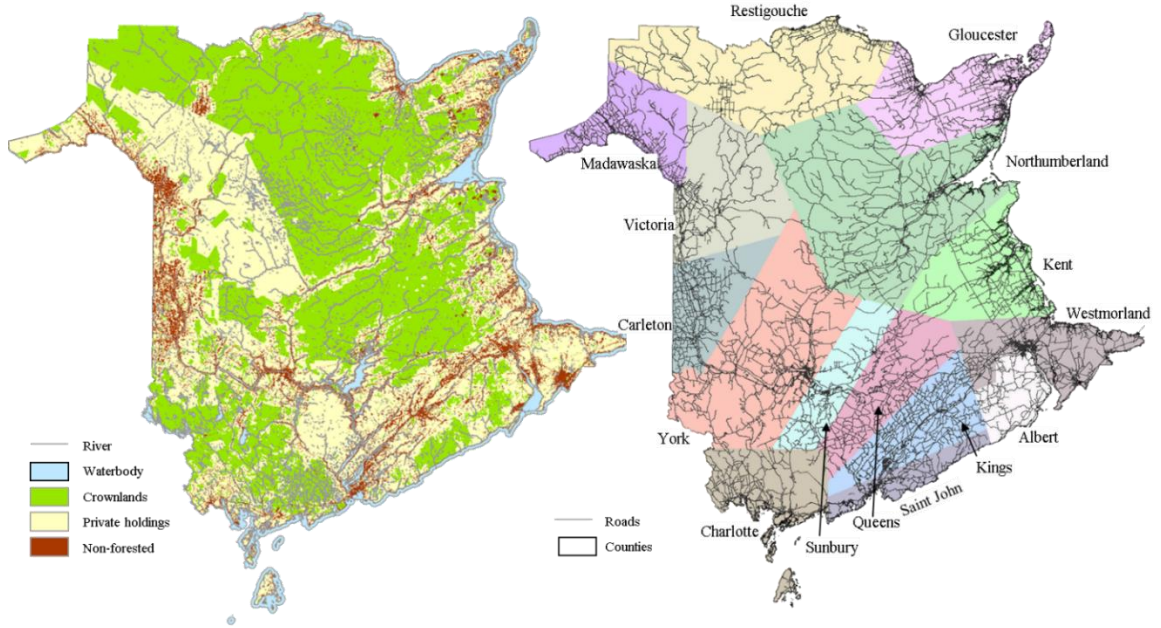


Figure 2.8. Mapping the distribution of crownlands, and of non-forested areas across NB, also showing water bodies and lakes (left), and roads overlaid on NB's counties (right). Source: GeoNB.

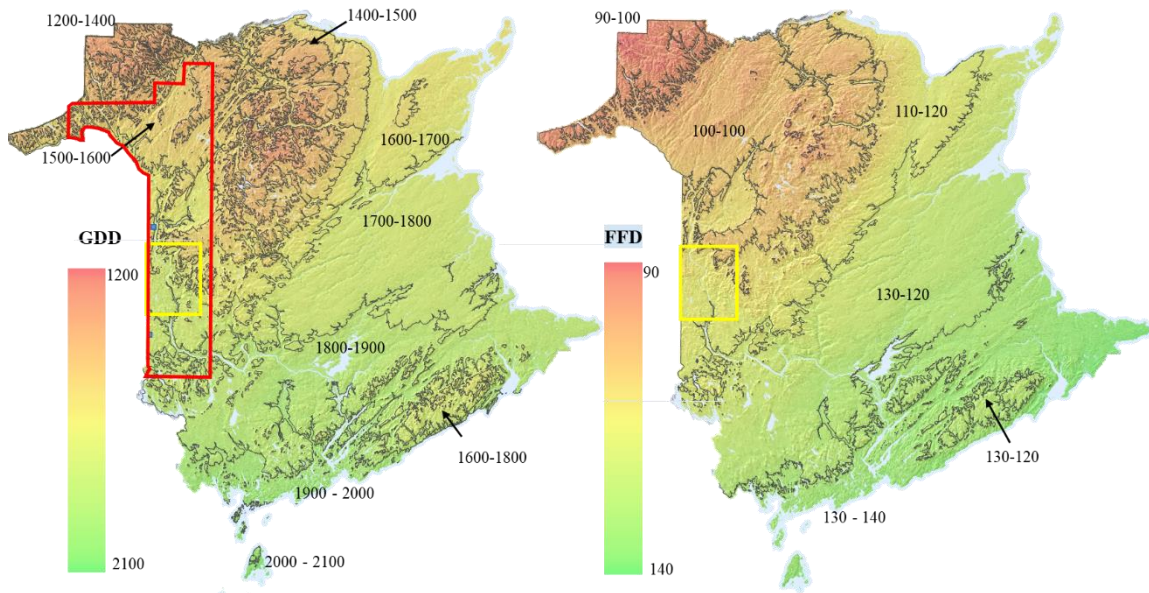


Figure 2.9. GDDs (left) and FFDs (right) across NB, generated from geospatially interpolating weather-station recorded air temperature data, extrapolated by elevation. Sources: UNB Forest Watershed Centre; Furze (2018).

### 2.2.3. Crop Suitability Mapping by Soil Association

**By soil texture.** While potato crops can be grown in differently textured soil, they grow best in well-drained sandy loams and other loam-containing soils (Rees et al., 2011; Redulla et al., 2002). Clay containing soils (i.e., sandy clay loam, clay loam, and clay) are not recommended because fine-textured soils are easily compacted. This compaction would result in poor soil aeration followed by potato rot when moist to wet. Across NB, soil textures vary primarily by mode of geological surface deposition. Basal tills as well as lacustrine to marine deposits tend to produce fine-textured soil whereas ablation till, riparian and glaciofluvial deposits tend to be coarse textured. Among these, ablation and basal tills together with their combinations of ablation till on top of basal till are prevalent.

**By CF.** CF refer to gravel, cobbles, stones, and boulders from smallest < 2 millimeters (mm) to largest. Where possible, large CF should be removed from fields to facilitate seedbed preparations and potato harvesting. Additionally, CF removal increases the soil availability for rooting, improves water filtration thereby reducing surface runoff and erosion, decreases heat conduction and related day-and-night soil temperature extremes, and minimizes tuber injuries during harvesting (Chow et al., 2007).

**By soil depth.** Potatoes will not root into firm to very firm soil. Restrictions in soil-related rooting depth are encountered on traffic compacted or naturally compacted soils, such as fine-textures lacustrine and marine deposits and basal tills. Moderate rooting restrictions occur on basal tills overlain by ablation till. Lowest restrictions are associated with deep ablation tills, outwash plains, and sandy deposits along riverbanks and well-drained floodplains.

**By calcareousness.** Soil parent materials containing limestones and/or calcareous siltstones, sandstones, mudstones, and slates generally improve and maintain good soil qualities in terms of elevated pH, increased exchangeable Ca and magnesium (Mg) contents, reduced soil acidity, and enhanced Ca-soil aggregation, and particularly so on loamy and clay enriched soils.

**By soil crop suitability ratings combined.** The variations of the above soil properties across NB were reported and mapped by Colpitts et al. (1995) by soil association. The information so obtained was crop-suitability coded 0.1 from poor to 1 for best (Table 2.1). The extent of soil calcareousness was coded 0 (absent) to 1 (limestones) depending on the stated mineral mix of each soil association. Table 2.2 shows this rating by the forest soil-association mapping units, along with parent material lithology of and areal extent.

Table 2.1. Potato crop suitability rating by topsoil texture, subsoil texture, depth-to compaction of soil, CF content, and calcareousness.

Topsoil Texture		Subsoil Texture		Depth-to-Compaction		Coarse Fragments		Calcareousness			
<b>C</b>	0.6	<b>C</b>	0.6	<b>1</b>	0.1	<b>H</b>	0.1	<b>Cornhill</b>	0.1	<b>Carleton</b>	0.75
<b>C-M</b>	0.8	<b>C-M</b>	0.8	<b>1-2</b>	0.2	<b>M-H</b>	0.25	<b>Kennebecasis</b>	0.1	<b>Muniac</b>	0.75
<b>M-C</b>	1	<b>M-C</b>	1	<b>1-2/R</b>	0.2	<b>M</b>	0.5	<b>Parleeville/ Tobique</b>	0.1	<b>Thibault</b>	0.75
<b>M</b>	0.6	<b>M</b>	0.6	<b>1-3</b>	0.3	<b>L-H</b>	0.75	<b>Parry</b>	0.1	<b>Caribou</b>	1
<b>M-F</b>	0.3	<b>M-F</b>	0.3	<b>1-3/R</b>	0.3	<b>L-M</b>	0.75	<b>Salisbury</b>	0.1	<b>Siegas</b>	1
<b>F</b>	0.1	<b>F-M</b>	0.2	<b>2</b>	0.45	<b>L</b>	1	<b>Tracadie</b>	0.1	<b>Kedgwick</b>	1
				<b>F</b>	0.1			<b>2-3</b>	0.6	<b>Erb Settlement</b>	0.5
		<b>3</b>	0.8					<b>Saltsprings</b>	0.5	<b>Others</b>	0
		<b>3-4</b>	0.9								
		<b>3-4/R</b>	0.9								
		<b>4 or 2-3/</b>	0.9								
		<b>4</b>	1								

Texture code: [C = coarse, C-M = coarse-medium, M-C = medium-coarse, M= medium, M-F = medium-fine, F = fine]; Depth-to-compaction code: [1 = <= 30 cm, 2= 31-65 cm, 3 = 66-100 cm, 4 = > 100 cm, R = rock] Coarse fragment code: [H = high, M-H = medium-high, M = medium, L-H = low-high, L-M = low-medium, L = low].

Table 2.2. Forest soil units with soil rating, total hectare province-wide, and primary lithology of parent materials. Forest soil units within the study area (Figure 2.2) are bolded.

Forest soil units	Code	Soil Rating	Total Ha Province-Wide	Primary Lithology of Parent Materials
<b>Siegas</b>	SE	1	45,698	Argillaceous limestones. Minor limestones.
<b>Caribou</b>	CA	1	198,213	
<b>Undine</b>	UN	1	17,416	
<b>Kedgwick</b>	KE	1	94,304	Calcareous siltstones, calcareous sandstones and/or calcareous slates.
<b>Carleton</b>	CR	0.75	242,574	
<b>Thibault</b>	TH	0.75	214,897	
<b>Muniac</b>	MU	0.75	26,441	
Saltspings	SS	0.5	9,282	Grey calcareous mudstones and/or feldspathic to lithic sandstones. Minor polymictic conglomerates
Erb Settlement	EB	0.5	8,904	
<b>Salisbury</b>	SA	0.1	167,047	Red polymictic conglomerates, feldspathic to lithic sandstones and/or mudstones. Calcium carbonates presents
<b>Parry</b>	PR	0.1	155,879	
Cornhill	CH	0.1	23,771	
<b>Parleeville-Tobique</b>	PT	0.1	1743,501	
<b>Kennebecasis</b>	KN	0.1	20,616	

Tracadie	TD	0.1	33,923	in the cementing material.
<b>Holmesville</b>	HM	0	325,472	Metaquartzites, slates, metasiltstones, metaconglomerates and/or metawackes.
<b>Victoria</b>	VI	0	145,859	
<b>McGee</b>	MG	0	335,809	
<b>Glassville</b>	GE	0	193,900	
<b>Grand Falls</b>	GF	0	71,227	
Stony Brook	SB	0	466,591	Red mudstone (weathered). Minor grey-ed lithic-feldspathic sandstones, quartzose sandstones and/or polymictic conglomerates
Tracy	TR	0	53,942	
Harcourt	HT	0	531,746	
Becaguimec	BE	0	13,078	
Barrieau-Buctouche	BB	0	95,444	
Reece	RE	0	522,674	Grey lithic-feldspathic sandstones. Minor quartzose sandstones, polymictic conglomerates, quartz pebble conglomerates, and/or red mudstones.
<b>Sunbury</b>	SN	0	281,388	
Fair Isle	FA	0	63,650	
Riverbank	RI	0	148,791	
<b>Tetagouche</b>	TT	0	43,445	Mafic volcanic rocks, gabbros and/or diorites
<b>Kingston</b>	KI	0	63,546	
Mafic Volcanic	MV	0	106,595	
Tuadook	TU	0	142,527	Gneiss, granites, alkali granites, granodiorites and/or quartz diorites
Juniper	JU	0	245,307	
Big Bald Mountain	BD	0	48,283	
<b>Popple Depot</b>	PD	0	200,003	Felsic volcanic or mixed igneous rocks and/or felsic pebble conglomerates
<b>Jacquet River</b>	JR	0	100,974	
<b>Lomond</b>	LO	0	168,872	
<b>Gagetown</b>	GG	0	85,311	
<b>Long Lake</b>	LL	0	336,934	Metasedimentary rocks mixed with igneous rocks. [Igneous clasts 20-50 %]
<b>Britt Brook</b>	BR	0	233,494	
<b>Serpentine</b>	SP	0	41,033	
<b>Catamaran</b>	CT	0	117,735	Igneous rocks mixed with metasedimentary rocks. [Sedimentary clasts 20-50 %].
<b>Irving</b>	IR	0	121,426	
<b>Pinder</b>	PI	0	38,828	
<b>Rogersville</b>	RG	0	39,529	Grey-ed sandstones or mudstones mixed

				with igneous rocks. [Igneous clasts 20-50 %]
<b>Interval</b>	IN	0	45,185	Undifferentiated.
Acadia	AC	0	15,299	
Organic Soil	OS	0	235,644	
Mining Debris	MD	0	5,901	

**Overall soil suitability by soil association.** Assuming that the coded rate entries in Table 2.1 capture the soil-affected variations in potato cropping response, it is necessary to determine how these rates combine into a single potato crop suitability factor by soil association. To do this, it was decided that:

1. To multiply the ratings for topsoil and subsoil texture, rooting depth, and CF, i.e., similar to calculating the likely occurrence outcome of simultaneously occurring random events.
2. To add the calcareousness rating to the resulting multiplication product assuming that calcareousness is one third as important as the best combination of the other four variables.
3. To normalize the results so obtained by dividing this result with its maximum value.
4. To transform the normalized values so generated to obtain a linear 0.3 to 1 suitability progression across the range of soil associations. This was accomplished through 0.33 exponentiation.

The result of doing so generated Eq. 2.1:

$$R_{\text{Soil Association}} = \left[ \frac{R_{\text{Topsoil}} \times R_{\text{Subsoil}} \times R_{\text{Depth-to-Compaction}} \times R_{\text{Coarse Fragments}} + 0.33 \text{ Calcareousness}}{\max(R_{\text{Topsoil}} \times R_{\text{Subsoil}} \times R_{\text{Depth-to-Compaction}} \times R_{\text{Coarse Fragments}} + 0.33 \text{ Calcareousness})} \right]^{0.3} \quad \text{Eq. 2.1.}$$

Table 2.3. Potato crop suitability rating by soil association across NB.

Potato Crop Suitability Rating by Soil Association					
*Not adjusted by drainage, growing-degree days, frost-free days, or slope					
Glassville	0.30	Gagetown	0.62	Holmesville	0.79
Stony Brook	0.33	Saltsprings	0.63	Catamaran	0.79
Mafic Volcanic	0.34	Kingston	0.64	Grand Falls	0.79
Tetagouche	0.34	Parleeville Tobique	0.65	Juniper	0.79
Big Bald	0.35	Kennebecasis	0.65	Kedgwick	0.80
Mountain					
Harcourt	0.38	McGee	0.66	Jacquet River	0.81
Fair Isle	0.39	Irving	0.66	Muniac	0.81
Pinder	0.43	Erb Settlement	0.68	Parry	0.82
Serpentine	0.44	Barrieau-	0.70	Caribou	0.83
		Buctouche			
Acadia	0.44	Riverbank	0.70	Thibault	0.83
Cornhill	0.45	Victoria	0.71	Long Lake	0.84
Lomond	0.46	Popple Depot	0.72	Carleton	0.86
Reece	0.50	Salisbury	0.72	Tracy	0.86
Tracadie	0.52	Tuadook	0.74	Becaquimec	0.92
Sunbury	0.54	Siegas	0.77	Britt Brook	0.92
Rogersville	0.61	Undine	0.78	Interval	1.00

**Soil suitability mapping.** Applying the soil suitability rating in Table 2.2 province-wide required updating of GeoNB’s catalogued forest soils shapefile to conform to GeoNB’s waterbodies and wetland layers. This was done in ArcMap 10.7.1 using procedures dealing with:

1. Eliminating all waterbodies and wetlands features in the forest soil shapefile for NB.
2. Converting the resulting shapefile into a 5 m resolution raster with “no data” pixels at the forest-soil registered waterbodies and wetlands locations.
3. Systematically extending existing soil-association identified pixels into all their adjacent “no data” spaces.

4. Once completed, replacing the resulting pixels with GeoNB's identified waterbodies or wetlands pixels where needed, done through conditional raster calculations.
5. Converting the resulting raster into the updated soil association shapefile, followed by feature outline smoothing to reduce and/or eliminate their pixelated appearance.
6. Applying Eq. 2.1 using the shapefile field calculator to generate the province-wide crop suitability layer by soil association, with all of GeoNB's waterbodies and wetlands features in place, as shown in Figure 2.8.

#### **2.2.4. Crop Suitability Mapping by Soil Drainage and Slope**

The crop suitability mapping parts by DTW and slope was done using the 1 m resolution coverage for elevation across NB. For this, the slope was derived using the *Slope* tool in ArcMap 10.7.1 as steepest percent rise over distance among the eight-cardinal directions adjacent to each DEM pixel. The DTW layer as shown in Figure 2.4 was derived using the ArcMap 10.7.1 *Cost Distance* tool, with the delineated flow channel network marking DTW = 0 reference cells, and the slope percent raster used as the cost raster. The resulting DTW and slope rasters are shown in Figure 2.4. In detail, DTW refers to the distance between the soil surface and the water table associated with the nearest waterbody and the flow channel locations, as affected by slope. The flow channels were developed using the D8 algorithm that derives the r flow accumulation and flow network rasters from the depression filled DEM according to the pixel-determined flow directions. The resulting flow channels were subsequently classified to have no data for any pixels with > 4 ha upslope flow accumulation. This threshold generally equates to mapping the extent of permanent streams under open end-of-summer field conditions. This being so, end-of-

summer conditions for  $DTW < 0.1\text{m}$ ,  $0.1\text{ m} < DTW < 0.25\text{ m}$ ,  $0.25\text{ m} < DTW < 0.5\text{ m}$ ,  $0.5\text{ m} < 1\text{m}$ ,  $1\text{ m} < DTW \leq 10\text{ m}$ ,  $DTW > 20\text{ m}$  generally correspond to: very poor, poor, imperfect, moderately well, well and excessive soil drainage, respectively.

The 0 to 1 crop suitability rating function for DTW was estimated by setting:

$$R_{DTW} = a [1 - \exp(-b DTW)]^c \exp(-d DTW) \quad \text{Eq. 2.2}$$

with  $a = 1.065$ ,  $b = 3.5$ ,  $d = 0.03$ ,  $c = 4.8$

As illustrated in Figure 2.4 (left),  $R_{DTW}$  starts from 0 when  $DTW = 0$  (too wet) reaches a maximum at 1.5 m (sufficiently moist most of the time), and trails downward from there to about 0.5 m as DTW approached 20 m and beyond (becoming drier with increasing DTW towards the upper ridges).

The 0 to 1 crop suitability rating function for slope (%) was estimated by setting:

$$R_{\text{slope}} = 1 / \{1 + \exp[-3(\text{slope} - 10)]\} \quad \text{Eq. 2.3}$$

This slope rating equation uses slope = 10 % as the DEM-derived slope threshold for ensuring that if slope < 10 %, then:

1. Field operations pertaining to seedbed preparation, seeding, harvesting, etc. remain safe.
2. Soil erosion remains minimal. This threshold is modified by approaching slope = 10 % gradually from 8 % upwards, and leaving it gradually towards 12 % (Figure 2.4, right).

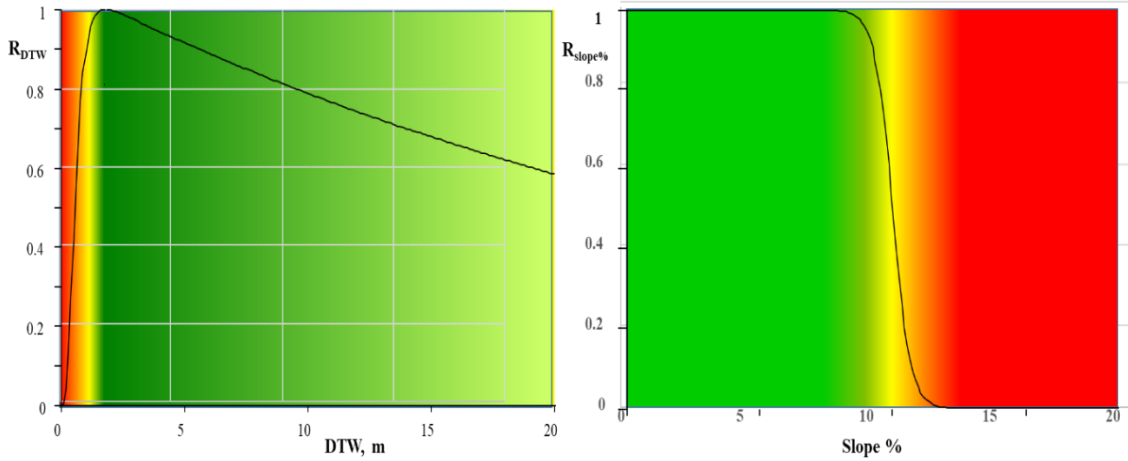


Figure 2.10. Potato crop rating specific to variations in DEM-derived DTW and slope %.

The overall soil-based crop suitability rating accommodates the DEM-captured DTW and slope variations by resetting Eq. 2.1 to Eq. 2.4. (i.e., with  $R_{DTW}$  and  $R_{Slope}$  as additional multiplication factors.

$$R_{Soil} = \left[ \frac{R_{Topsoil} \times R_{Subsoil} \times R_{Depth-to-Compaction} \times R_{Coarse\ Fragments} + 0.33\ Calcareousness}{\max(R_{Topsoil} \times R_{Subsoil} \times R_{Depth-to-Compaction} \times R_{Coarse\ Fragments} + 0.33\ Calcareousness)} \right]^{0.3} \times R_{DTW} \times R_{Slope\%} \quad \text{Eq. 2.4.}$$

### 2.2.5. Crop Suitability Mapping by Growing Degree Days and Frost-Free Days

In general, potatoes require about nine weeks (63 days) for full canopy development, and 18 weeks (126 days) to initiate senescence and thereby completing tuber growth (Figure 2.11). Late frost in spring affects foliage development. Early frost in fall affects tuber quality by tissue damaging. For example, early intermittent freezing leads to black external spots. FFDs generally exceed 100 days across NB except for the elevated areas in the northwest (Figure 2.9). This implies that the number of growing season days for potatoes is sufficiently long province-wide, with only minor FFD rating adjustments needed for the high elevation areas in the northwest.

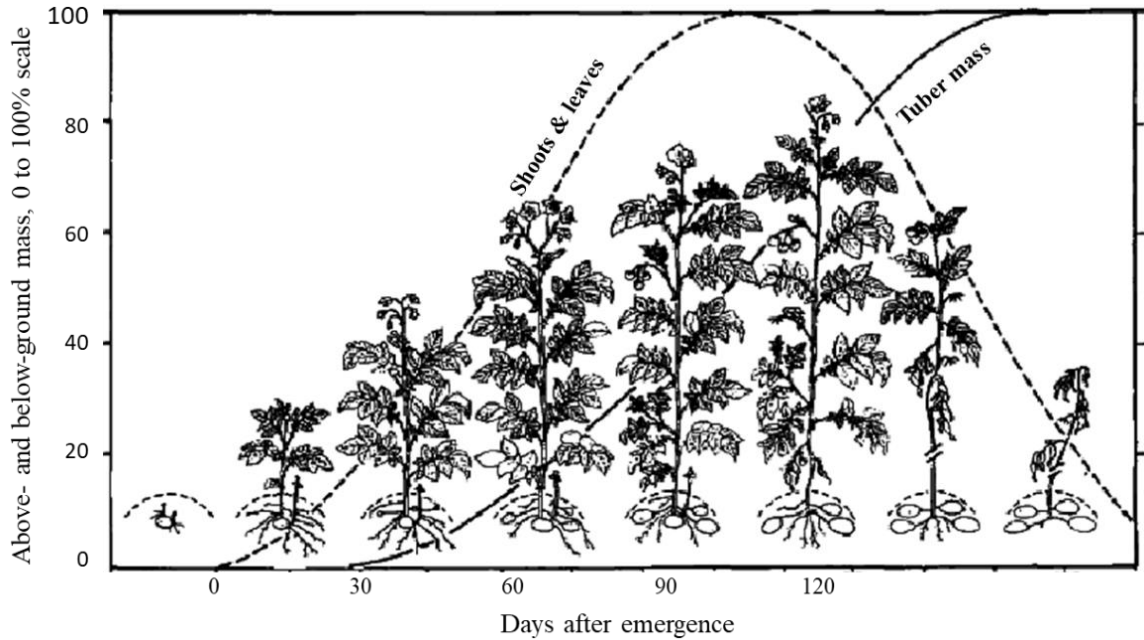


Figure 2.11. Percent extent of potato shoot, foliage, and tuber development by days after emergence. Source: Rosen & Bierman (2008).

In terms of GDDs, potatoes require about 1,000 and 1,500 GDDs from emergence to tuber initiation and harvesting (Figure 2.12). Across NB and according to Figure 2.9, GDDs range from 1400 to 2100, therefore potato cropping is essentially not climate restricted across NB except for the high elevation location in the northwest. Where conditions are suitable, GDDs > 1500 lead to additional tuber growth, particular for Russet potatoes (Figure 2.12).

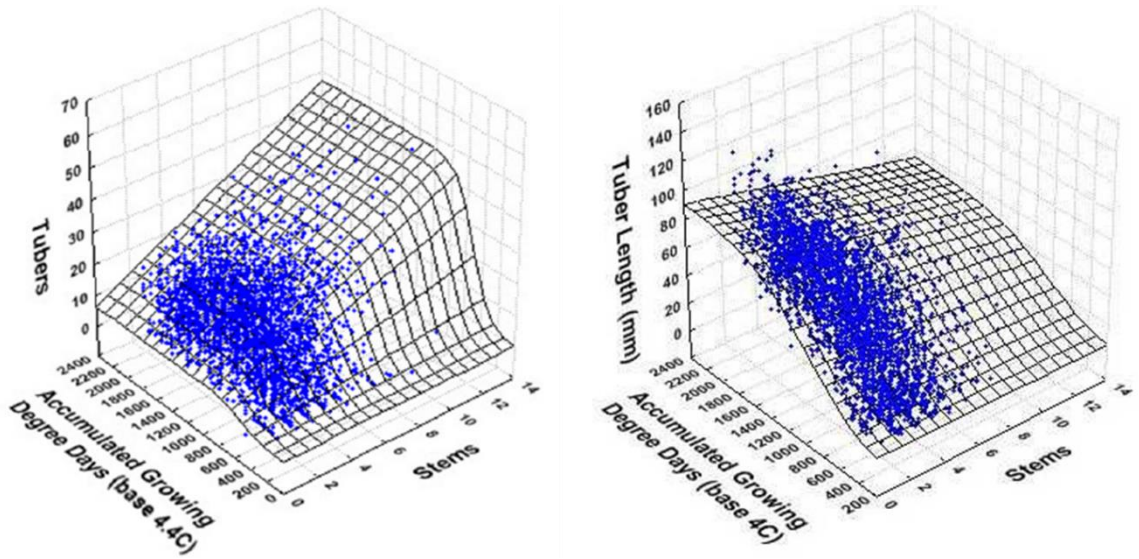


Figure 2.12. Russet potato tuber numbers and length in relation to the number of stems and increasing GDDs > 5 °C. Source: Goeser et al. (2012).

Accounting for increasing FFDs and GDDs benefits on potato suitability rating modifies Eq. 2.4 to Eq. 2.5:

$$R_{\text{soil \& Climate}} = R_{\text{soil}} \times R_{\text{GDD}} \times R_{\text{FFD}} \quad \text{Eq. 2.5}$$

with

$$R_{\text{FFD}} = 1 / [1 + \exp(-a_{\text{FFD}} (\text{FFD} - b_{\text{FFD}}))] \quad \text{Eq. 2.6}$$

and

$$R_{\text{GDD}} (\text{tuber length}) = 1/[1+\exp(-a_{\text{GDD}} (\text{GDD}-b_{\text{GDD}}))] \quad \text{Eq. 2.7}$$

Varying from 0 to 1 with increasing GDD and FFD values. Tentative,  $a_{\text{GDD}}$ ,  $b_{\text{GDD}}$ ,  $a_{\text{FFD}}$ , and  $b_{\text{FFD}}$  are set at 0.006, 1250, 0.1, and 100, respectively, with the result shown in Figure 2.13.

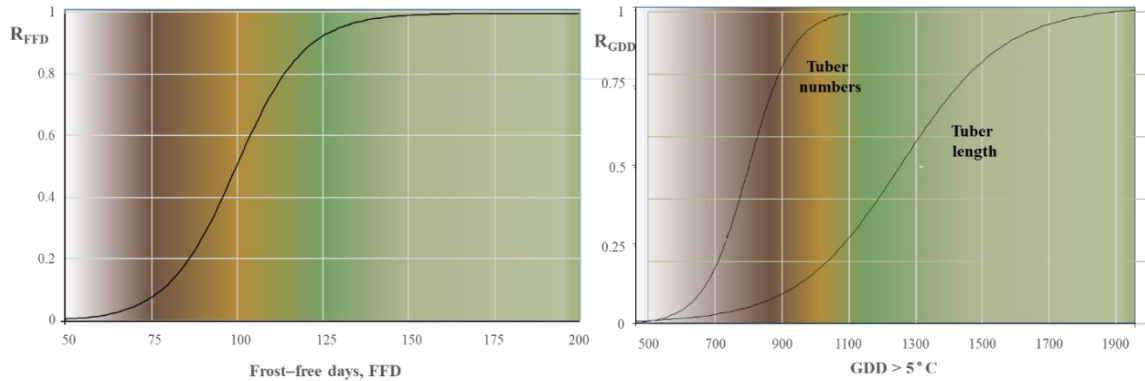


Figure 2.13. Increasing the rating for FFD and GDD as generated with Eq. 2.5, 2.6, and 2.7 marks the time available for potato cropping number of days within and across regions depending on local climate conditions.

### 2.2.6. Crop Suitability Mapping by Socioeconomic Factors

This thesis does not rate potato crop suitability within the context of socioeconomic realities such as distance to potato processing facilities and market but evaluates the outcome of these realities by examining the extent of farm- and woodland-based property taxation across NB. To this effect, farm and woodland tax assessment values - as listed for each property - were compared with the property-corresponding values for:

1. Mean crop suitability ratings.
2. Area (ha).
3. Footprint area of buildings (m<sup>2</sup>).
4. Binary variable coded 0 for farm fields properties only and coded 1 for farm and wood lands property combinations.

The data layers used to do this examination refer to:

1. The PID layer (Figure 2.3).
2. The soil, slope, DTW, and climate assessed potato crop suitability layers, as presented in Chapter 3.

3. GeoNB's building footprint layer.

The results for this socio-economic evaluation are described in Chapter 4.

### 2.3. Results

Figure 2.3 shows the potato crop suitability mapping results for the whole AOI. In Chapter 3, the results so obtained per PID will be discussed across the study area as a whole and per three subsections (Woodstock area, Hartland to Florenceville area, and the northern section above Florenceville).

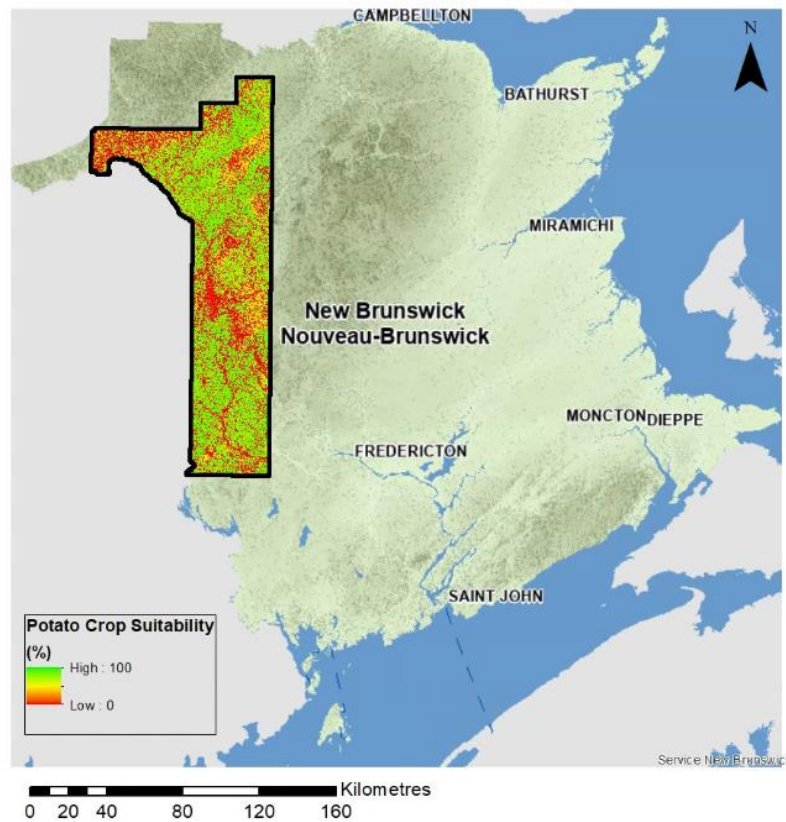


Figure 2.14 LiDAR-based potato crop suitability mapping results within the AOI (black boundary). Basemap source: GeoNB.

### 2.4. Discussion and Conclusion

The approach taken above differs from the literature on potato crop suitability mapping, as follows:

1. The approach makes use of high-resolution airborne 1 m LiDAR data. The preceding articles on potato suitability listed in Chapter 1 do this at significantly coarser resolution [Trigoso et al. (2017), Asfaw et al. (2017), Daccache et al. (2012), Yusianto et al. (2012), Wang et al. (2021), and Zhao et al. (2018)]. The province-wide GDD and FFD data layers as described above are elevation adjusted at LiDAR-DEM generated 10 m resolution. In contrast, Internet available GDD and FFD data layers are based on much coarser resolutions (e.g., Gridded 5 kilometre (km); National Centers for Environmental Information, 2022).
2. While GDDs and FFDs tend to decrease with increasingly northern latitudes, it appears that these variations- according to Figure 2.9 - remain within the feasible GDD and FFD ranges for potato cropping across NB, except on the high northwest elevations.
3. The above potato crop suitability analysis explicitly accounts for five soil characteristics that effect potato cropping fundamentally, i.e., subsoil and topsoil texture, CF content, depth-to-compaction of soil, and calcareousness. The corresponding literature-based soil selection listed in Table 1.1 range from eclectic to selective. For example, Trigoso et al. (2017) accounted for soil pH, OM, P, K, cation exchange capacity (CEC), and EC. Asfaw et al. (2017) used generalized soil type information from Selassie et al. (2014) and Kollias & Kalivas (1999) about pH, OM, total nitrogen (N), and available P in Ethiopian soils while Kollias & Kalivas (1999) provides soil information about slope, drainage, texture, carbonates, and erosion risk in Greek soils. Daccache et al. (2012) only accounted for soil

texture, OM, and soil structure. For establishing the potato suitability context over wide regions, Yusianto et al. (2020) dealt with soil texture only.

4. Socioeconomic factors can be included into the overall potato suitability rating scheme through location-specific add-on considerations. For NB, this would amount to assessing (i) the transportation costs from fields and farms to nearby processing facilities, (ii) the costs needed for upgrading existing fields or adjacent forested areas to enable potato cropping, and (iii) the costs required to establish new farms and processing facilities.

## 2.5. Literature Cited

- Asfaw, M., & Asfaw, D. 2017. Agricultural Land Suitability Analysis for Potato Crop by Using GIS and Remote Sensing Technology, in the Case of Amhara Region, Ethiopia. *Journal of Biology, Agriculture and Healthcare*, 7, 5-16.
- Chow, T. L., Rees, H. W., Monteith, J. O., Toner, P., & Lavoie, J. 2007. Effects of coarse fragment content on soil physical properties, soil erosion and potato production. *Canadian Journal of Soil Science*, 87(5), 565–577.
- Colpitts, M. C., Fahmy, S. H., MacDougall, J. E., Ng, T. T. M, McInnis, B. G., & Zelazny, V. F. 1995. Forest Soils of New Brunswick. Retrieved from [https://www2.gnb.ca/content/dam/gnb/Departments/nrrn/pdf/en/Publications/forest\\_soils\\_of\\_NB-e.pdf](https://www2.gnb.ca/content/dam/gnb/Departments/nrrn/pdf/en/Publications/forest_soils_of_NB-e.pdf).
- Daccache, A., Keay, C., Jones, R. J. A., Weatherhead, E. K., Stalham, M. A., & Knox, J. W. 2012. Climate change and land suitability for potato production in England and Wales: Impacts and adaptation. *The Journal of Agricultural Science*, 150(2), 161-177.
- Furze, S. 2018. *A high-resolution digital soil mapping framework for New Brunswick, Canada* [PhD Thesis, University of New Brunswick].
- GeoNB. n.d. Website: <http://www.snb.ca/geonb1/>.
- Goeser, N. J., Mitchell, P. J., Esker, P. D., Curwen, D., Weis, G., & Bussan, A. J. 2012. Modeling Long-Term Trends in Russet Burbank Potato Growth and Development in Wisconsin. *Agronomy*, 2(1), 14-27.
- Government of New Brunswick. 2018. Agriculture Site Suitability. Retrieved from <https://www2.gnb.ca/content/gnb/en/departments/10/agriculture/content/agriculture-suitability.html>.
- Jong, Q. B., Gameda, R., Huffman, S., Neilsen, T., Desjardins, D., Wang, R., Mcconkey, H.B.G. 2013. Impact of climate change scenarios on Canadian agroclimatic indices. *Canadian Journal of Soil Science*, 93, 243-259.
- National Centers for Environmental Information. 2022. NOAA Monthly U. S. Climate Gridded Dataset (NCLimGrid). Retrieved from: <https://www.ncei.noaa.gov/access/metadata/landing-page/bin/iso?id=gov.noaa.ncdc:C00332>.
- Pedlar, J. H., McKenney, D. W., Lawrence, K., Papadopol, P., Hutchinson, M. F., & Price, D. 2015. A Comparison of Two Approaches for Generating Spatial Models of Growing-Season Variables for Canada. *Journal of Applied Meteorology and Climatology*, 54(2), 506-518.
- Redulla, C. A., Davenport, J. R., Evans, R. G., Hattendorf, M. J., Alva, A. K., & Boydston, R. A. 2002. Relating potato yield and quality to field scale variability in soil characteristics. *American Journal of Potato Research*, 79(5), 317–323.

- Rees, H. W., Chow, T. L., Zebarth, B. J., Xing, Z., Toner, P., Lavoie, J., & Daigle, J. L. 2011. Effects of supplemental poultry manure applications on soil erosion and runoff water quality from a loam soil under potato production in northwestern New Brunswick. *Canadian Journal of Soil Science*, 91(4), 595–613.
- Rosen, C. J., & Bierman, P. M. 2008. Potato yield and tuber set as affected by phosphorus fertilization. *American Journal of Potato Research*, 85(2), 110-120.
- Selassie, Y. G., Ayalew, G., Elias, E., & Getahun, M. 2014. Soil Characterization and Land Suitability Evaluation to Cereal Crops in Soil Characterization and Land Suitability Evaluation to Cereal Crops in Yigossa Watershed, Northwestern Ethiopia. *Journal of Agricultural Science* 6(5), 199-206.
- Trigoso, D. I., López, R. S., Briceño, N. B. R., López, J. O. S., Fernández, D. G., Oliva, M., Huatangari, L. Q., Murga, R. E. T., Castillo, E. B., & Gurbillón, M. Á. B. 2020. Land Suitability Analysis for Potato Crop in the Jucusbamba and Tincas Microwatersheds (Amazonas, NW Peru): AHP and RS-GIS Approach. *Agronomy*, 10(12), 1898.
- Kollias, V. J., & Kalivas, D. P. 1999. Land evaluation methodology and GIS for soil resource management. Example with cotton crop in Greece. *Agronomie* 19(1999), 107-118.
- Wang, C., Shi, X., Liu, J., Zhao, J., Bo, X., Chen, F., & Chu, Q. 2021. Agriculture, Ecosystems and Environment Interdecadal variation of potato climate suitability in China. *Agriculture, Ecosystems and Environment*, 310, 107293.
- Yusianto, R., Dian, U., Semarang, N., Marimin, M., Suprihatin, S., & Hardjomidjojo, H. H. 2020. Spatial Analysis for Crop Land Suitability Evaluation: A Case Study of Potatoes Cultivation in Wonosobo, Indonesia. *South China University of Technology*. 313-319.
- Zhao J., Zhan X., Jiang Y., & Xu J. 2018. Variations in climatic suitability and planting regionalization for potato in northern China under climate change. *PLoS ONE* 13, 1–19.

## **CHAPTER 3: MAPPING RESULTS, QUALITATIVE EVALUATIONS**

### **3.1. Introduction**

This chapter evaluates and presents some of the potato crop suitability mapping results generated by the workflow processes detailed in Chapter 2 across the area as depicted in Figure 2.2 and detailed by soil association in Table 2.2. This was done for three areas: around Woodstock, Edmundston and Grand Falls (Figure 3.1), with property-specific examples for each area viewed in terms of hill-shaded DEM and recent satellite images with and without the resulting potato crop suitability layer overlaid. Also overlaid in these presentations are (i) the DEM-derived flow channels with > 4 ha upslope flow-accumulation areas and (ii) the GeoNB-catalogued wetlands, water bodies, roads, and PIDs. Subsequently, the potato crop suitability mapping examples so generated are compared with the corresponding clipped portions of the coarser-grained province-wide crop suitability map as provided by NB's DAAF.

The evaluation of the individual property pieces across the study area refers to separating each property by its agricultural field and forest components. This is done to determine the total areas and the average crop suitability rating for these two components. The hypothesis is that the agricultural field components have higher suitability ratings than the forest components.

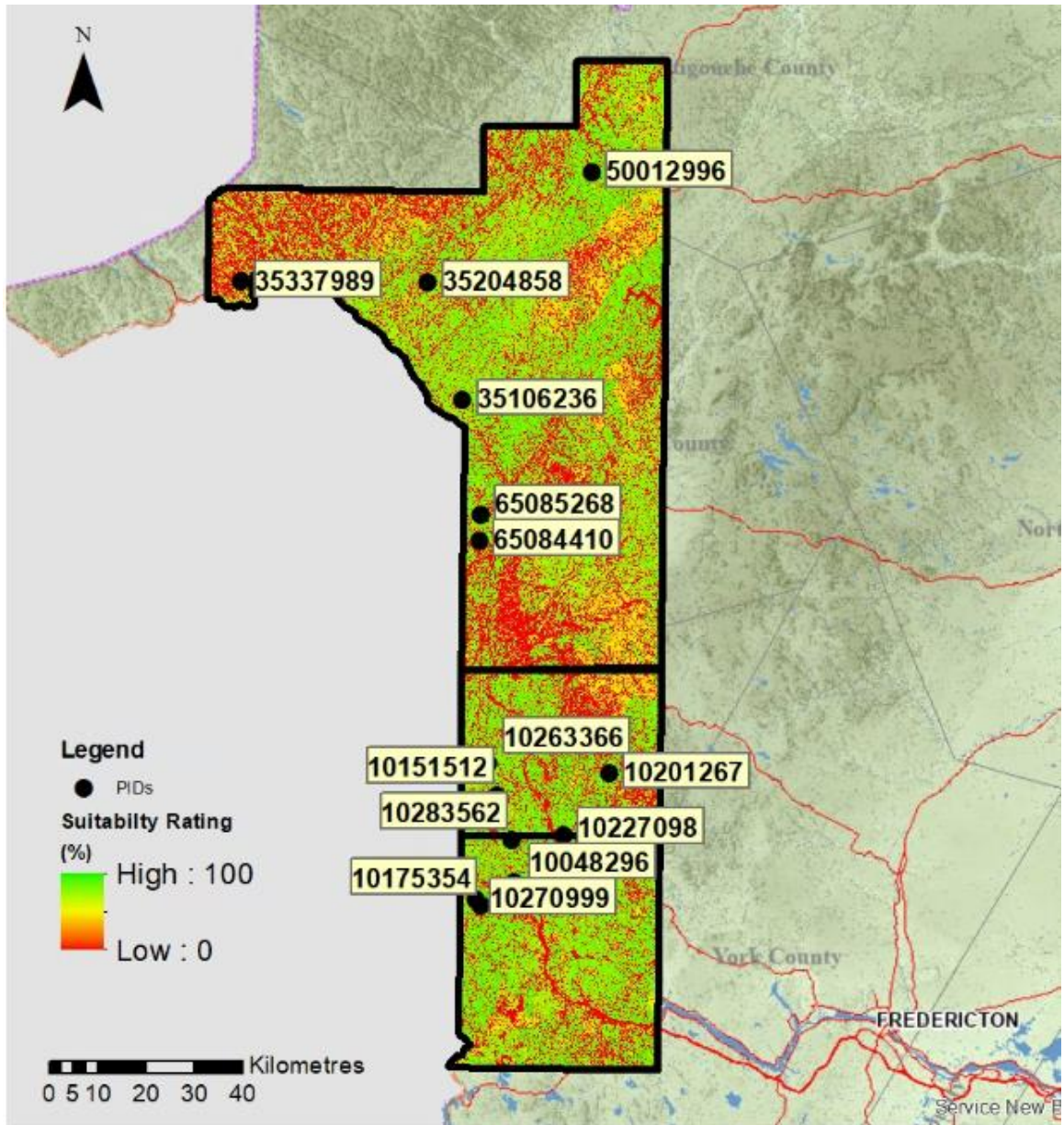


Figure 3.1. NB topographic map overlaid on the potato crop suitability (%) map within the study area within the AOI (black boundaries), with the locations of the field-based map examples for the Woodstock, Florenceville and northern NB sectors overlaid. Basemap source: GeoNB.

## 3.2. Methods

### 3.2.1. Qualitative Assessments

LiDAR-based potato crop suitability mapping was done according to workflow and procedures described in Chapter 2. Province-wide shapefiles referring to properties as well

as waterbodies, wetlands, and roads were obtained through GeoNB. These files were clipped to produce examples of property-based crop suitability examples by forested and agricultural field components (e.g., Figure 3.2) for the Woodstock (4 examples), Florenceville (4 examples) and northern NB (5 examples) areas. These examples contained the mask-extracted crop suitability raster overlaid on the (i) hill-shaded DEM and (ii) ESRI satellite images or georeferenced Google Earth images. This procedure was repeated to enable example-specific comparisons with the Chapter 2-generated and the coarser-grained on-line provincial potato site suitability maps (Government of New Brunswick, 2018).

### **3.2.2. Quantitative Assessment**

Basic statistics of the mean potato crop suitability (%), numbers of PANs, and total area of PANs (ha) by land class (farm, woodlot, and farm and wood combinations lands) and split by sections (Woodstock area, Hartland-Florenceville area, and Northwestern NB area) were generated to compare potato crop suitability across the AOI and by current land use. PANs were used instead of PIDs since it is possible to identify which properties contains both agricultural and forested components as opposed to PIDs.

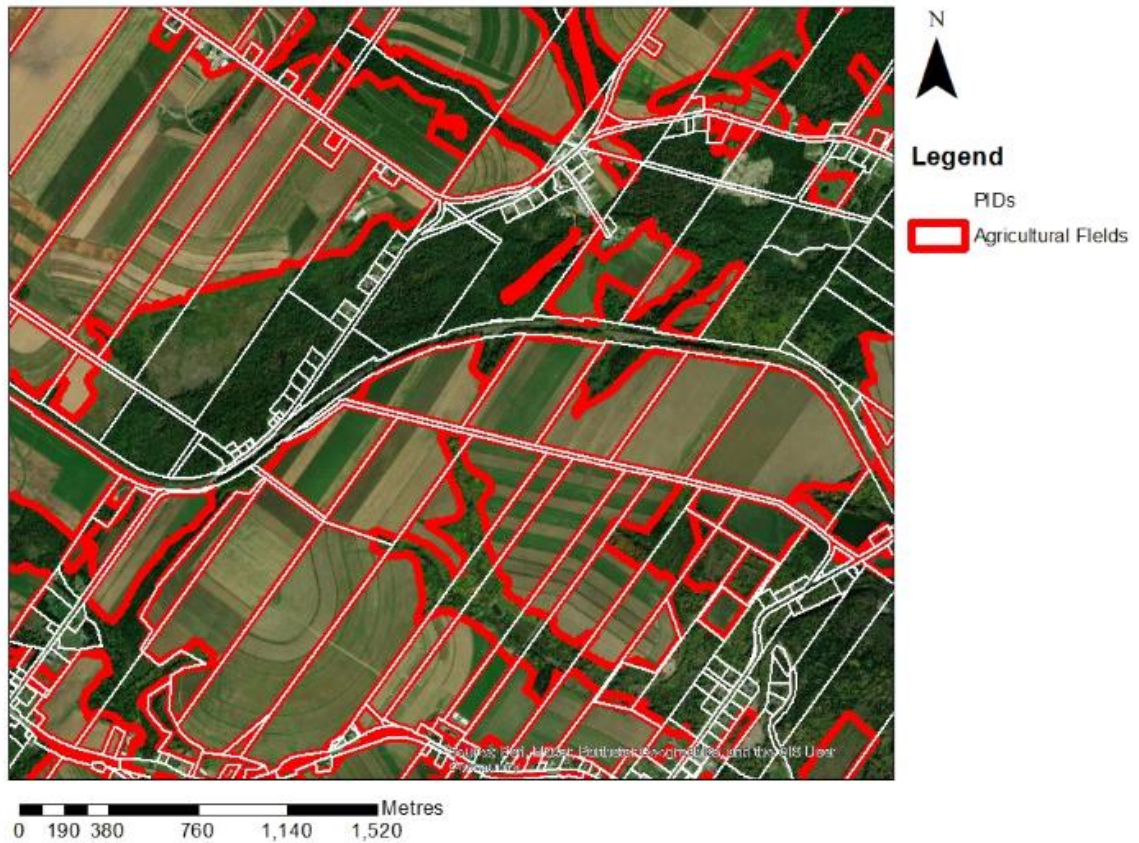


Figure 3.2. Close-up of an area within the AOI. World imagery with GeoNB-retrieved property outlines (“PIDs”, white borders) and their agricultural field components (red borders) overlaid. Basemap source: GeoNB.

### 3.3. Results

#### 3.3.1. Qualitative Assessment: Woodstock Area

Figure 3.3 shows the four locations of the crop suitability examples for the Woodstock area, overlaid on the forest soil association unit within this area, with close-ups shown in Figures 3.4, 3.5, 3.6, and 3.7.

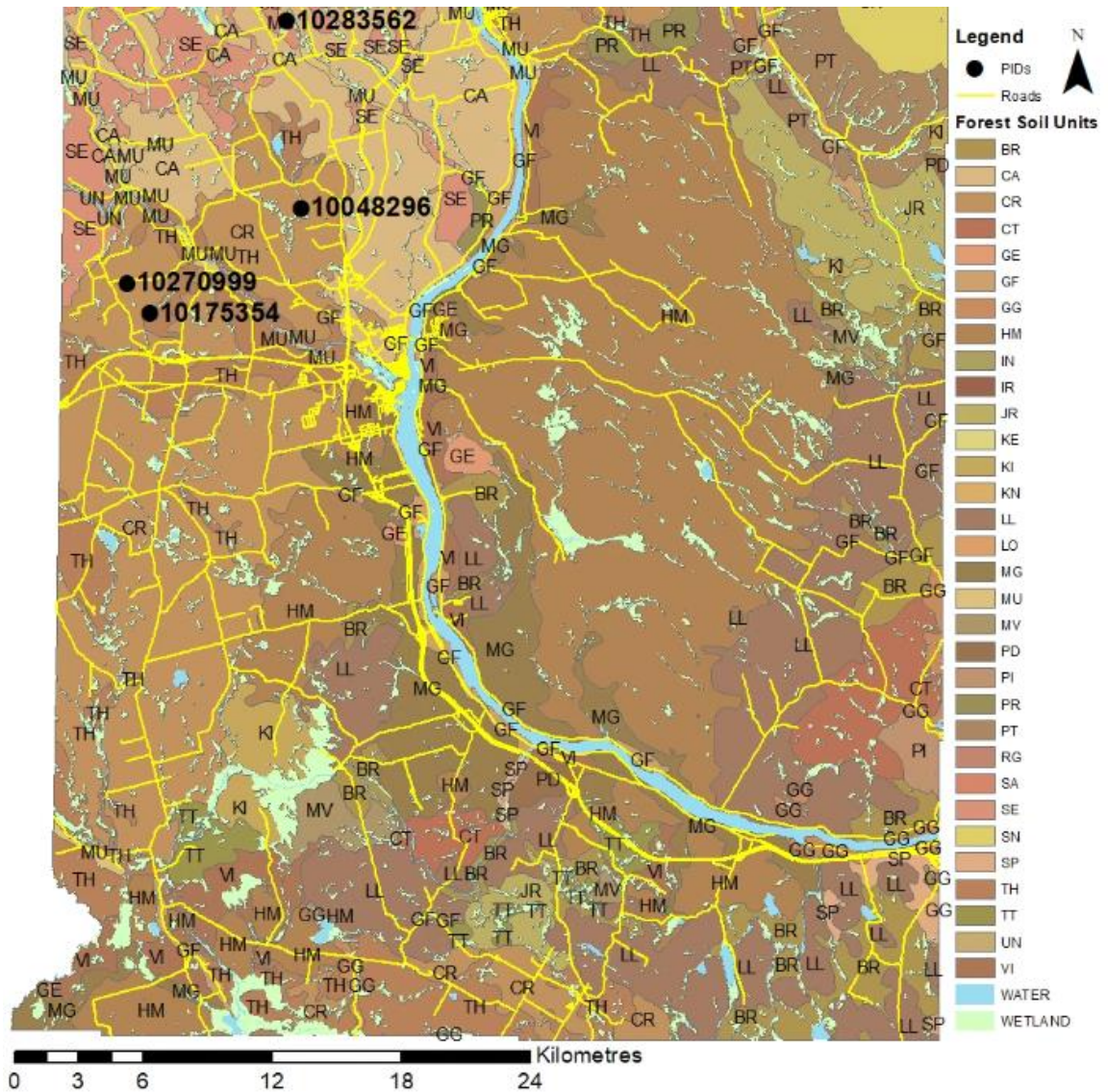


Figure 3.3. Locations of the crop suitability examples (PIDs 10283562, 10048296, 10270999, 10175354) within the Woodstock area, overlaid on the forest soil units for the area and roads (yellow lines). Source: Colpitts et al. (1995).

In detail, the PID 10048296 entry (84.50 ha) is located in Wakefield Parish (46°13'12.0"N 67°38'14.3"W). The underlying soil for this PID refers to CR, which is derived from calcareous siltstones, sandstones and/or slates. Figure 3.4 indicates poor to moderate potato crop suitability along the streams and associated wet areas with poor soil drainage. The steeper slopes are also categorized by poor crop suitability. Otherwise, most of the PID is deemed to be suitable for potato cropping, as is already the case for most of its eastern field portion.

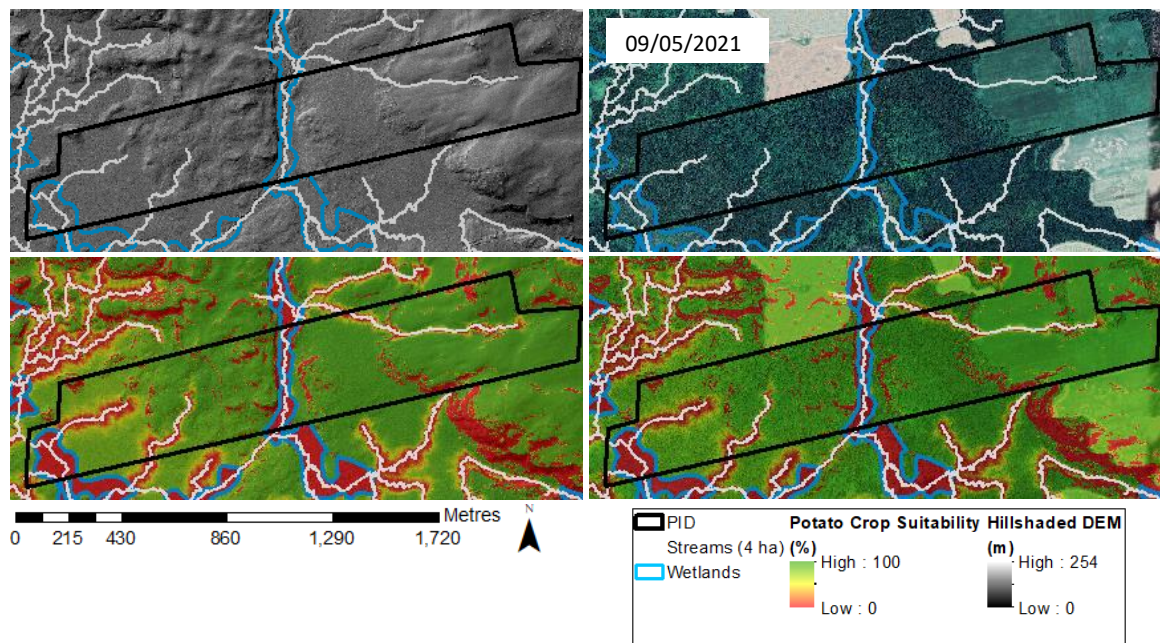


Figure 3.4. Images of PID 10048296 close-ups. From left to right, and from up to down: hillshaded DEM, hillshaded DEM with potato crop suitability (%) overlaid (layer transparency set to 50 %), satellite imagery, satellite imagery with potato crop suitability overlaid (layer transparency set to 50 %). All images also showing streams (4 ha), PIDs, roads, waterbodies, and wetland. Forest soil unit: CR. Basemap source: GeoNB. Potato crop suitability varies from 0 to 100 %, coloured from red through yellow to green, respectively.

Figure 3.5 shows close-ups of PIDs 10270999 (33.58 and 29.82 ha, north to south), located in Richmond Parish (46°11'14.8"N 67°44'30.8"W). The field also occur on CR soil. The satellite images indicate that the fields are highly suitable for potato cropping.

Exceptions occur along the mapped > 4 ha flow channels that run cross the fields. Three of these channels (southern PID, bottom left and middle, northern PID white line) run along image-detectable ditches.

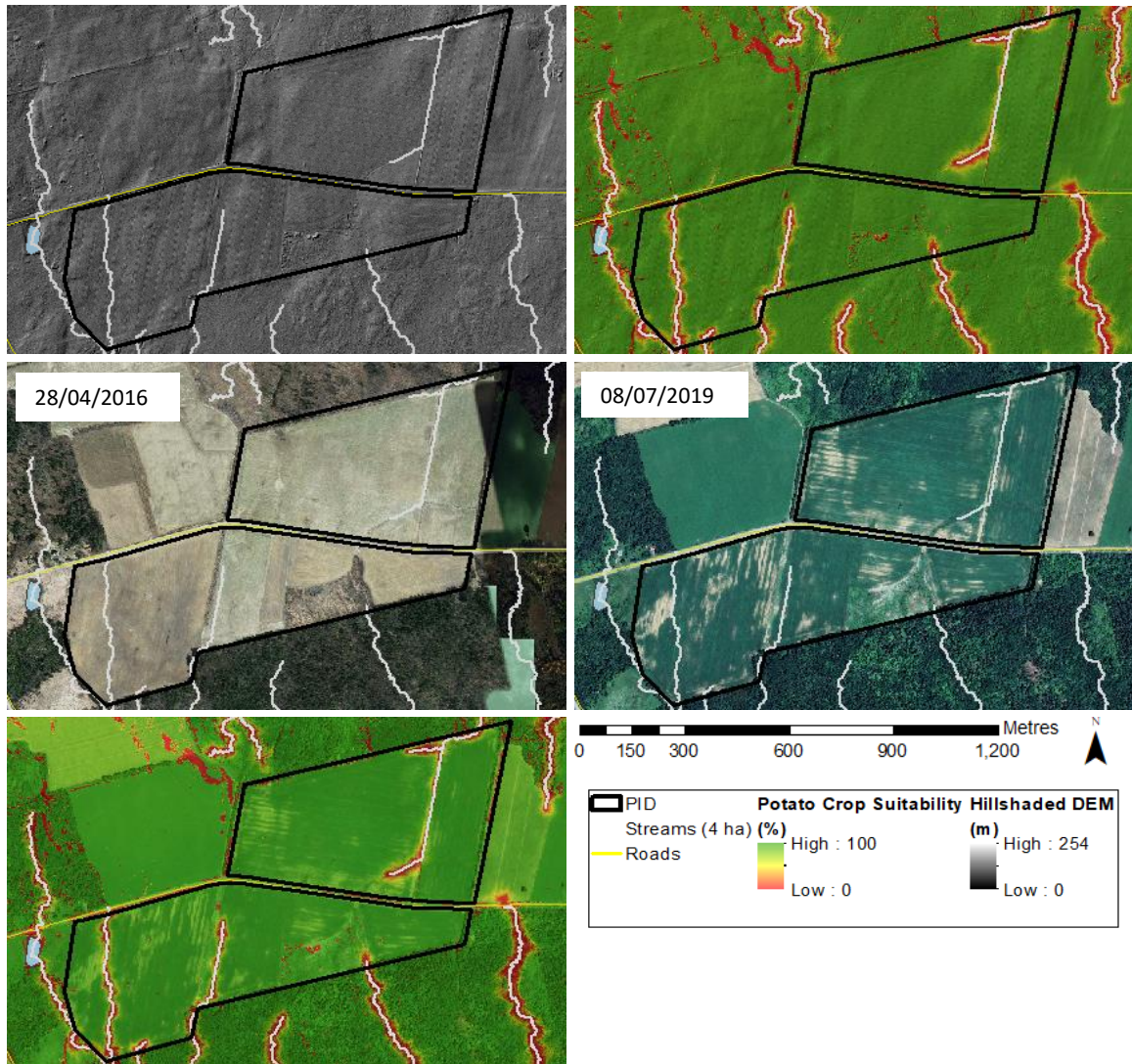


Figure 3.5. Images of PID 10270999 close-ups. From left to right, and from up to down: hillshaded DEM, hillshaded DEM with potato crop suitability (%) overlaid (layer transparency set to 50 %), satellite imagery, satellite imagery with potato crop suitability overlaid (layer transparency set to 50 %). All images also showing streams (4 ha), PIDs, roads, waterbodies, and wetland. Forest soil unit: CR. Basemap source: GeoNB. Potato crop suitability varies from 0 to 100 %, coloured from red through yellow to green, respectively.

Figure 3.6 shows close-ups of PID 10175354 (61.14 ha), located in Richmond Parish ( $46^{\circ}10'30.4''N$   $67^{\circ}43'38.9''W$ ). This PID occurs on calcareous CR and TH soils. Due to the steep slope conditions this forested PID is not suitable for potato cropping.

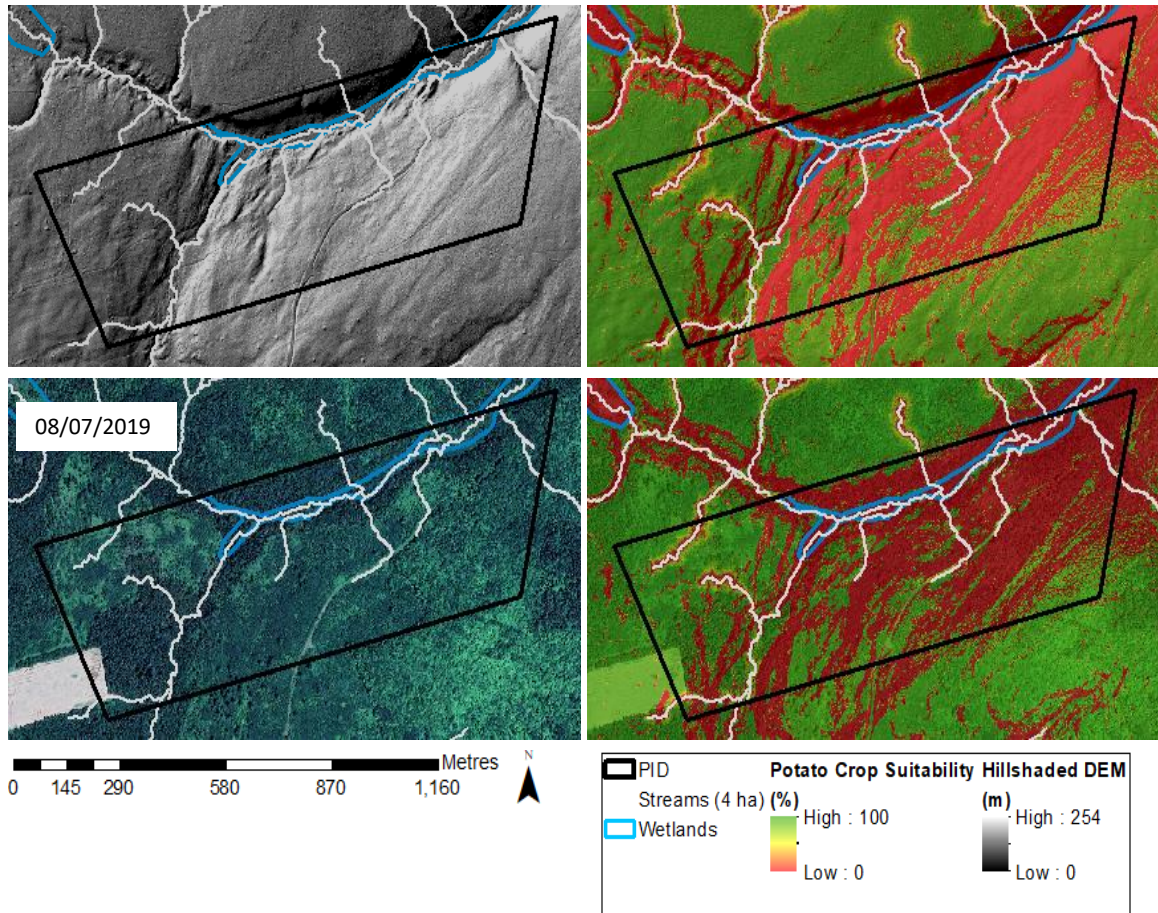


Figure 3.6. Images of PID 10175354 close-ups. From left to right, and from up to down: hillshaded DEM, hillshaded DEM with potato crop suitability (%) overlaid (layer transparency set to 50 %), satellite imagery, satellite imagery with potato crop suitability overlaid (layer transparency set to 50 %). All images also showing streams (4 ha), PIDs, roads, waterbodies, and wetland. Forest soil units: CR and TH. Basemap source: GeoNB. Potato crop suitability varies from 0 to 100 %, coloured from red through yellow to green, respectively.

Figure 3.7 shows close-ups of PID 10283562 (113.66), located in Wilmot Parish ( $46^{\circ}17'53.0''N$   $67^{\circ}38'53.2''W$ ). This PID occurs on calcareous CA and SE soils. Potato crop suitability varies across this PID from unsuitable for the middle part on the flat area along

the main flow channel from west to east at near to suitable for the norther and southern parts. According to the historical Google Earth images, the northern part was forest cleared from west to east between 2017 and 2019, but with the forest portions within wet areas of this section remaining intact.

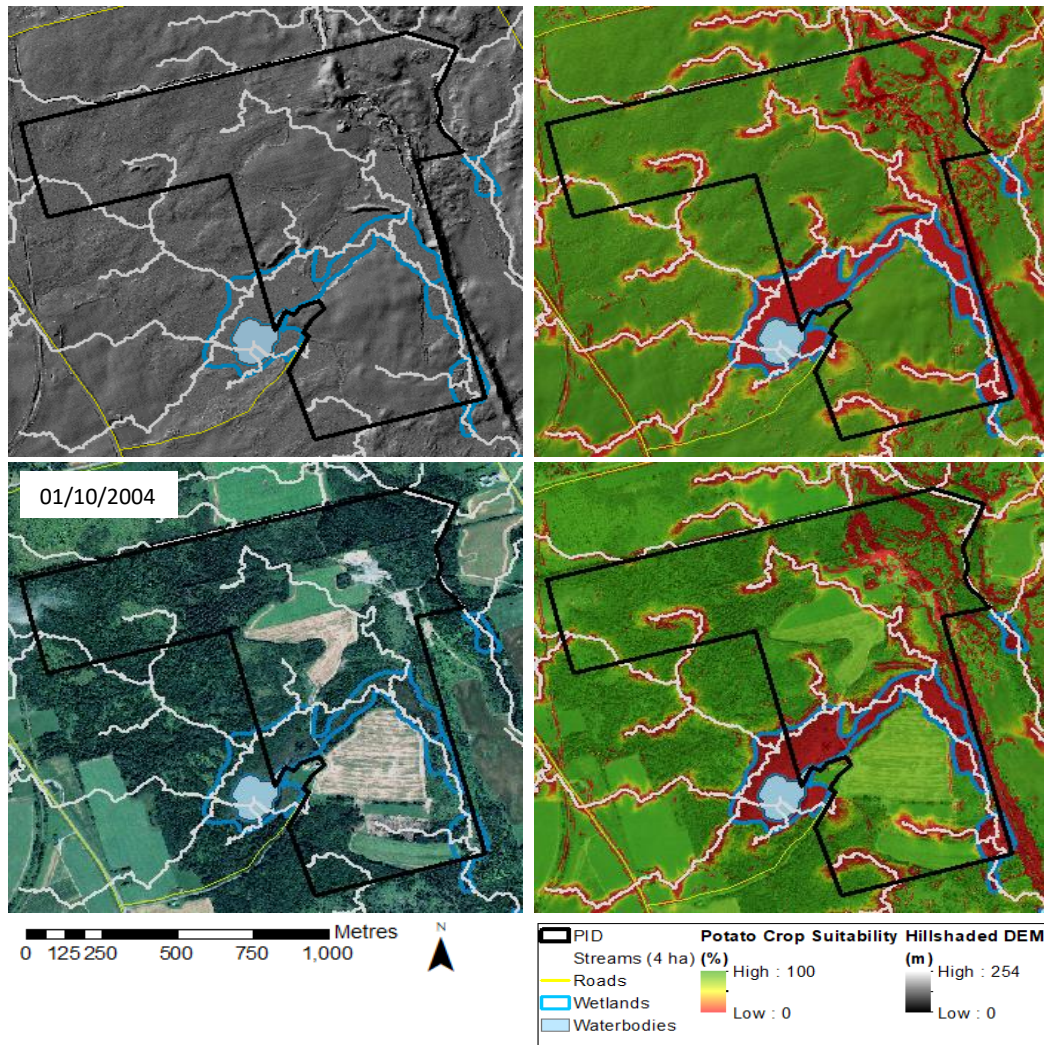


Figure 3.7. Images of PID 10283562 close-ups. From left to right, and from up to down: hillshaded DEM, hillshaded DEM with potato crop suitability (%) overlaid (layer transparency set to 50 %), satellite imagery, satellite imagery with potato crop suitability overlaid (layer transparency set to 50 %). All images also showing streams (4 ha), PIDs, roads, waterbodies, and wetland. Forest soil units: CA and SE. Basemap source: GeoNB. Potato crop suitability varies from 0 to 100 %, coloured from red through yellow to green, respectively.

### 3.3.2. Qualitative Assessment: Hartland-Florenceville Area

Figure 3.8 shows the four locations of the crop suitability examples for the Hartland-Florenceville area, overlaid on the forest soil association units within this area, with close-ups shown in Figures 3.9, 3.10, 3.11, and 3.17.

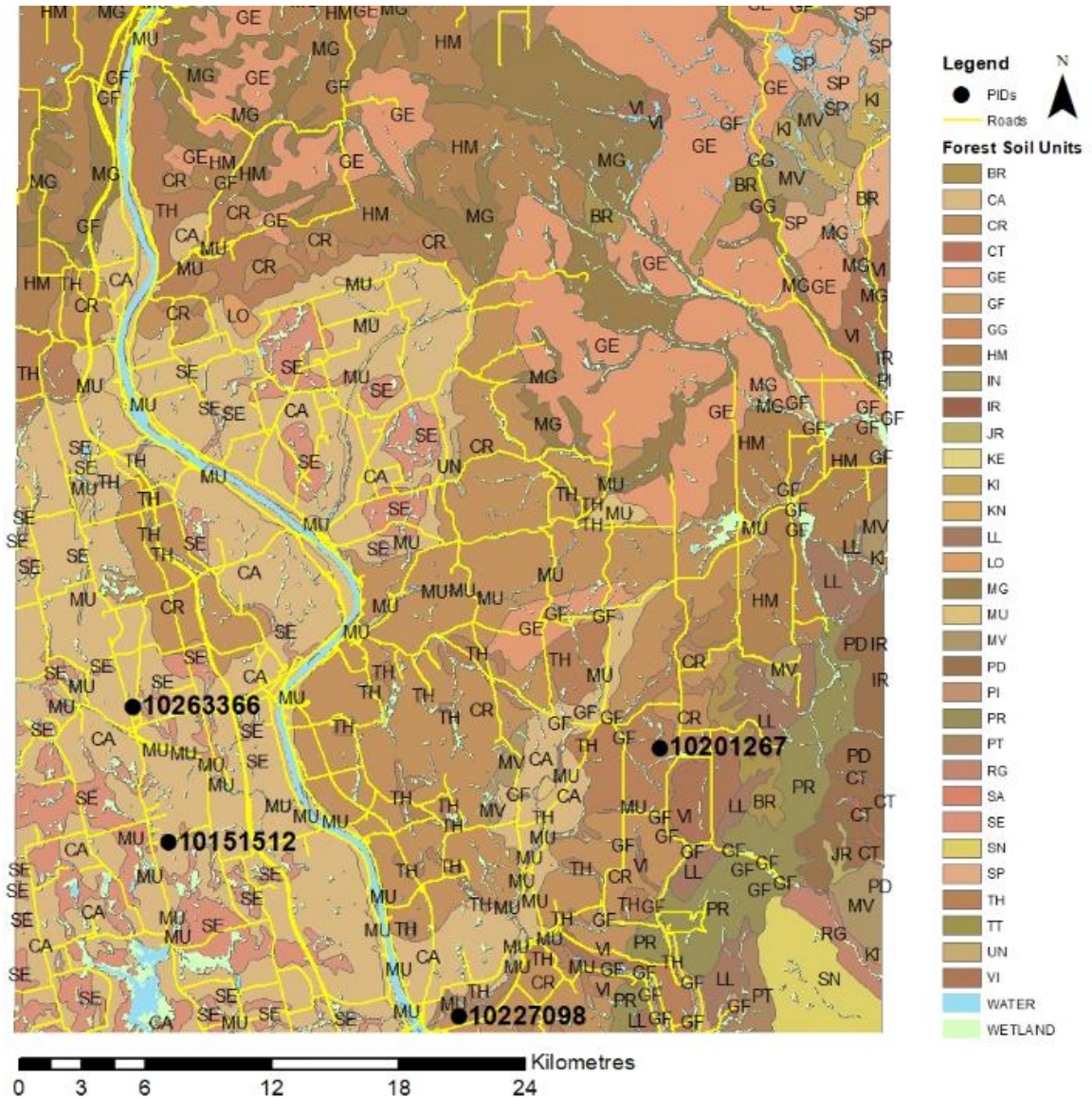


Figure 3.8. Locations of the crop suitability examples within the Hartland-Florenceville area, overlaid on the forest soil units for the area. Source: Colpitts et al. (1995). Yellow lines: roads.

In detail, Figure 3.9 shows a close-up collage of PID 10227098 (87.60 ha), located east of the Harland High School (46°18'30.11"N, 67°30'29.46"W). The PID occurs on CR soil. Along the less hummocky and less steeper portions, this parcel has been used for agricultural production since settlement, with the steeper and not suitable portions remaining forested. More details about this PID are presented in Chapter 6.

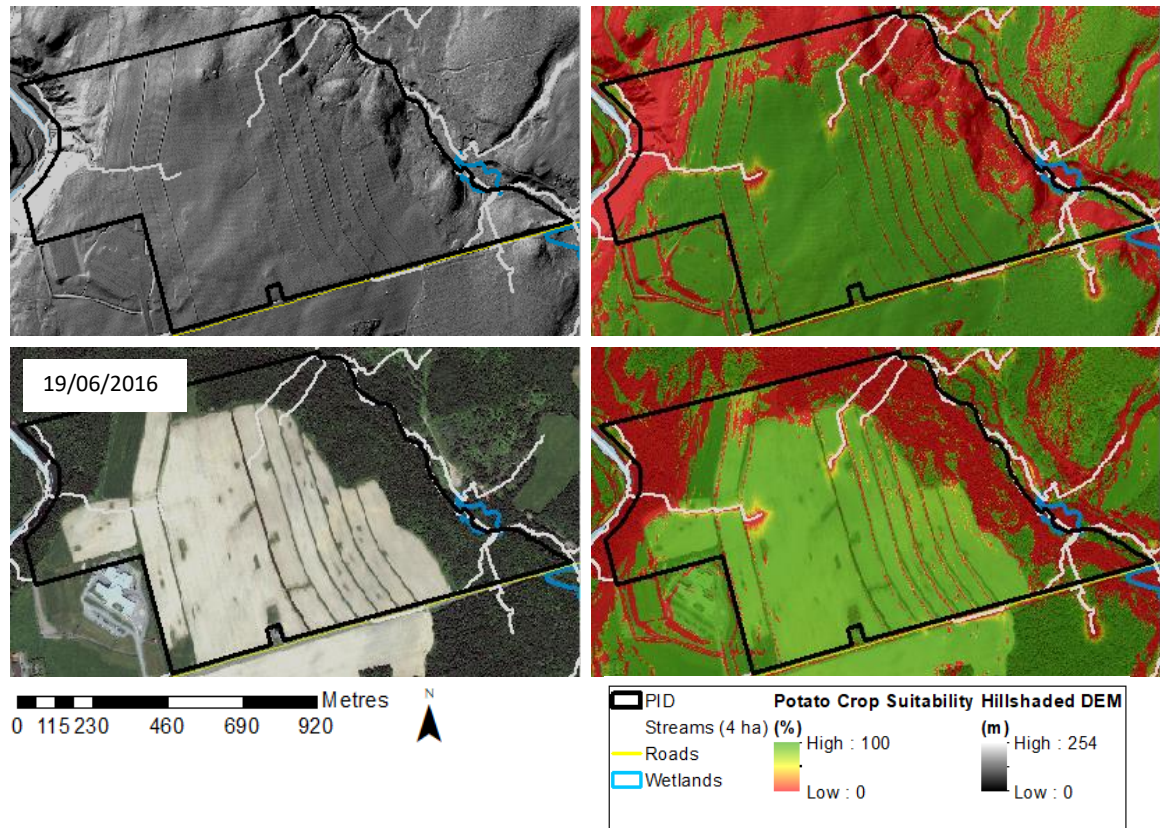


Figure 3.9 Images of PID 10227098 close-ups. From left to right, and from up to down: hillshaded DEM, hillshaded DEM with potato crop suitability (%) overlaid (layer transparency set to 50 %), satellite imagery, satellite imagery with potato crop suitability overlaid (layer transparency set to 50 %). All images also show streams with > 4 ha upslope flow accumulation areas, PIDs, roads, waterbodies, and wetland. Forest soil unit: CR. Basemap source: GeoNB. Potato crop suitability varies from 0 to 100 %, coloured from red through yellow to green, respectively.

Figure 3.10 shows a close-up collage of PID 10263366 (20 ha), located in Centreville (46°26'20.89"N, 67°42'43.14"W). The PID is on CA soil. The hillshaded DEM

reveals a smooth to hummock terrain which is mostly mapped to be suitable for potato cropping.

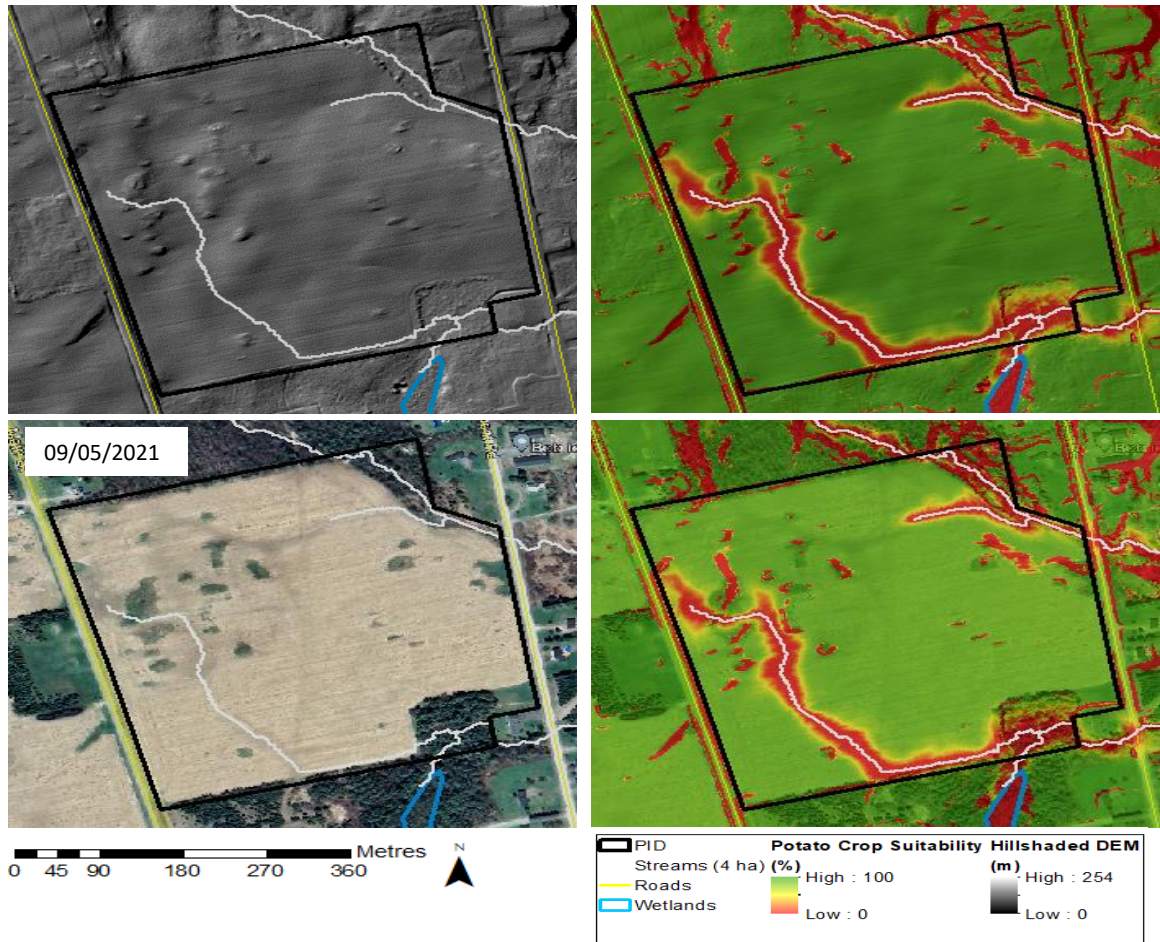


Figure 3.10. Images of PID 10263366 close-ups. From left to right, and from up to down: hillshaded DEM, hillshaded DEM with potato crop suitability (%) overlaid (layer transparency set to 50 %), satellite imagery, satellite imagery with potato crop suitability overlaid (layer transparency set to 50 %). All images also show streams with > 4 ha upslope flow accumulation areas, PIDs, roads, waterbodies, and wetland. Forest soil unit: CA. Basemap source: GeoNB. Potato crop suitability varies from 0 to 100 %, coloured from red through yellow to green, respectively.

The flow channels along the western part of this PID are mapped to have low crop suitability. Looking at the historical Google Earth images reveals a darkening of the surface colour towards this channel, thereby trending towards wetter and lower soil drainage conditions. Historically poor soil drainage along this channel may have been addressed by

installing subsoil drainage tiles. Along the northeastern portion, the PID remains in part forested. The portion of the forested area south of the PID is- for the most part - mapped to be potato-crop suitable.

Figure 3.11 shows a close-up collage of PID 10151512 (13.38 ha), located in Wilmot Parish ( $46^{\circ}22'54.8''\text{N}$   $67^{\circ}41'18.7''\text{W}$ ). The PID is located on CA soil. The southwestern forested part of the field is not suitable for potatoes due to hilly topography. In addition, there are parts mapped to be unsuitable near flow-channel location conditions. Looking at the historical images reveals that cropping took place across the non-forested portion of the field, but surface colouration within the May 2021 Google Earth image changed along the hill-shade revealed lower lying portions of this field.

Figure 3.12 shows close-up collage of PID 10201267 (36.03 ha), located in Brighton Parish ( $46^{\circ}25'30.0''\text{N}$   $67^{\circ}23'12.7''\text{W}$ ) on TH soil. Overall, this field is suitable for potato crops, expected for the small and steeply sloping forested area at its southern boundary and the small poorly-drained area around the stream located at the northern boundary. The flatter areas around this PID are also mapped to be suitable for potato cropping.

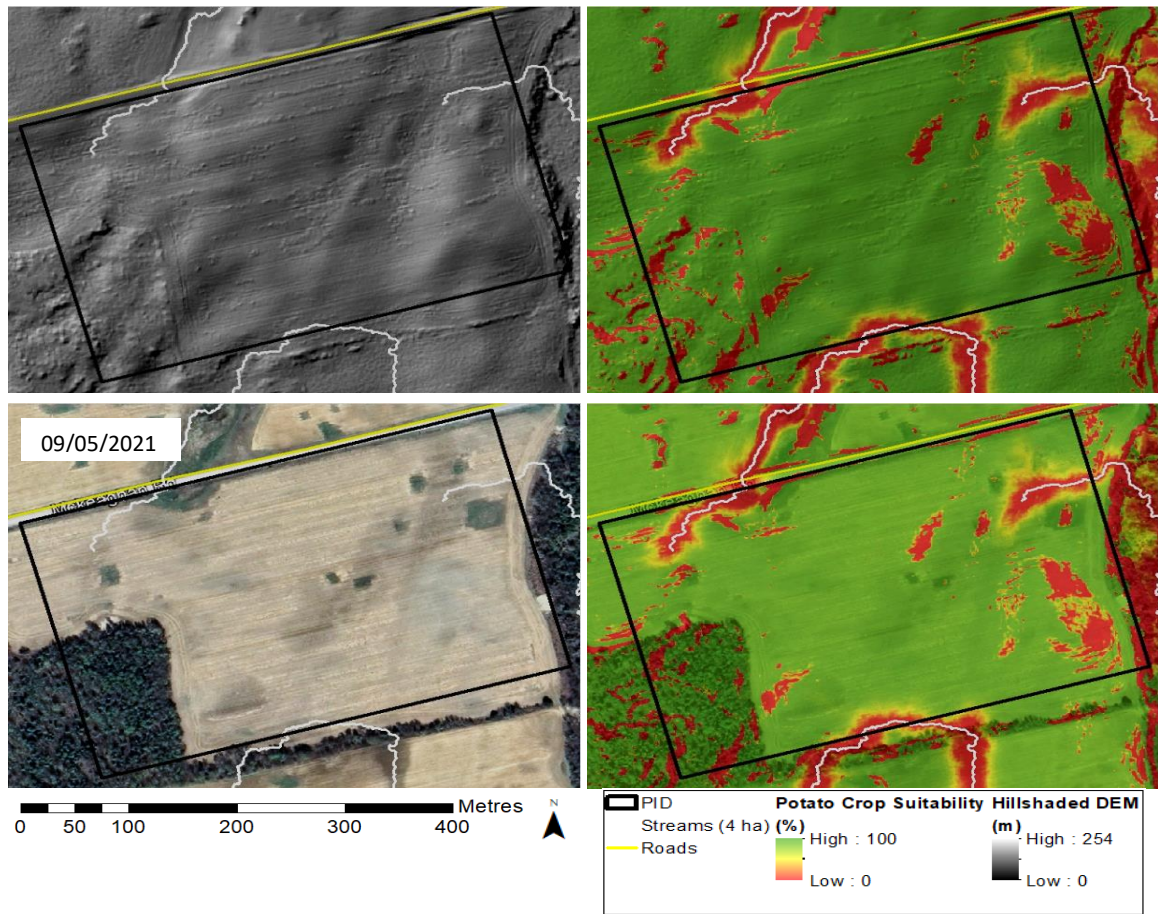


Figure 3.11. Images of PID 10151512 close-ups. From left to right, and from up to down: hillshaded DEM, hillshaded DEM with potato crop suitability (%) overlaid (layer transparency set to 50 %), satellite imagery, satellite imagery with potato crop suitability overlaid (layer transparency set to 50 %). All images also show streams with > 4 ha upslope flow accumulation areas, PIDs, roads, waterbodies, and wetland. Forest soil unit: CA. Basemap source: GeoNB. Potato crop suitability varies from 0 to 100 %, coloured from red through yellow to green, respectively.

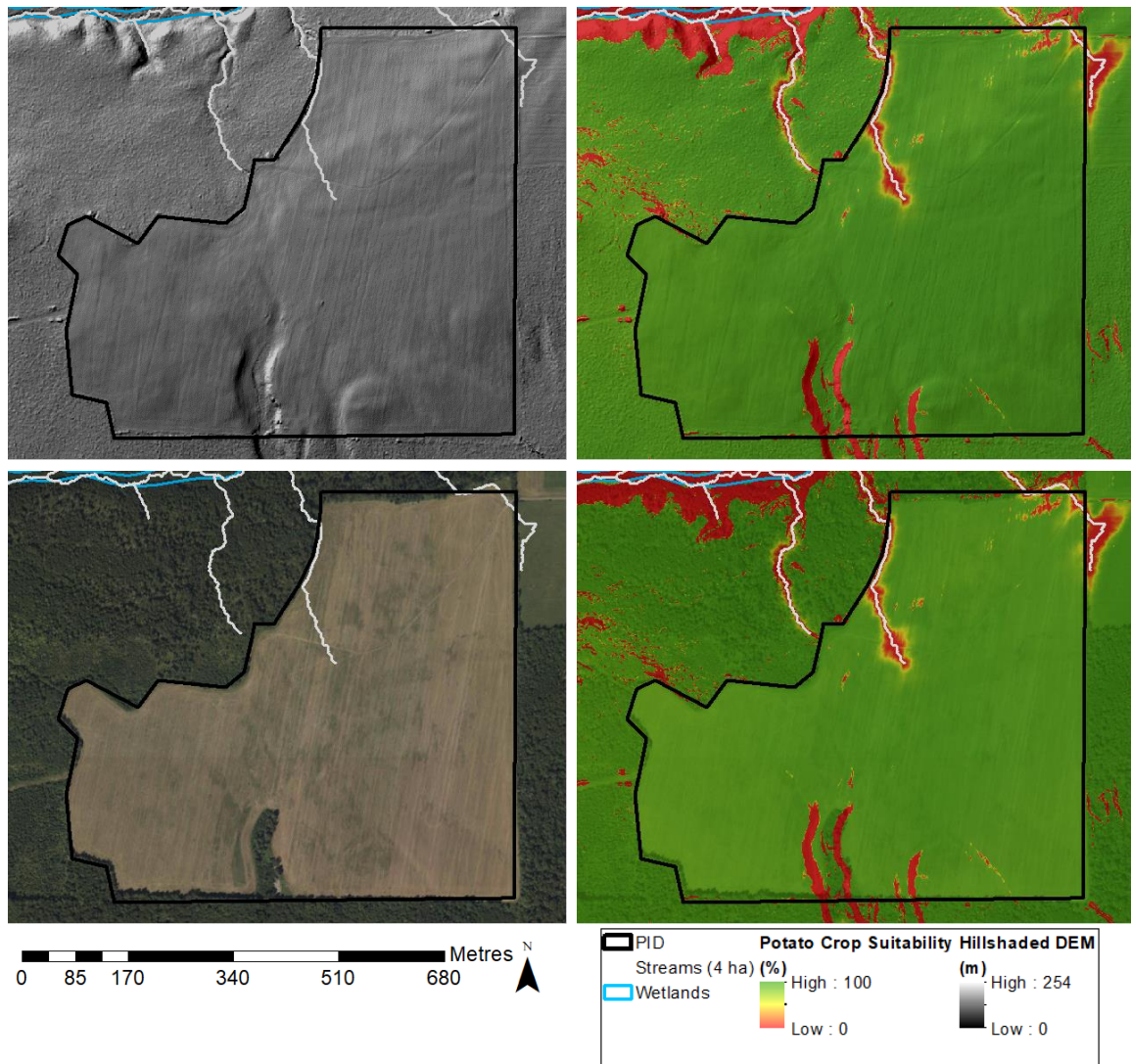


Figure 3.12. Images of PID 10201267 close-ups. From left to right, and from up to down: hillshaded DEM, hillshaded DEM with potato crop suitability (%) overlaid (layer transparency set to 50 %), satellite imagery, satellite imagery with potato crop suitability overlaid (layer transparency set to 50 %). All images also show streams with > 4 ha upslope flow accumulation areas, PIDs, roads, waterbodies, and wetland. Forest soil unit: TH. Basemap source: GeoNB. Potato crop suitability varies from 0 to 100 %, coloured from red through yellow to green, respectively.

### 3.3.3. Qualitative Assessment: Northwestern NB

Figure 3.13 shows the northwestern study area by soil association, with roads, wetlands and waterbodies overlaid, followed by the close-up collage examples in Figures 3.14 to 3.19.

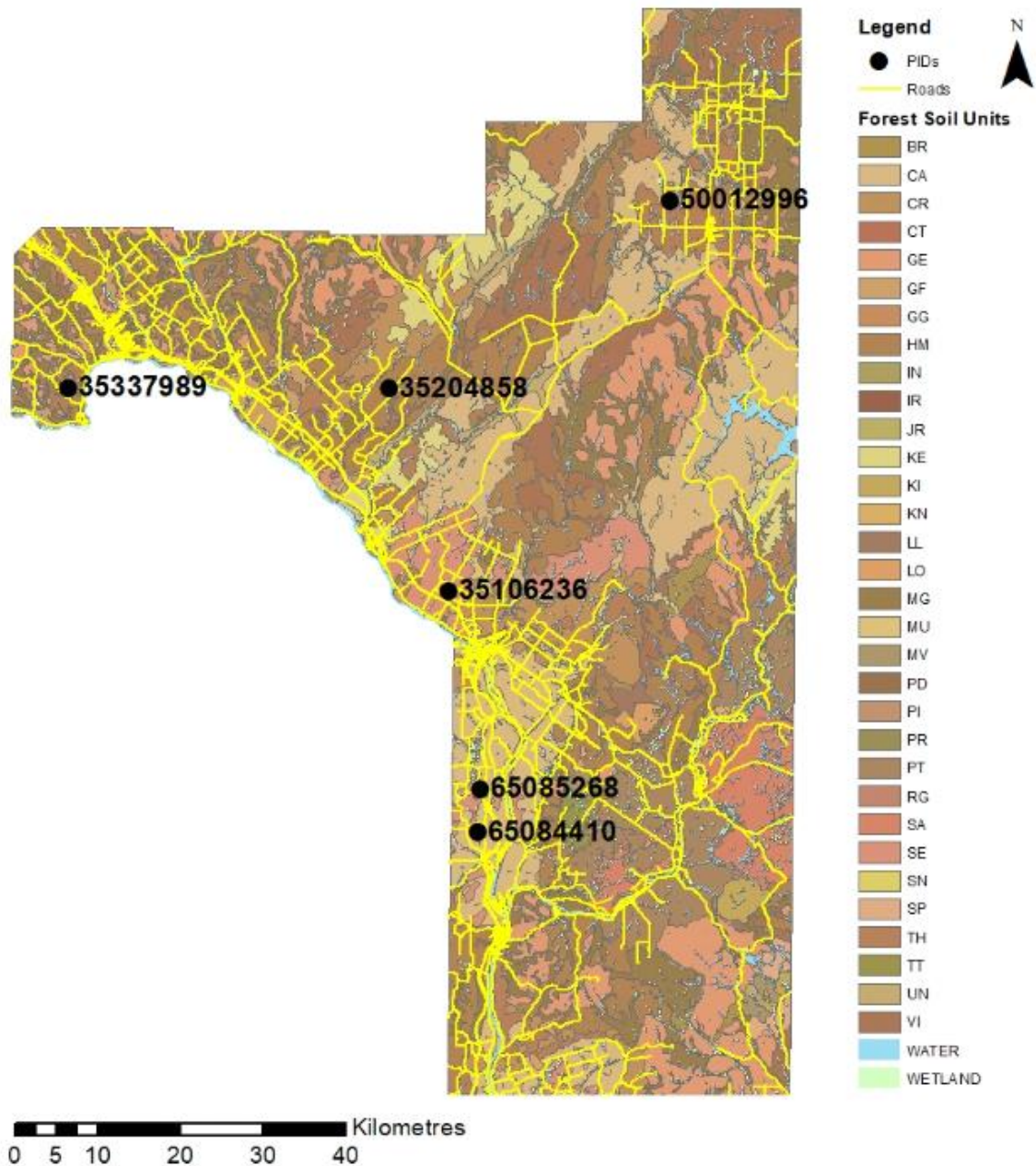


Figure 3.13. Locations of the crop suitability examples within the Grand Falls area, overlaid on the forest soil units for the area. Source: Colpitts et al. (1995). Yellow lines: roads.

Figure 3.14 presents the close-ups for PID 65084410 (58.50 ha), located in Grand Falls Parish (46°51'18.8"N 67°44'47.3"W) on SE and CA soils. The smooth field section on this PID contains a 60 m drainage pattern obliquely aligned from south to north and leading into the major flow channels along the PID perimeter. This pattern was likely installed to overcome the slow drainage nature of the poorly draining and compacted basal till that underlies SE soil. Overall, the drained portions of the field are mapped to be well suited for potato production. In contrast, the field portions that are steep and are mapped to be poorly-drained have remained forested.

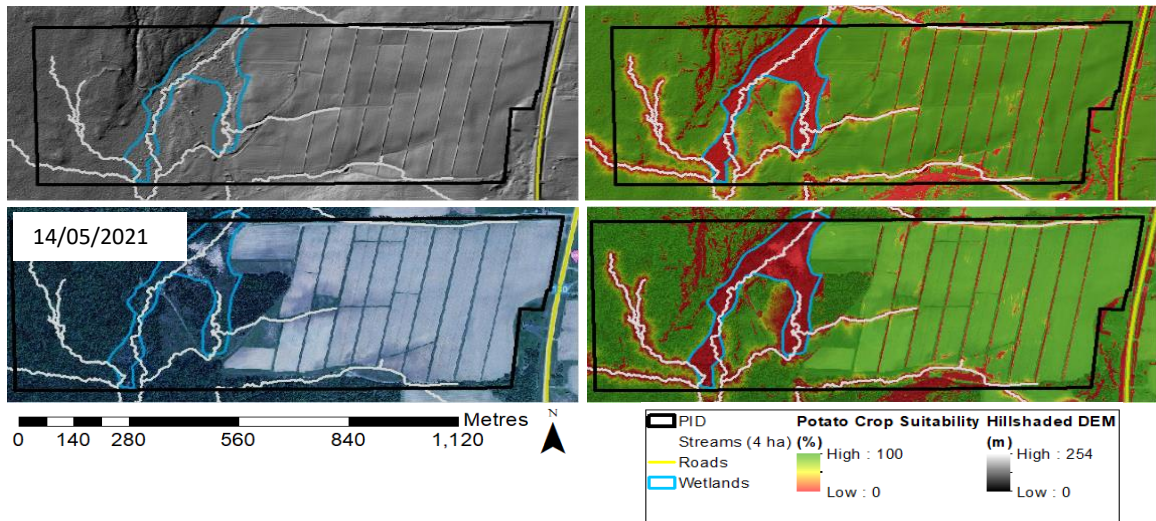


Figure 3.14. Images of PID 65084410 close-ups. From left to right, and from up to down: hillshaded DEM, hillshaded DEM with potato crop suitability (%) overlaid (layer transparency set to 50 %), satellite imagery, satellite imagery with potato crop suitability overlaid (layer transparency set to 50 %). All images also show streams with > 4 ha upslope flow accumulation areas, PIDs, roads, waterbodies, and wetland. Forest soil units: SE and CA. Basemap source: GeoNB. Potato crop suitability varies from 0 to 100 %, coloured from red through yellow to green, respectively.

Figure 3.15 shows close-up collage of PID 65085268 (34.74 ha), located in Grand Falls Parish (46°54'07.2"N 67°44'38.3"W). The field also occurs on SE and CA soils and contains a south-north curved 60 m ditch drainage pattern along its western section. Cropping pattern within this PID changed between 2011 and 2019 by dividing the PID into smaller management units. The forested area is suitable for potato growth, except for the steep slope terrain at the southeastern boundary. The eastern portion along the highway and to the south of this PID, while mapped crop suitable, has remained forested.

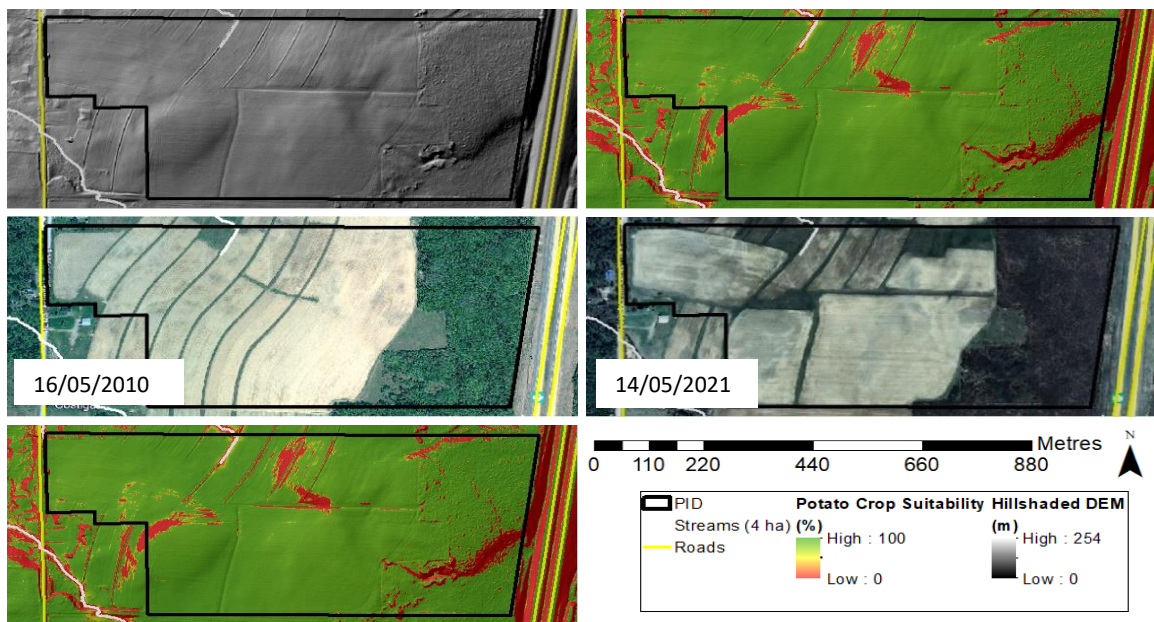


Figure 3.15. Images of PID 65085268 close-ups. From left to right, and from up to down: hillshaded DEM, hillshaded DEM with potato crop suitability (%) overlaid (layer transparency set to 50 %), satellite imagery, satellite imagery with potato crop suitability overlaid (layer transparency set to 50 %). All images also show streams with > 4 ha upslope flow accumulation areas, PIDs, roads, waterbodies, and wetland. Forest soil units: CA and SE. Basemap source: GeoNB. Potato crop suitability varies from 0 to 100 %, coloured from red through yellow to green, respectively.

Figure 3.16 shows the close-up collage for PID 35106236 (39.82 ha), located in Saint-André Parish (47°06'58.6"N 67°47'54.2"W). The PID is mapped to occur on SE soil but appears to be well-drained for potato cropping except along the east-west middle

portion and the northern section which is in part still forested. More details about this PID are presented in Chapter 5.

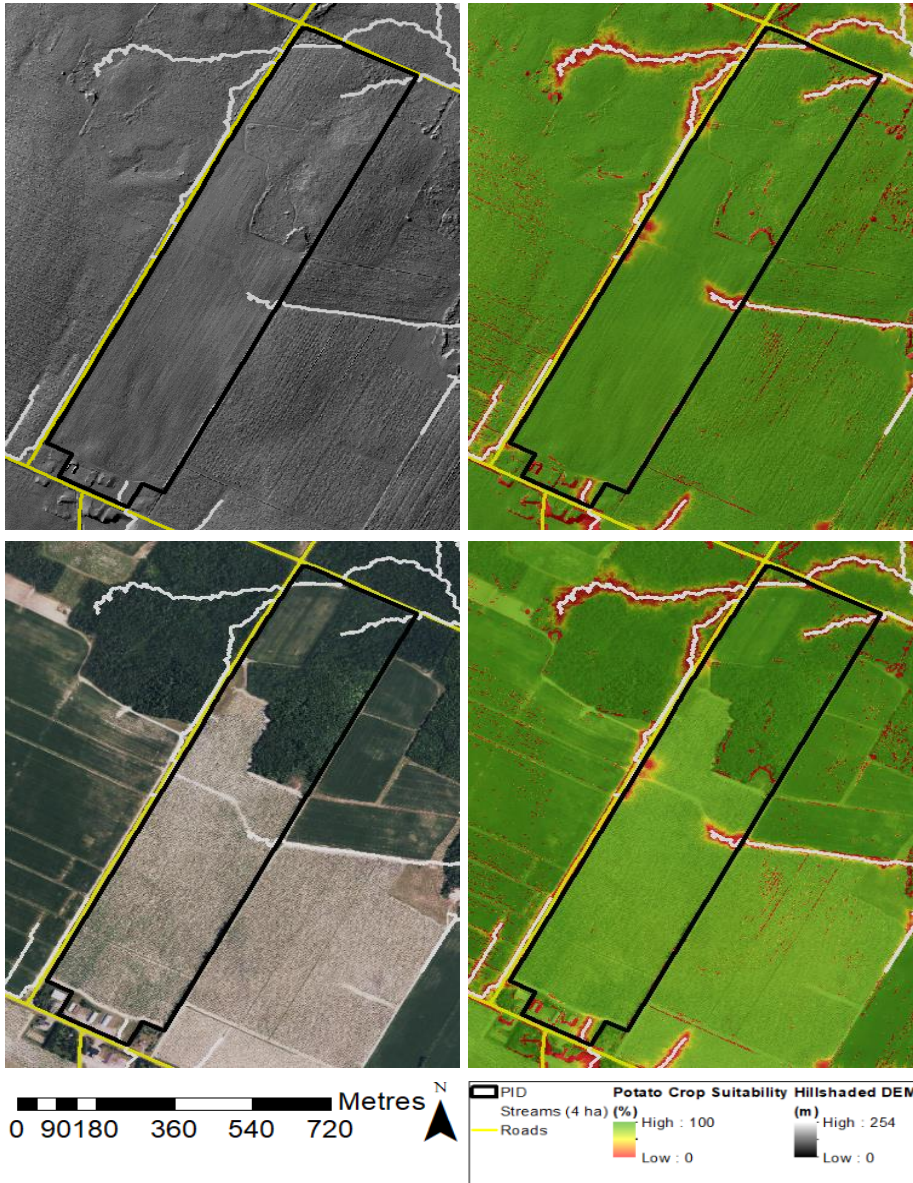


Figure 3.16. Images of PID 135106236 close-ups. From left to right, and from up to down: hillshaded DEM, hillshaded DEM with potato crop suitability (%) overlaid (layer transparency set to 50 %), satellite imagery, satellite imagery with potato crop suitability overlaid (layer transparency set to 50 %). All images also show streams with > 4 ha upslope flow accumulation areas, PIDs, roads, waterbodies, and wetland. Forest soil unit: SE. Basemap source: GeonB. Potato crop suitability varies from 0 to 100 %, coloured from red through yellow to green, respectively.

Figure 3.17 shows the close-up collage for PID 35337989 (44.37 ha), located in Edmundston (47°19'39.4"N 68°24'39.3"W). The PID occurs on non-calcareous well-draining MG and HM soils, both derived from a mix of metaquartzites, slates, metasiltstones, metaconglomerates and/or metawackes. The terrain is hummocky along the northern part, and gentler along the southern part. Except for the strongly hummocky areas, the field portions are mapped to be suitable for potato cropping. The area along the southern perimeter of this PID has remained forested. Examining the historical Google Earth images reveals frequent management zone changes within the field portions of this PID.

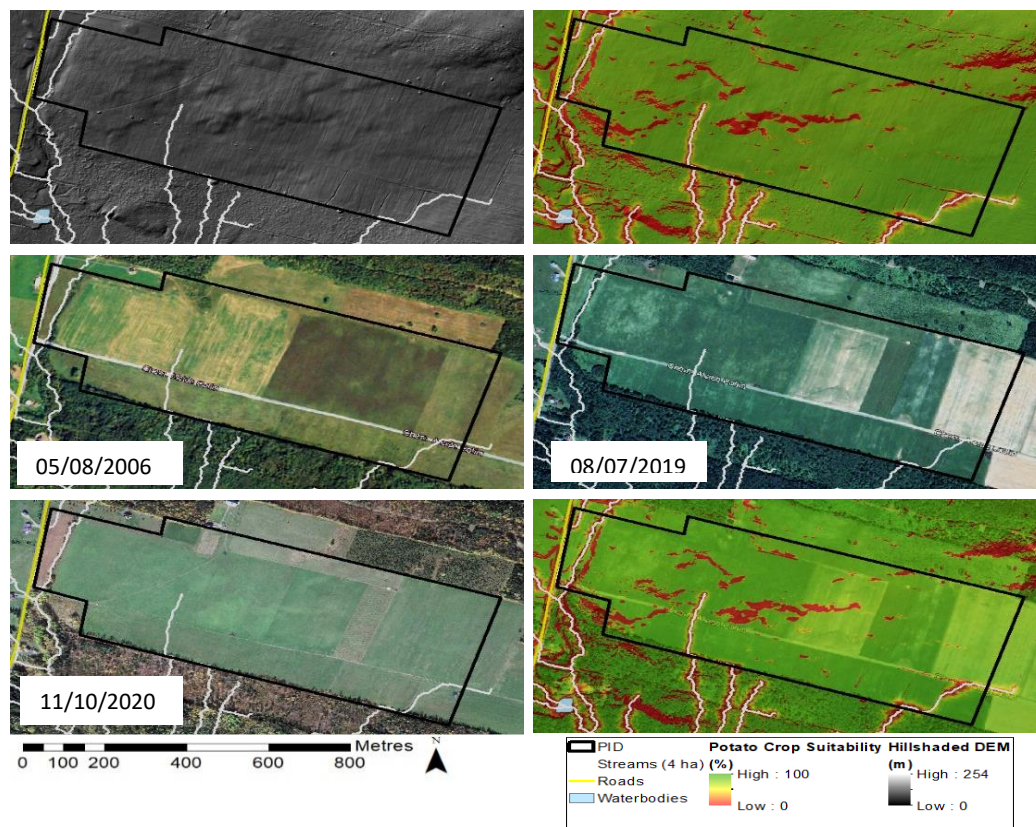


Figure 3.17. Images of PID 35337989 close-ups. From left to right, and from up to down: hillshaded DEM, hillshaded DEM with potato crop suitability (%) overlaid (layer transparency set to 50 %), satellite imagery, satellite imagery with potato crop suitability overlaid (layer transparency set to 50 %). All images also show streams with > 4 ha upslope flow accumulation areas, PIDs, roads, waterbodies, and wetland. Forest soil units: HM and MG. Basemap source: GeoNB. Potato crop suitability varies from 0 to 100 %, coloured from red through yellow to green, respectively.

Figure 3.18 shows close-ups of PID 35204858 (41.61 ha), located in Sainte-Anne Parish (47°20'04.0"N 67°53'55.8"W) and on well-draining and in part steeply sloping HM soil. Overall, this PID remains subject to forest management and is generally unsuitable for potato cropping.

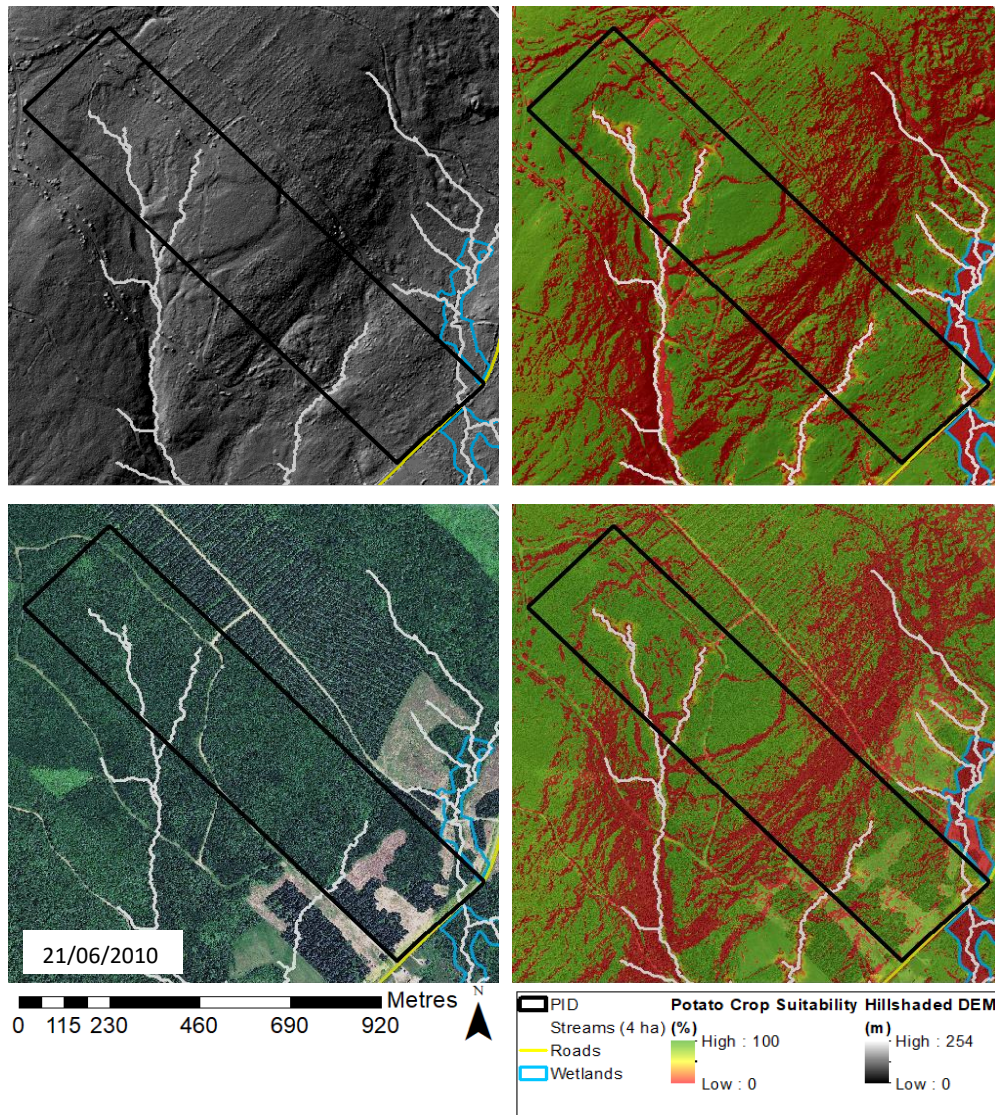


Figure 3.18. Images of PID 35204858 close-ups. From left to right, and from up to down: hillshaded DEM, hillshaded DEM with potato crop suitability (%) overlaid (layer transparency set to 50 %), satellite imagery, satellite imagery with potato crop suitability overlaid (layer transparency set to 50 %). All images also show streams with > 4 ha upslope flow accumulation areas, PIDs, roads, waterbodies, and wetland. Forest soil unit: HM. Basemap source: GeoNB. Potato crop suitability varies from 0 to 100 %, coloured from red through yellow to green, respectively.

Figure 3.19 shows close-ups of PID 50012996 (41.00 ha), located in Saint-Quentin Parish ( $47^{\circ}32'35.8''N$   $67^{\circ}27'16.5''W$ ) on calcareous TH soil. Potato cropping is mapped to be suitable except along the flow channels within this PID. Examining the July 2019 Google Earth image reveals (i) a greener surface colouring along these channels, and (ii) that the forested area above the northern PID perimeter and flow channels has been cleared.

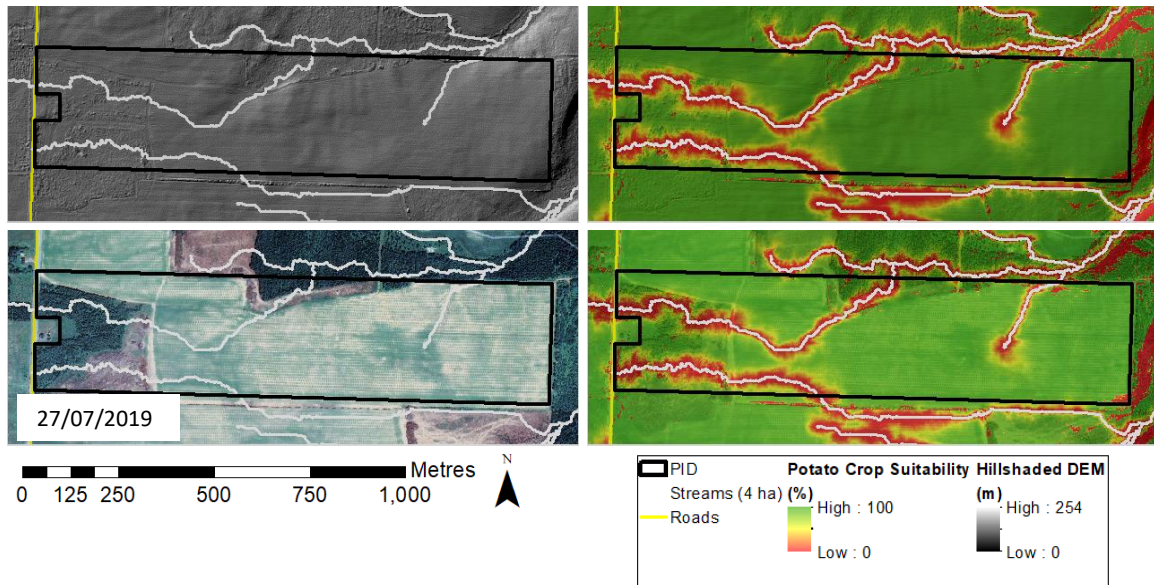


Figure 3.19. Images of PID 50012996 close-ups. From left to right, and from up to down: hillshaded DEM, hillshaded DEM with potato crop suitability (%) overlaid (layer transparency set to 50 %), satellite imagery, satellite imagery with potato crop suitability overlaid (layer transparency set to 50 %). All images also show streams with > 4 ha upslope flow accumulation areas, PIDs, roads, waterbodies, and wetland. Forest soil unit: TH. Basemap source: GeoNB. Potato crop suitability varies from 0 to 100 %, coloured from red through yellow to green, respectively.

### 3.3.4. Qualitative Assessment: LiDAR-DEM versus Coarse-Grained Crop Suitability Mapping

The LiDAR-DEM versus the province-wide coarse-grained suitability maps for potato cropping are presented in Figures 3.20, 3.21 and 3.22 and are all based on the above collage illustrations for the Woodstock, Hartland-Florenceville and northern NB areas. The differences in suitability mapping across these examples are mainly due to:

1. using the original non-LiDAR DEM coverage across NB for flow channels and cartographic depth-to-water mapping;
2. not using provincial soil maps for differentiating crop suitability by varying soil conditions;
3. blocking out wetland areas and areas deemed too steep for potato cropping.

For the Woodstock area, the provincial productivity map in comparison with the LiDAR-derived map:

1. rated poorly-drained areas in the southern part of PID 10283562 suitable for potato cropping;
2. rated more areas in PID 10048296 and PID 10270999 unsuitable, by not accounting for local variations in soil type and the presence of flow channels with > 4 ha upslope flow accumulation areas;
3. provides no rating for PID 10175354.

For the Hartland-Florenceville area, the provincial productivity map in comparison with the LiDAR-derived map produced similar although less detailed results for PIDs 10263366, 1020126, 10151512, and 1022709. However, actual locations and extent for crop suitability differ.

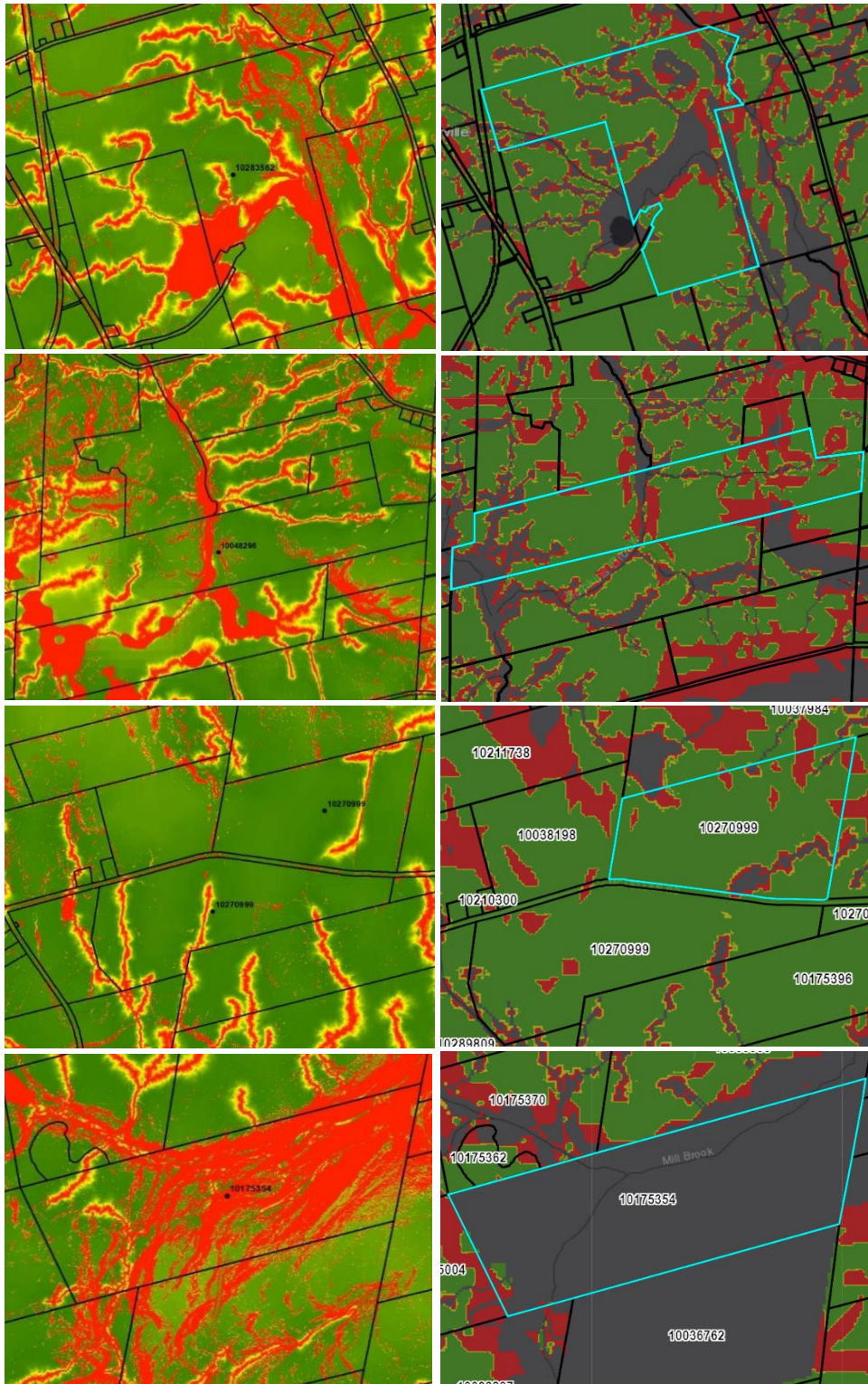


Figure 3.20. Comparison of potato crop suitability rating from LiDAR-based results (left) and provincial results (right) for PIDs 10283562, 10048296, 10270999, and 10175354.

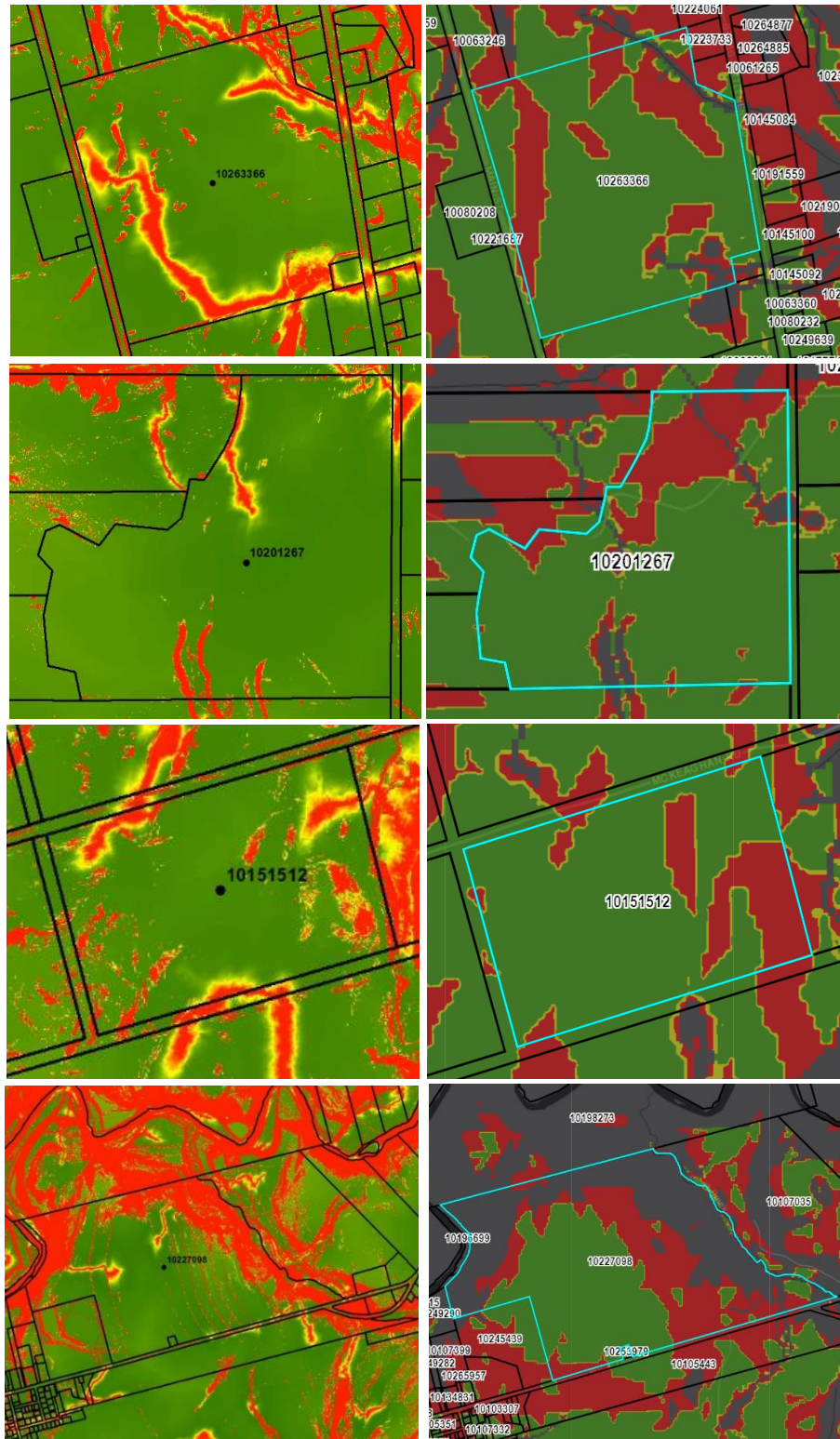


Figure 3.21. Comparison of potato crop suitability rating from LiDAR-based results (left) and provincial results (right) for PIDs 10263366, 10201267, 10151512, 10227098.

For the northern NB area, the provincial productivity map in comparison with the LiDAR-derived map showed more areas for PIDs 35337989 and 35204858 to be unsuitable, while the suitability results for PID 50012996.

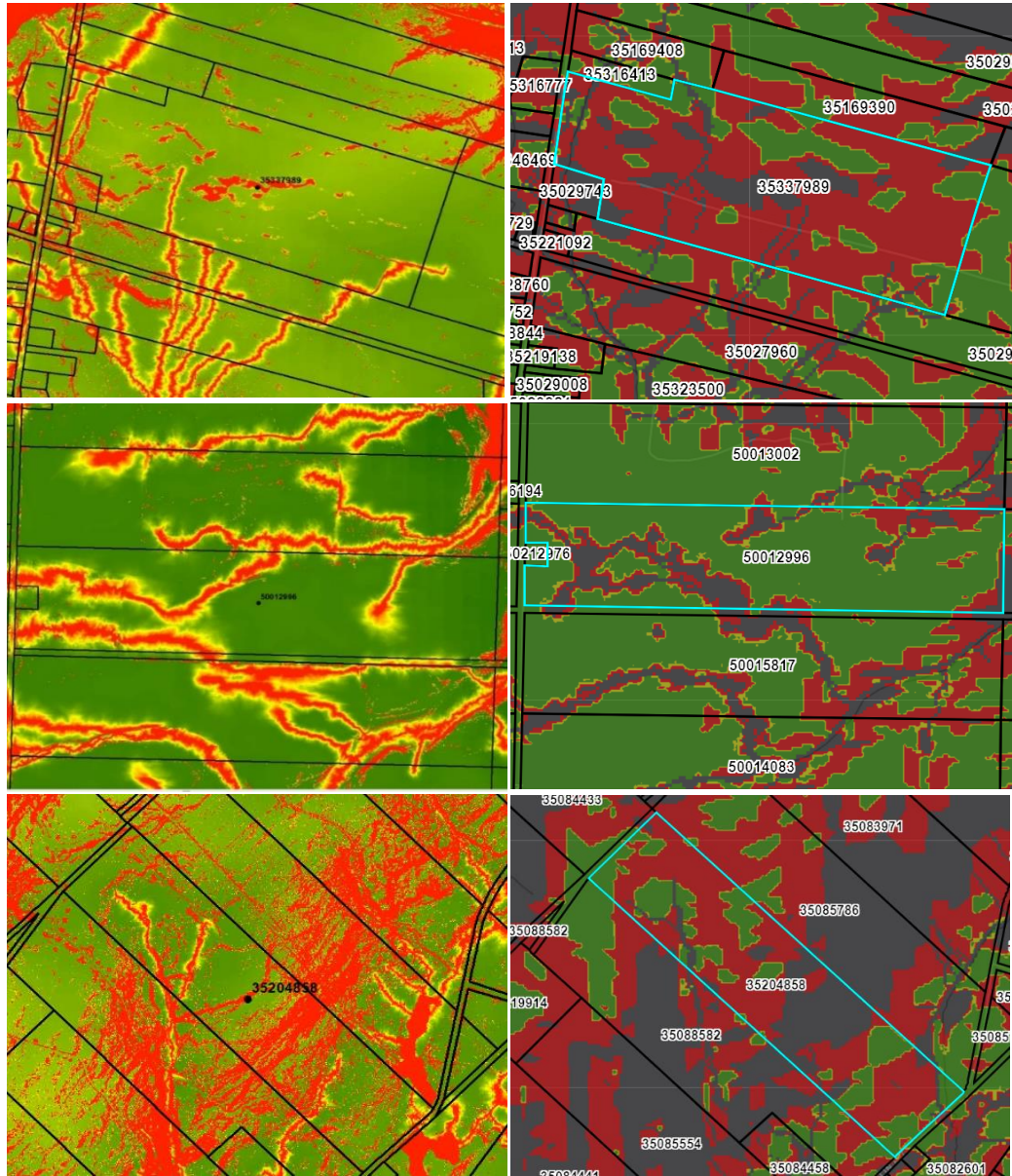


Figure 3.22. Comparison of potato crop suitability rating from LiDAR-based results (left) and provincial results (right) for PIDs 35337989, 50012996, and 35204858.

For the remaining examples for Northern NB area, the provincial productivity map again mapped larger areas in PIDs 35106236, 65085268 and PID 65084410 to be unsuitable for potato cropping.

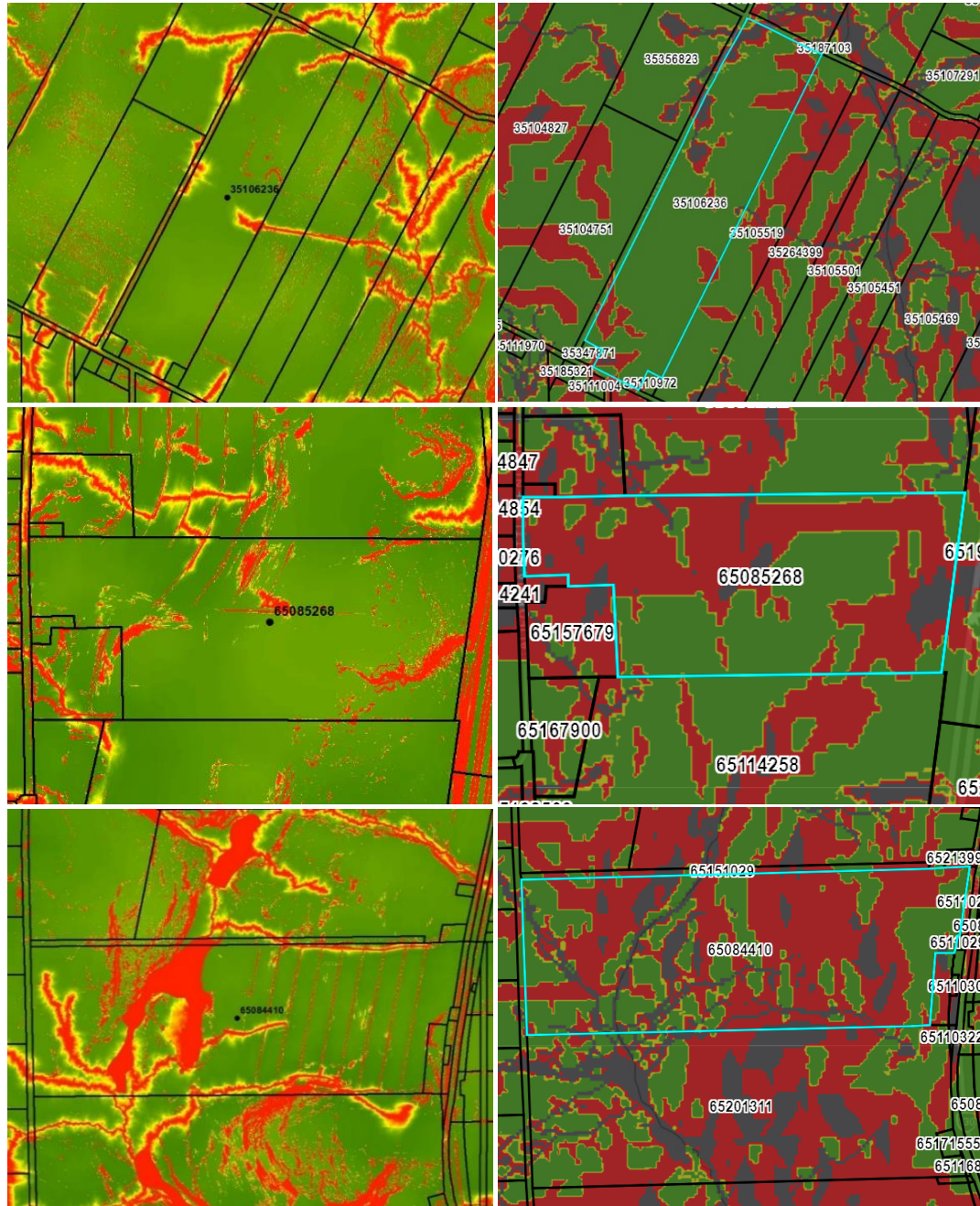


Figure 3.23. Comparison of potato crop suitability rating from LiDAR-based results (left) and provincial results (right) for PIDs 35106236, 65085268, and 65084410.

In summary, the qualitative crop suitability rating results including the comparisons with the NB rating map for potato cropping as portrayed above suggest the following:

1. The LiDAR generated crop suitability map is rated 0-100 %. In contrast, the provincial potato crop suitability map is rated using three categories: limited potential, modest potential, and good (best) potential. However, the modest potential rating is limited to the perimeter of the other limited and best classes and is therefore not able to locate transitional areas from poor to best.
2. The 0 to 100 % crop suitability display allows for field-by-field inspections to ascertain within-field limitations regarding soil drainage and steep slopes.
3. Areas where slopes are deemed too steep for agricultural activities (i.e., > 10 %) are left out of the provincial potato crop suitability mapping, as opposed to LiDAR-derived results, showing where these areas grading become unsuitable, or good in part be used by way of, e.g., contour terracing.
4. This project's results identify greater areas suitable for potato production than the provincial mapping results. This is mainly due to the 1 m elevation resolution, which deems many small areas between flow channels and with > 10 % slopes to be crop suitable.
5. For the most part, fields - as revealed above through historical surface images - are aligned with LiDAR-generated crop suitability extents. Exceptions occur in fields where areas adjacent to LiDAR-generated flow channels parts are mapped to be poorly-drained and are therefore rated unsuitable but appear to be well-drained. In part, these channels are present, but the water would have been diverted either along ditches or through underground drainage tiles (Milburn & Gartley, 1987). Still, in

many cases, low-lying areas in fields along DEM-generated flow channels with > 4 ha upslope flow accumulation appears to be darker, lighter or greener.

### 3.3.5. Quantitative Assessment

The forest and agricultural segments across the study area and across its Woodstock, Hartland to Florenceville and the northern sections were analyzed in terms of (i) property numbers, (ii) combined farm, farm & forest and forest areas, and (iii) mean potato crop suitability ratings. The results so obtained are listed in Table 3.1.

Table 3.1. Statistics (mean and/or sum) of PANs area (ha), soil quality rating (%), assessment values (\$), and PANs; split by section and land class.

	Land Class	Woodstock area	Hartland-Florenceville area	Northwestern NB
Number of PANs	Farm	633	889	1000
	Forest	1402	1050	2660
	Farm & Forest	251	374	514
	Total	2,286	2,313	4174
Combined areas of PANs (ha)	Farm	29,071	37,904	33,021
	Forest	109,688	65,496	334,821
	Farm & Forest	11,394	17,610	18,461
	Total	150,153	121,010	386,302
Mean potato crop suitability rating (%)	Farm	56.04	52.72	51.10
	Forest	47.72	36.85	32.75
	Farm & Forest	54.42	50.50	43.08
	Average	52.73	46.69	42.31

Across the study area, the forested areas exceed the agricultural land portions by a factor of 8, i.e., 967,775 ha vs. 100,248 ha). The average potato crop suitability rating of forested land amounted to 34.4 %. This suggests that field and areas suited for potato cropping can be expanded but perhaps not to this extent because some of the areas between flow channels and steep slopes would be too narrow and/or too small in support of self-financing cropping operations. The average potato crop suitability rating of farm field PIDs

amounts to 51.1 % across the study area. This percentage would be higher upon excluding all within-field areas that either too wet or too steep. From the southern to the northern study areas, the within-field and forest suitability ratings decrease. This decrease can be attributed to the southern to northern increase in per-area frequencies pertaining to steeper slopes.

### **3.5. Conclusion**

To conclude, the existing provincial potato-crop suitability map does not account for cross-province soil association variations, and local slope and soil drainage conditions remain poorly resolved (Government of New Brunswick, 2018). Using the NB-wide LiDAR generated DEM in connection with the waterbodies and wetlands adjusted NB Forest Soil Association map overcomes this issue such that areas now rated suitable for potato cropping conform to image-captured field extent. Overall, the averaged potato crop suitability ratings for agricultural fields and forested areas amount to 51.1 % and 34.4 % across the study area, respectively. This suggests where potato and related crops can be expanded into forest areas but only where rated and found to be suitable. To do so, however, requires detailed on-site considerations including conducting on-site inspections and surveys pertaining to actual soil property determinations. In this regard, the above crop suitability rating scheme – by procedure influenced by the generalized soil association attributes listed in Tables 2.1 and 2.2 – does not yet represent actual within-field soil attribute distributions (see Chapters 5 and 6). To that end, digital soil mapping needs to be developed further to reliably account for within-field soil property variations as affected by, e.g., drainage and topography. In principle, conversion of forested lands into agricultural lands needs to be done carefully without degrading physical, chemical and

biological soil properties (Government of New Brunswick, n.d.) In this, maintaining if not enhancing existing soil organic matter pools is vital, especially for repeated potato cropping (Tolimir et al., 2020).

### 3.6. Literature Cited

Government of New Brunswick. 2018. Agriculture Site Suitability. Retrieved from <https://www2.gnb.ca/content/gnb/en/departments/10/agriculture/content/agriculture-suitability.html>

Government of New Brunswick. n.d. Soil Management. Retrieved from: [https://www2.gnb.ca/content/gnb/en/departments/10/agriculture/content/crops/potatoes/soil\\_management.html](https://www2.gnb.ca/content/gnb/en/departments/10/agriculture/content/crops/potatoes/soil_management.html)

Milburn, P., & Gartley, C. 1987. Subsurface drainage and land use in New Brunswick. *Canadian Agricultural Engineering*. 13-17.

Tolimir, M., Kresović, B., Životić, L., Dragović, S., Dragović, R., Sredojević, Z., & Gajić, B. 2020. The conversion of forestland into agricultural land without appropriate measures to conserve SOM leads to the degradation of physical and rheological soil properties. *Scientific Reports*, 10(1), 1–12.

## **CHAPTER 4: PARCEL ACCOUNT NUMBER GENERATED**

### **RESULTS**

#### **4.1. Introduction**

In NB, farm properties ( $\geq$  five ha) are assessed at market value. In contrast, freehold timberlands ( $\geq$  10 ha) and farm woodlots ( $\geq$  10 ha) are assessed at one hundred dollar and one dollar, respectively (Government of New Brunswick, 2005; Cook, 1992). A map of individual land parcels can be obtained through GeoNB, along with information on land use description, sale value, assessment value, tax levy, and area (PAN data file; GeoNB, n.d.). This information is updated annually and is available for public use. The objective of this chapter is to evaluate the extent to which the assessed market values of farmland PANs correspond with the 1 m crop suitability rating results for the study area depicted in Figure 4.1. The hypothesis is that soil quality in terms of potato cropping implicitly contributes to the NB tax assessment of farm as well as farm / forested properties.

#### **4.2. Methods**

##### **4.2.1. Study Area and Data**

The area in Carleton County (Bath to Woodstock), outlined red in Figure 4.1, represents the Proof-of-Concept area (POC; 142,839 ha). The area along the Upper Saint-John River Valley, outlined yellow in Figure 4.1, represents the entire Area of Interest (AOI; 971,665 ha).

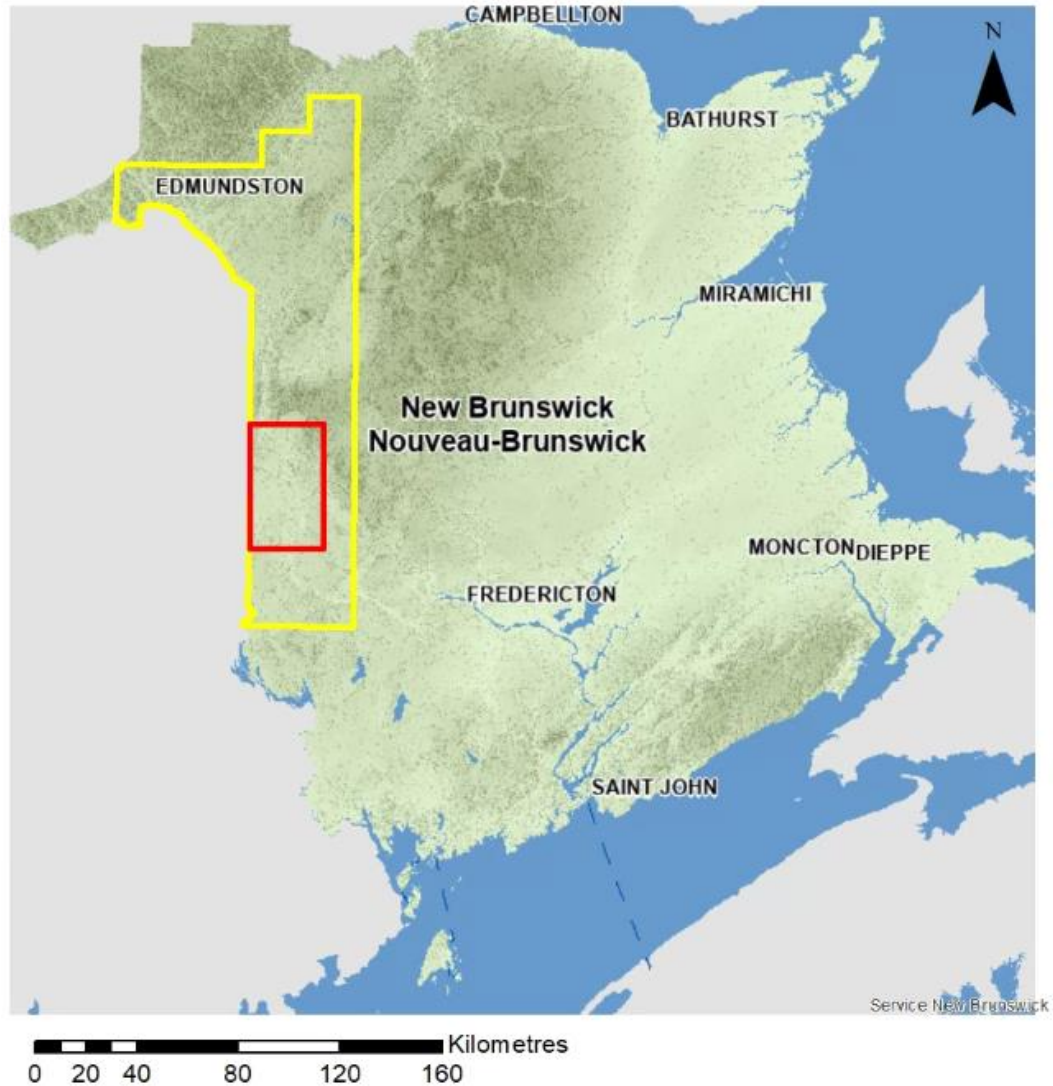


Figure 4.1. Evaluating the extent of soil-based potato crop rating on property tax assessment: POC (red outline), a portion of Carleton County; AOI (yellow outline), the Upper Saint John River Valley in NB.

Shown in Figure 4.2 are POC close-ups of:

1. The potato crop suitability map derived in Chapter 3, based on the procedures described in Chapter 2 (left).
2. The building footprint (building areas (m<sup>2</sup>) per PID) obtained from GeoNB (middle).

- Farmlands, woodlands, and farm and wood land combinations PANs obtained from GeoNB (right).

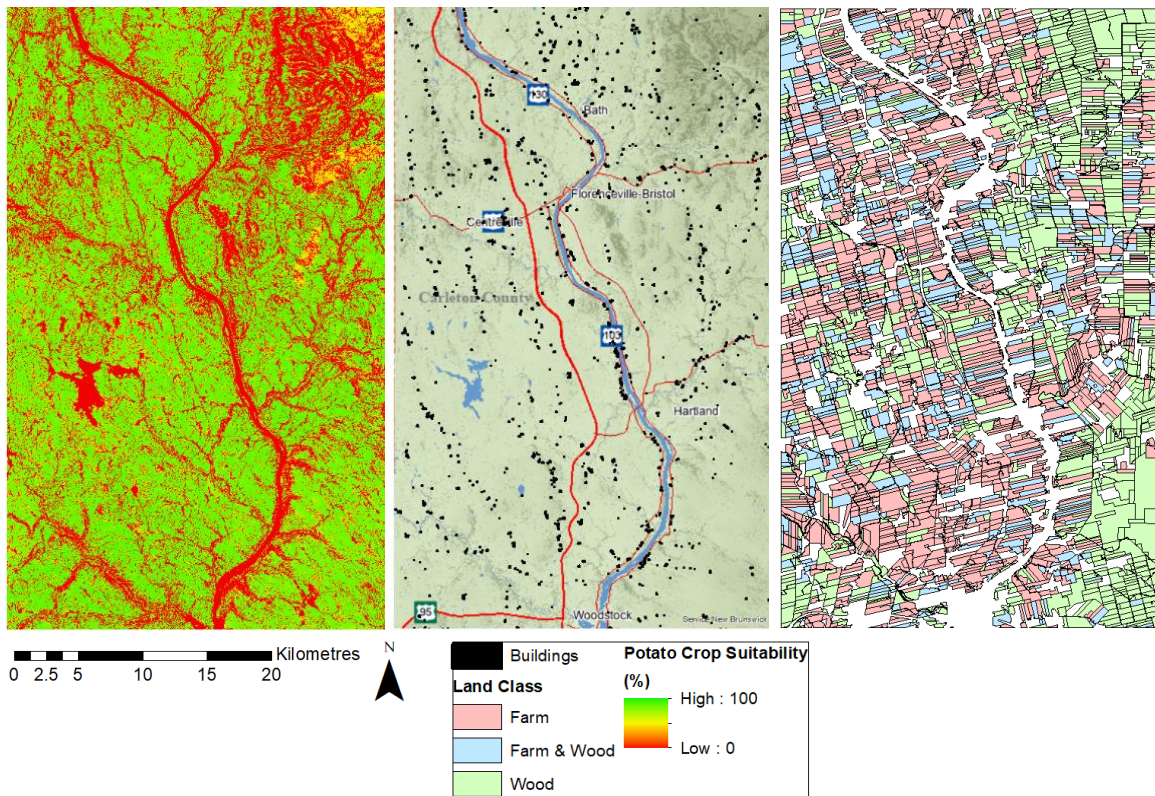


Figure 4.2. Maps of layers used to investigate the extent to which farmlands reflect soil quality with respect to potato production. a) potato crop suitability rating map (%), b) building footprint, and c) farmlands, woodlands, and farm and wood land combinations PANs. The layers are “zoomed in” the POC area. Basemap source: GeoNB.

The potato crop suitability rating map ranges from 0 to 100 %, with 0-33 %, 33-66 %, and 66-100 % considered poor, fair, and good, respectively. The PAN layer provides the data for tax assessment purposes and the PID layer (parcel identifier) is used for mapping purposes. A property can be assigned more than one PID if it contains multiple buildings. Altogether, the PAN layer also contains information on:

- Location (physical address).
- Description of property.

3. Tax assessment code and tax assessment description.
4. Assessment year.
5. Assessment value (\$).
6. Transaction date.
7. Sale value (\$).
8. Tax levy (\$).
9. Area of property (m<sup>2</sup>).

For the purpose of this research, only property assessment values, property areas, property footprint areas, and property type (i.e., farm, farm/woodland, forest are used for tax assessment analysis and geoprocessing. For this analysis, the building footprint layer provides details on all buildings that were present during the time of LiDAR data collection (2015 and 2018), as follows:

1. Date of creation.
2. Minimum and maximum elevation (m).poc
3. Building ID.
4. Building (polygon) area (m<sup>2</sup>).
5. For the purpose of this research, building area per PAN is chosen to be an additional variable for tax assessment analysis and geoprocessing.

#### **4.2.2. Geoprocessing**

Geoprocessing was conducted in ArcMap 10.7.1 with the following workflow:

1. The *Clip* tool was used to limit the PANs layer to the POC and AOI areas.

2. Farmlands smaller than five ha were removed from the selection using the *Select by Attribute* function and PANs intersecting the boundary of the POC and AOI areas were removed using the *Selection by Locations* function.
3. PANs with buildings were identified using the *Selection by Location* function. The *Intersect* tool was used to create a feature class of these buildings and output was joined to the PANs layer via shared field.
4. The *Select by Attribute* function was used to only select PANs pertaining to farmlands, woodlands, and farm/woods using the following query sequence:

Descript LIKE '\*Farm\*' OR  
 Descript LIKE '\*Agricole\*' OR  
 Descript LIKE '\*AGRICOLE\*' OR  
 Descript LIKE '\*FARM\*' OR  
 Descript LIKE '\*Ferme\*' OR  
 Descript LIKE '\*TIMBER\*' OR  
 Descript LIKE '\*Timber\*' OR  
 Descript LIKE '\*wood\*' OR  
 Descript LIKE '\*WOOD\*' OR  
 Descript LIKE '\*TIMBELAND\*' OR  
 Descript LIKE '\*TIMERLAND\*' OR  
 Descript LIKE '\*TIMBLD\*' OR  
 Descript LIKE '\*Boisée\*' OR  
 Descript LIKE '\*boisee\*' OR  
 Descript LIKE '\*BOISE\*' OR  
 Descript LIKE '\*boisée\*' OR  
 Descript LIKE '\*BOISÉES\*' OR  
 Descript LIKE '\*BOISÉE\*' OR  
 Descript LIKE '\*Agri.\*' OR  
 Descript LIKE '\*Boisee\*' OR

Descriptp LIKE '\*FERME\*' OR  
Descriptp LIKE '\*Woodland\*' OR  
Descriptp LIKE '\*Agricole\*' OR  
Descriptp LIKE '\*boisé\*' OR  
Descriptp LIKE '\*Boisé\*' OR  
Descriptp LIKE '\*Woodlot\*' OR  
Descriptp LIKE '\*AGRCIOLE\*' OR  
Descriptp LIKE '\*ABRICOLES\*' OR  
Descriptp LIKE '\*agri\*

5. The *Zonal Statistics as Table* tool was used to derive the mean potato crop suitability rating for each PAN. The table output so generated was joined to the clipped PANs layer via shared attribute.
6. The tabular data was exported using the *Excel to Table* tool.

#### **4.2.3. Statistical Analyses**

The statistical evaluations included summarizing the PAN-based information in terms of:

1. Numbers, averages and total POC and AOI values per PAN in relation to PAN building area by property type (farmlands, woodlands, and farm/woodlands), mean suitability ratings, and mean taxation values (Table 4.1).
2. Presenting the PAN based results using boxplots (Figure 4.3).
3. Multivariate regression analyses, by relating the PAN taxation values to PAN property and building areas by property type; and repeating the same for each PAN taxation per ha value. To linearize the analyses, it was necessary to log transform the PAN taxation numbers and the numbers for property building footprint areas.

### 4.3. Results

The basic summary results for all properties evaluated in the POC and AOI areas are listed in Table 4.1. In this, the averaged POC and AOI numbers are similar to one another in spite of the AOI area being seven times larger than the POC area and covers a wide range of GDD and FFD values, i.e., from 1400 to 1900 °C, and from 100 to 130 days, respectively. In terms of property numbers, AOI PIDs  $\approx$  3.3 POC PANs. This is mainly due to increasing woodland numbers from south to north. In contrast, there is little POC versus AOI difference in terms of the mean soil suitability and PAN taxation values. In addition, the POC versus AOI variations for  $\log_{10}$ (PAN area),  $\log_{10}$ (taxation value), mean soil suitability and  $\log_{10}$ (building areas) as split by PAN type all remain very similar as shown by the boxplots in Figure 4.4. There are, however, corresponding decreases in PAN suitability and taxation such that farms > farm/woodlands > forests.

Table 4.1. Statistics (numbers, means, sums) for PAN areas (ha), PAN building footprints (m<sup>2</sup>), PAN crop suitability ratings (%), PAN taxation assessment values (\$), all split by study area (POC versus AOI), and PAN type.

	Land Class	POC	AOI
Number of PANs	Farm	1154	2471
	Forest	1024	5031
	Farm & woodlot	444	1120
	Total	2622	8622
Combined areas of PANs (ha)	Farm	49,633	97,053
	Forest	61,783	490,812
	Farm & woodlot	20,166	46,583
	Total	131,582	634,447
Combined building area of PANs (m <sup>2</sup> )	Farm	421,822	797,189
	Forest	17,374	163,502
	Farm & woodlot	15,845	59,236
	Total	455,040	1,019,927
Average PAN area (ha)	Farm	43.0	39.3
	Forest	60.3	97.6
	Farm & woodlot	45.4	41.6
	Total	50.2	73.6
Average buildings area (m <sup>2</sup> )	Farm	365.5	322.6
	Forest	17.0	32.5
	Farm & woodlot	35.7	52.9
	Total	173.5	118.3
Mean soil quality rating (%) of PANs	Farm	54.2	52.9
	Forest	42.1	37.7
	Farm & woodlot	52.7	47.9
	Total	49.2	43.4
Mean tax assessment values of PANs (\$)	Farm	80,353	75,564
	Forest	13,074	14,649
	Farm & woodlot	37,006	33,785
	Total	46,738	34,592

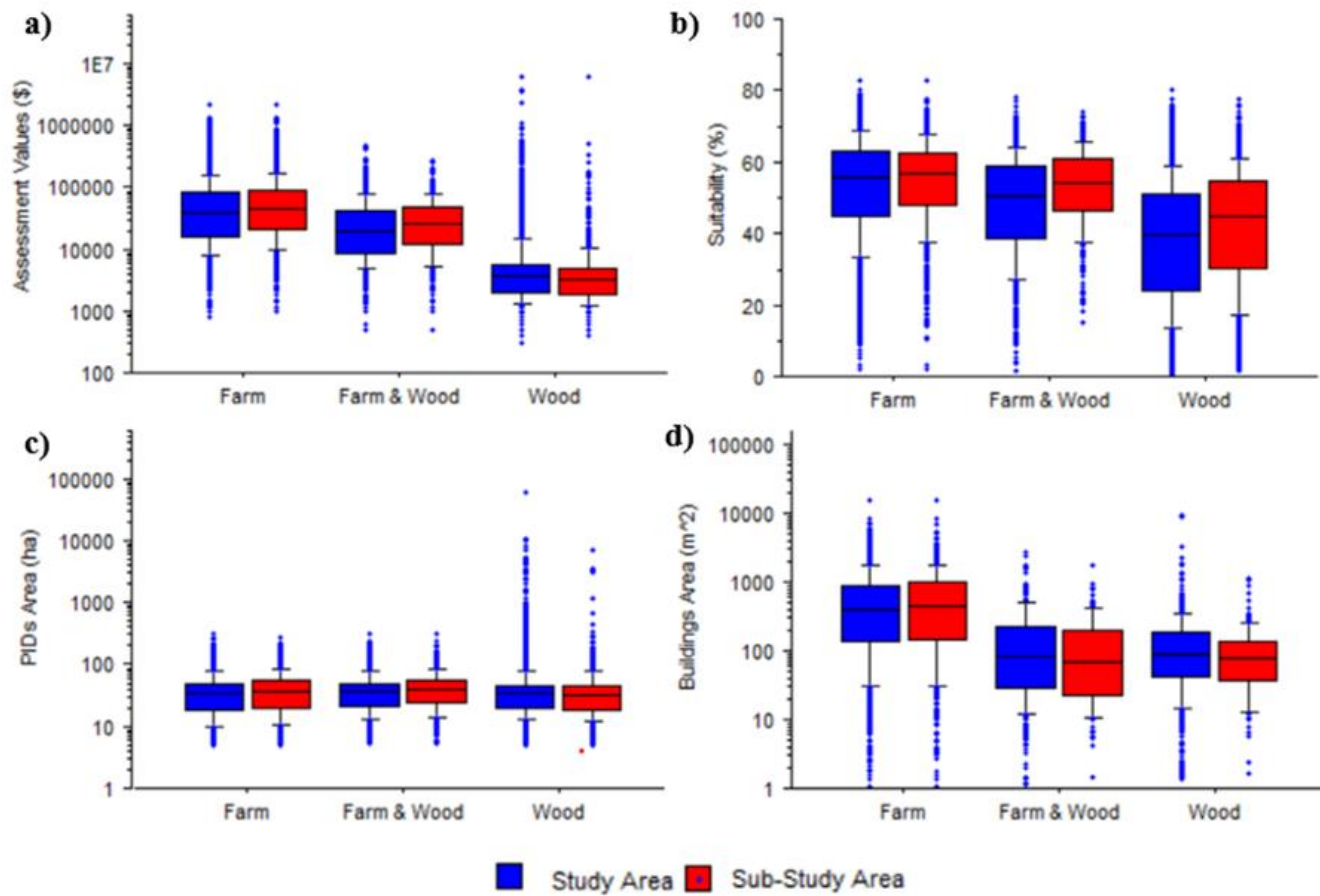


Figure 4.3. Boxplots of PANs a) assessment values (\$), b) suitability (%), c) area (ha), and d) building area (m<sup>2</sup>); split by land class (farmlands, woodlands, farm and wood land combinations).

The POC and AOI regression results obtained using  $\log_{10}(\text{\$ assessment values})$  and  $\log_{10}(\text{\$/ha assessment value})$  as dependent variable, and  $\log_{10}(\text{area})$ ,  $\log_{10}(\text{building footprint})$  for the farmlands, woodlands, and farm and wood land combinations properties as independent variables are shown in terms of:

1. The best-fitted regression results summaries (Table 4.2)
2. The corresponding regression coefficients together with their associated error and significance evaluations (Table 4.3).
3. The regression equations (Eq. 4.1, Eq. 4.2).
4. Scatterplots of actual versus best-fitted  $\log_{10}(\text{\$ assessment values})$  and  $\log_{10}(\text{\$/ha assessment values})$  are presented in Figure 4.4.

Table 4.2. PAN numbers (n), together with the best fitted R<sup>2</sup> and RMSE values for the PAN-based POC and AOI tax assessment analyses.

Tax assessment variable	n		R <sup>2</sup>		RMSE	
	POC	AOI	POC	AOI	POC	AOI
$\log_{10}(\text{assessment value (\$)})$	1588	3561	0.502	0.474	0.816	0.865
$\log_{10}(\text{assessment value (\$) / ha})$			0.431	0.424	0.337	0.360

Table 4.3. Intercept and regression coefficient with errors and significance levels for the PAN-based POC and AOI tax assessment analyses.

Tax assessment variable	Regression variable	Coefficient		Std. Error		Std. Coeff.		t-Value			p-Value	
		POC	AOI	POC	AOI	POC	AOI	POC	AOI	AOI/POC	POC	AOI
log <sub>10</sub> (assessment value (\$))	Intercept	2.87	2.9	0.06	0.04	2.87	2.9	48.5	75.9	1.57	<.0001	<.0001
	log <sub>10</sub> (PANs area)	0.64	0.61	0.03	0.02	0.42	0.38	22.8	30.5	1.34	<.0001	<.0001
	PAN suitability	0.0111	0.0113	0.0008	0.0005	0.42	0.37	22	29.1	1.32	<.0001	<.0001
	log <sub>10</sub> (PANs buildings area) <sup>0.33</sup>	0.164	0.158	0.008	0.005	0.26	0.31	14.7	25	1.7	<.0001	<.0001
	Agricultural & forested PANs	-0.143	-0.165	0.021	0.014	-0.13	-0.15	-6.8	-11.6	1.7	<.0001	<.0001
log <sub>10</sub> (assessment value (\$) / ha)	Intercept	2.85	2.88	0.06	0.004	2.85	2.88	50.6	78.5	1.55	<.0001	<.0001
	log <sub>10</sub> (PANs area)	0.064	0.064	0.002	0.002	0.54	0.47	26.4	35.1	1.33	<.0001	<.0001
	PAN suitability	0.0107	0.0110	0.0007	0.0004	0.28	0.33	14.9	25.4	1.7	<.0001	<.0001
	log <sub>10</sub> (PANs buildings area) <sup>0.33</sup>	-0.380	-0.412	0.027	0.019	-0.28	-0.28	-14.3	-21.3	1.49	<.0001	<.0001
	Agricultural & forested PANs	-0.119	-0.142	0.02	0.014	-0.12	-0.14	-6	-10.3	1.73	<.0001	<.0001

The regression results presented in Table 4.3 can, in principle, be used for approximate soil suitability tax evaluation purposes, by way of the following AOI regression-derived equations per PAN area (Eq. 4.1) and per PAN hectare (Eq. 4.2):

$$\log_{10}(\text{PAN assessment value, \$}) = 2.90 + 0.61 \log_{10}(\text{PAN area, ha}) + 0.158 (\text{PAN building footprint, m}^2) + 0.0113 \log_{10}(\text{PAN Suitability, \%}) - 0.165(\text{PAN farm/woodlot})$$

Eq. 4.1

$$\log_{10}(\text{PAN assessment value, \$ / ha}) = 2.88 + 0.064 (\text{PAN building footprint, m}^2)^{1/3} + 0.0110(\text{PAN suitability, \%}) - 0.412 \log_{10}(\text{PAN area, ha}) - 0.142(\text{PAN farm/woodlot})$$

Eq. 4.2

In these equations, note that:

- The negative farm/woodland coefficient for taxation indicates that farm/woodland areas are – by definition and as explained above - assessed lower than farmlands with woodlots.
- The PAN \$ assessment values correlate positively with the PAN area while the PAN \$/ha assessment values correlate negatively with PAN area. This means that PAN \$/ha taxation values decrease with increasing PAN area.
- The suitability rating coefficients (Table 4.3) for the POC and AOI PAN \$ and PAN \$/ha values effectively remain the same, i.e., 0.0113 versus 0.0110, respectively. Similarly, the actual versus best-fitted values for the POC and AOI PAN \$ and PAN \$/ha (Figure 4.4) also remain affectively the same This confirms that the assessment values for farmlands and farm/woodland combinations increase with increasing potato crop suitability, as rated above and it does so regardless of total or per hectare PAN area.

- The building footprint coefficient for taxation is positive which indicates that taxation by property increases with increasing building footprints.
- For example, applying Eq. 4.1 to a 100 ha PAN with a 100 % suitability rating and buildings with a 100 m<sup>2</sup> footprint yields an assessment value of \$274,979. This turns out to be 12 times higher than a field with a “0” suitability rating.

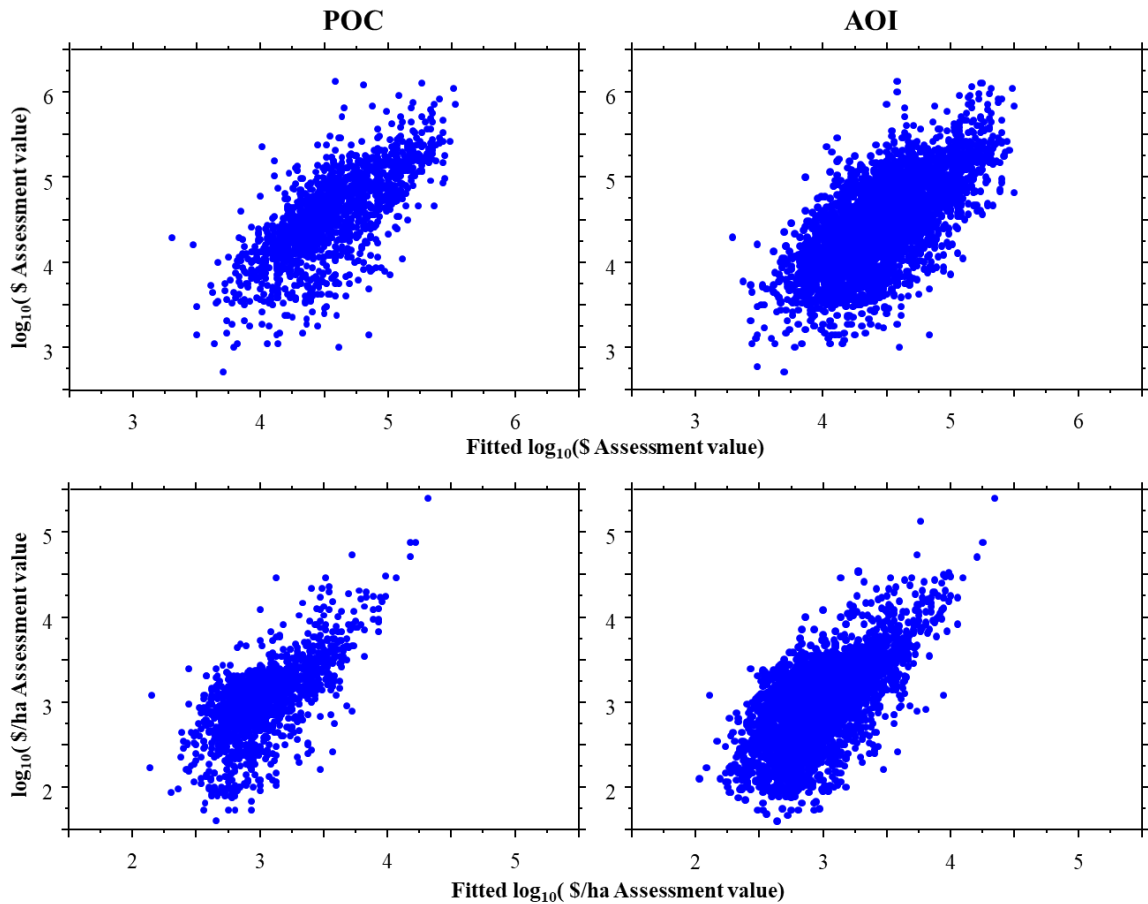


Figure 4.4. Actual versus best-fitted tax assessment scatterplots for \$ and \$/ha for each POC and AOI PAN, using PAN area, building area, and property type (farmlands versus farm and wood land combinations) as PAN-specific predictor variables.

#### **4.4. Conclusion**

The results obtained for the POC and AOI areas do not differ greatly according to results listed in Tables 4.1, 4.2, 4.3 and Figures 4.3 and 4.4. However, the mean suitability rating that is assigned to each PAN with soil drainage, slope and soil association as primary rating criteria is a significant tax assessment predictor along with PAN-specific property areas and building footprints. This suggests the following:

1. The crop suitability rating as described in Chapter 3 and Chapter 4 would in principle correlate with per-property income histories.
2. Since there is little POC versus AOI difference among the best-fitted regression coefficients, it is reasonable to expect that the methodology so established would work equally well to all other PAN-identified farmlands and farm/woodland combinations across NB. In general (Faber & Fonseca, 2014), choosing smaller areas for analysis such has greater extrapolation limitations than choosing larger areas as illustrated by the POC and AOI areas in Figure 4.1 and the standard error and t-value listings in Table 4.3.
3. While the actual procedures used to assess the tax base of individual farm and farm/woodland are in detail much more technical than what is represented above, it would seem that Eqs. 4.1 and 4.2 are helpful in reasonably estimating \$ assessment values of fields and properties by area and per hectare following forest clearing.
4. In so doing, once suitable areas are located for each specific socioeconomic context (e.g., locations adjacent to existing farmlands, active or abandoned farm fields),

these should be inspected regarding mapping veracity, and especially so by slope, drainage, and soil property conditions.

#### 4.5. Literature Cited

Cook, B. A. 1992. Forest property taxation in New Brunswick: A comment. *The Forestry Chronicle*, 335-338.

Faber, J., & Fonseca, L. M. 2014. How sample size influences research outcomes. *Dental Press Journal of Orthodontics*, 19(4), 27–29.

GeoNB. n.d. Website: <http://www.snb.ca/geonb1/>.

Government of New Brunswick. 2005. Report of the Auditor General. Chapter 3 Service New Brunswick Property Assessment for Taxation Purposes. Retrieved from <https://www.agnb-vgnb.ca/content/dam/agnb-vgnb/pdf/Reports-Rapports/2005v1/Chap3e.pdf>.

## **CHAPTER 5: COMPARISONS OF PUBLISHED FIELD- GENERATED CROP AND SOIL DATA WITH DSM- AND GIS- GENERATED DATA LAYERS**

### **5.1. Introduction**

This chapter presents and discusses results obtained by re-analyzing soil and potato crop properties from the perspective of terrain analysis (Moore et al., 1993). This is done for two published on-site fields (Perron et al., 2018). The re-analyzed soil and potato crop properties in this publication refer to (i) SM, (ii) electrical conductivity (EC), (iii) pH, (iv) clay content, (v) Mehlich-3 extracted P, and (vi) tuber yields for the Saint-André field, and (i) EC, (ii) Mehlich-3 extracted Ca and P, and (iii) tuber yields for the Centreville field (Figure 5.1). In this chapter, these properties are re-examined and re-interpreted by taking advantage of (i) the NB-wide availability of LiDAR-generated DEM at 1 m resolution, and (ii) the LiDAR-DEM projected cartographic depth-to-water concept (DTW).

### **5.2. Methods**

#### **5.2.1. Study Area**

The study area is comprised of two fields: one in Saint-André (21 ha; 47°06'58.6"N 67°47'54.2"W; PID 3510623) and one in Centreville (18 ha; 46°26'22.0"N 67°42'43.2"W; PID10263366). Both fields are located within the AOI, in northwestern NB (Figure 5.2 and Figure 5.3). Figure 5.1 shows historic aerial photos of the Saint-André field in September 2013, September 2015, September 2016, and October 2020. Figure 5.2 shows historic aerial photos of the Centreville field in September 2014, August 2016, July 2019, and May 2021.



Figure 5.1. Air photos of the Saint-André field (47°06'58.6"N 67°47'54.2"W) on A. 9/16/2013, B. 8/24/2015, C. 9/26/2016, and D. 10/11/2020. Source: Google Earth Pro.



Figure 5.2. Air photos of the Centreville field (46°26'22.0"N 67°42'43.2"W) on A. 9/1/2014, B. 8/22/2016, C. 7/8/2019, and D. 5/9/2021. Source: Google Earth Pro.

Perron et al. (2018) choose these fields to conduct their analyses because they have been well studied and are intensively used for potato (Russet Burbank) production. The Saint-André field has sandy loam soil texture while the Centreville field has a loamy to silt loamy soil texture. Drainage along the Saint-André field ranges from poor to well while the Centreville field drain varies from moderately well to well. Both fields are of glacial till origin, with coarse fragment representing 15-25 % of soil volume. The Saint-André field has a slope range of 0.5-5.0 % whereas the Centreville field has a slope range of 0.5-9.0 %. Neither field is subject to irrigation.

Figure 5.4 shows the LiDAR-DEM derived elevations for both fields. Figure 5.5 shows the 0 to 100 % crop suitability map for both the Saint-André and Centreville fields, derived according to the procedures described in Chapter 2. For this rating, the 0-33, 33-

66, and 66-100 % ranges can be considered poor (coloured red), fair (coloured yellow), and good (coloured green), respectively.

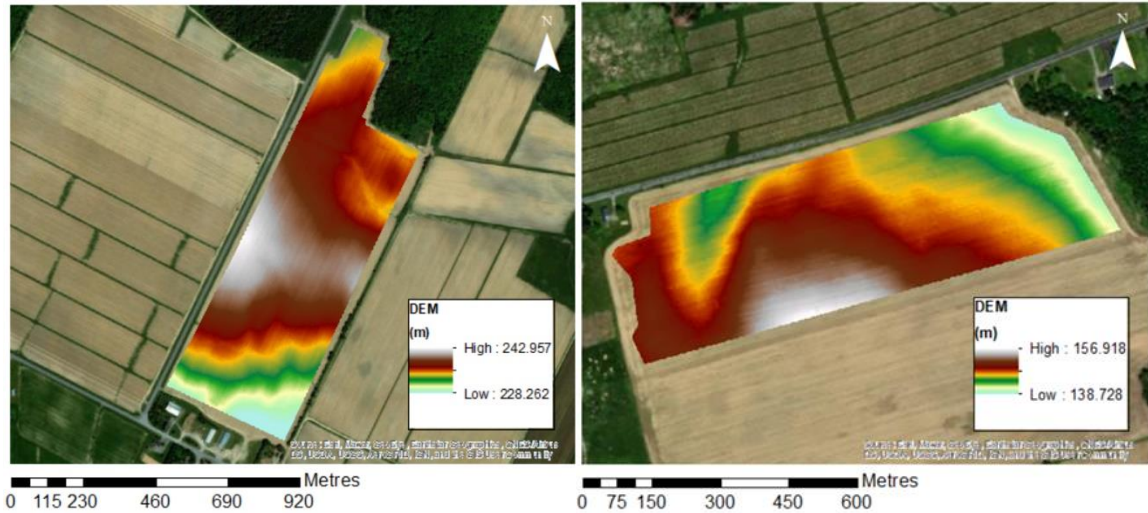


Figure 5.3. LiDAR DEMs for the Saint-André field (left; elevations 228.3 to 243.0 m) and the Centreville field (right, elevations 138.7 to 156.9 m). Source: GeoNB.

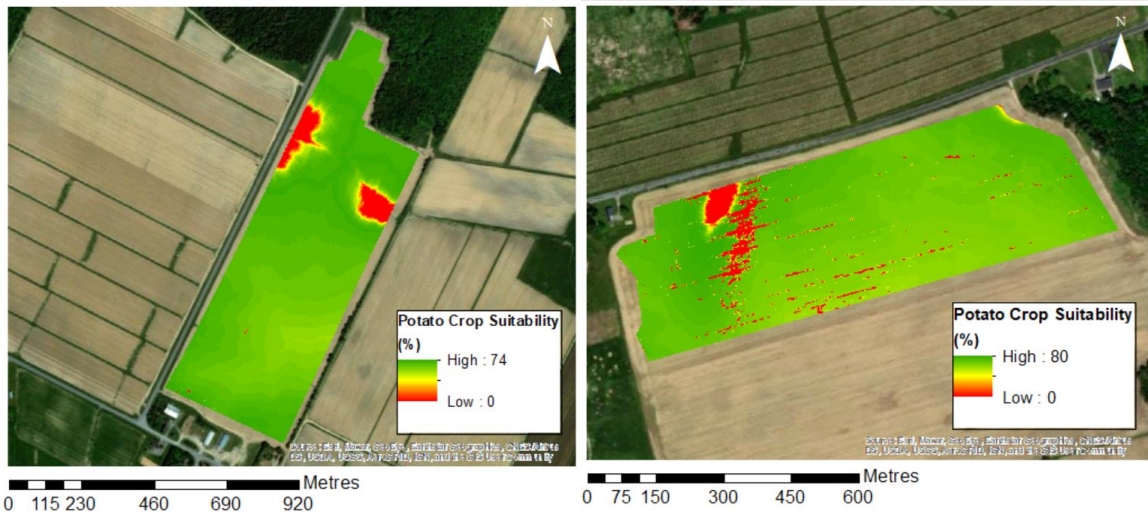


Figure 5.4. Potato crop suitability rating in % for the Saint-André and Centreville fields, with crop suitability coloured red (poor) through yellow (fair) to green (good).

The NB-wide DEM coverage was used to generate the 1 m resolution DEM rasters for the two fields in Figure 5.4. The map-presented soil and tuber yield data in Perron et al. (2018) refer to (i) EC ( $EC_{a0-0.3m}$  and  $EC_{a0-1m}$ ), (ii) tuber yield during 2013, 2014, and 2016 (Mg/ha); (iii) clay (g/kg), (iv) SM (%), (v) P (mg/kg), and (vi) Ca (mg/kg) of the two

fields were taken from paper. These images were “geo-processed” as described below. DSM-derived layers on SOC (%), pH, EC (mS/m), clay (%), PWP (%), Sand (%), Db (g/cm<sup>3</sup>), and FC (%) at soil depth 0-20 cm were obtained from Furze (2018). Figure 5.6 provides a collage of the individual soil property maps for the St-André and Centreville field locations.

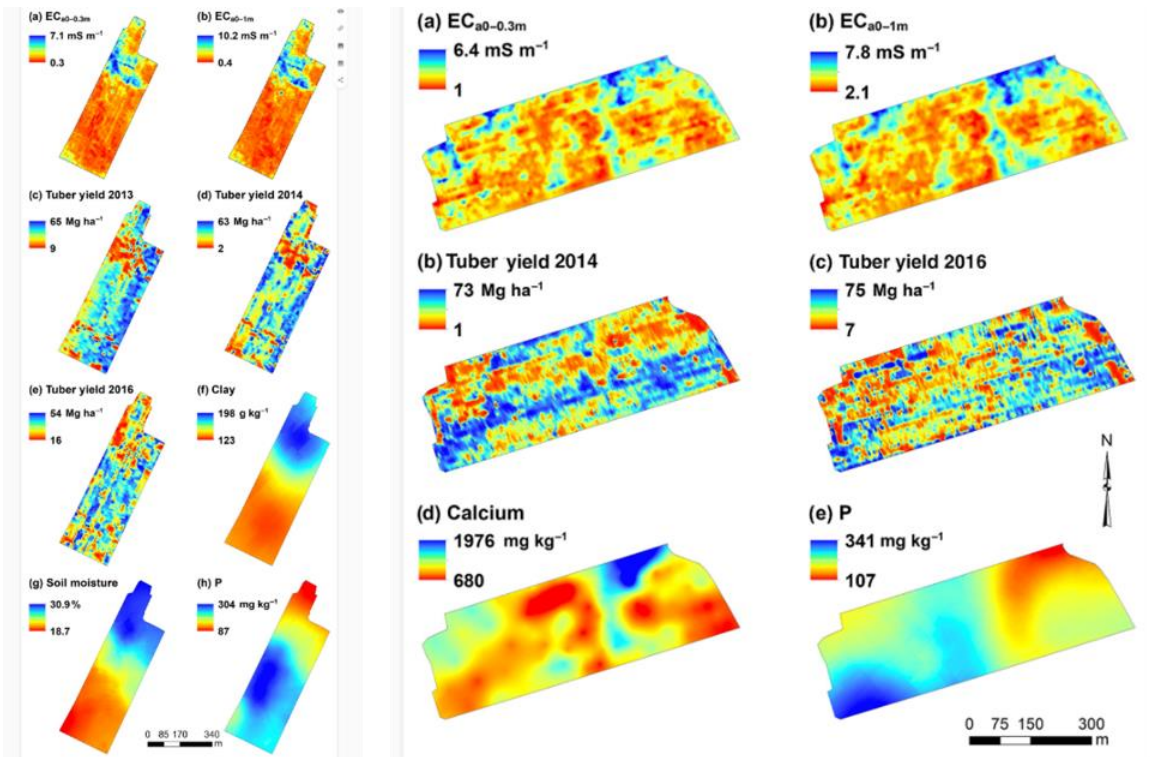


Figure 5.5. To the right: Kriging maps of the apparent soil EC measured (a)  $EC_{a0-0.3m}$  and (b)  $EC_{a0-1m}$ ; tuber yield (c) 2013, (d) 2014, and (e) 2016; and (f) clay, (g) SM, and (h) Mehlich-3 extracted P of the Saint-André field. To the left: kriging maps of the apparent soil EC (a)  $EC_{a0-0.3m}$  and (b)  $EC_{a0-1m}$ ; tuber yield (c) 2014 and (d) 2016; and Mehlich-3 extracted (e) Ca and (f) P for the Centreville field. Source: Perron et al. (2018).

### 5.2.3. Geoprocessing and Statistical Analyses

The images were “geo-referenced” in ArcMap 10.7.1 using the *Add Control Points* function. Then, the *IsoCluster Unsupervised Classification* tool was used to reclassify the images raster bands. The resulting layers were then reclassified with their appropriate scale.

The *Focal Statistics* tool was used to smooth out the layers. Then, the maps so re-created were point-digitized for each soil and crop property along 10 m fishnet grid using the *Create Fishnet* tool. This point-digitization was also applied to the field-specific elevation and DTW rasters. The *Extract Multi Values to Points* tool was used to extract cell values of above-mentioned layers. The resulting layers containing the point data for elevation, DTW, soil properties and tuber yields were analyzed in terms of basic statistical summaries and multivariate and non-linear regression analyses in StatView 5.0. The DTW mapping and analysis processes involved two steps:

1. Applying the DTW=0 definition to all flow channels with > 4 ha upslope flow accumulation areas.
2. Inspecting the soil moisture determination by Perron to locate drainage-promoting flow-channel segments to remove the DTW = 0 definition along these segments (Figure 5.7). This was done to ensure that field-measured SM (%) content would be proportion to increasing DTW.

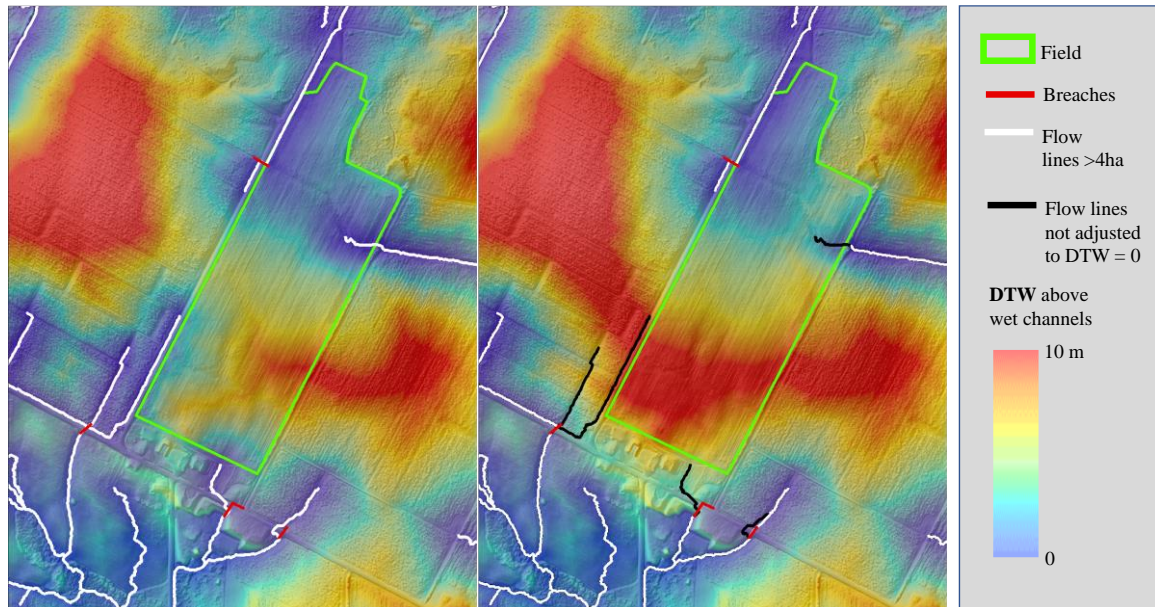


Figure 5.6. LiDAR-DEM generated DTW with > 4 ha upslope flow accumulations centered on the Saint-André field before (left) and after (right) DTW = 0 flow-channel adjustments.

### 5.3. Results and Discussion

#### 5.3.1. Saint-André Field

Figure 5.8 shows the Perron et al. (2018) reconstructed data layers for the Saint-André field regarding a)  $EC_{a0-1m}$ , b)  $EC_{a0-0.3m}$ , c) clay, d) tuber yield 2013, e) tuber yield 2014, f) tuber yield 2016, g) P, h) SM (%). The best-fitted regression equations for these layers are presented Table 5.1 and by the corresponding plots in Figure 5.9. The equations for  $EC_{a0-1m}$ ,  $EC_{a0-0.3m}$ , clay, and P were generated using the fishnet-point extracted values for these properties and for the channel-modified DTW layer. The 2013, 2014 and 2016 tuber yield equations were analyzed by averaging the tuber yield per each DTW 1 m class from 0.5 m upwards, with the results shown in Figure 5.10.

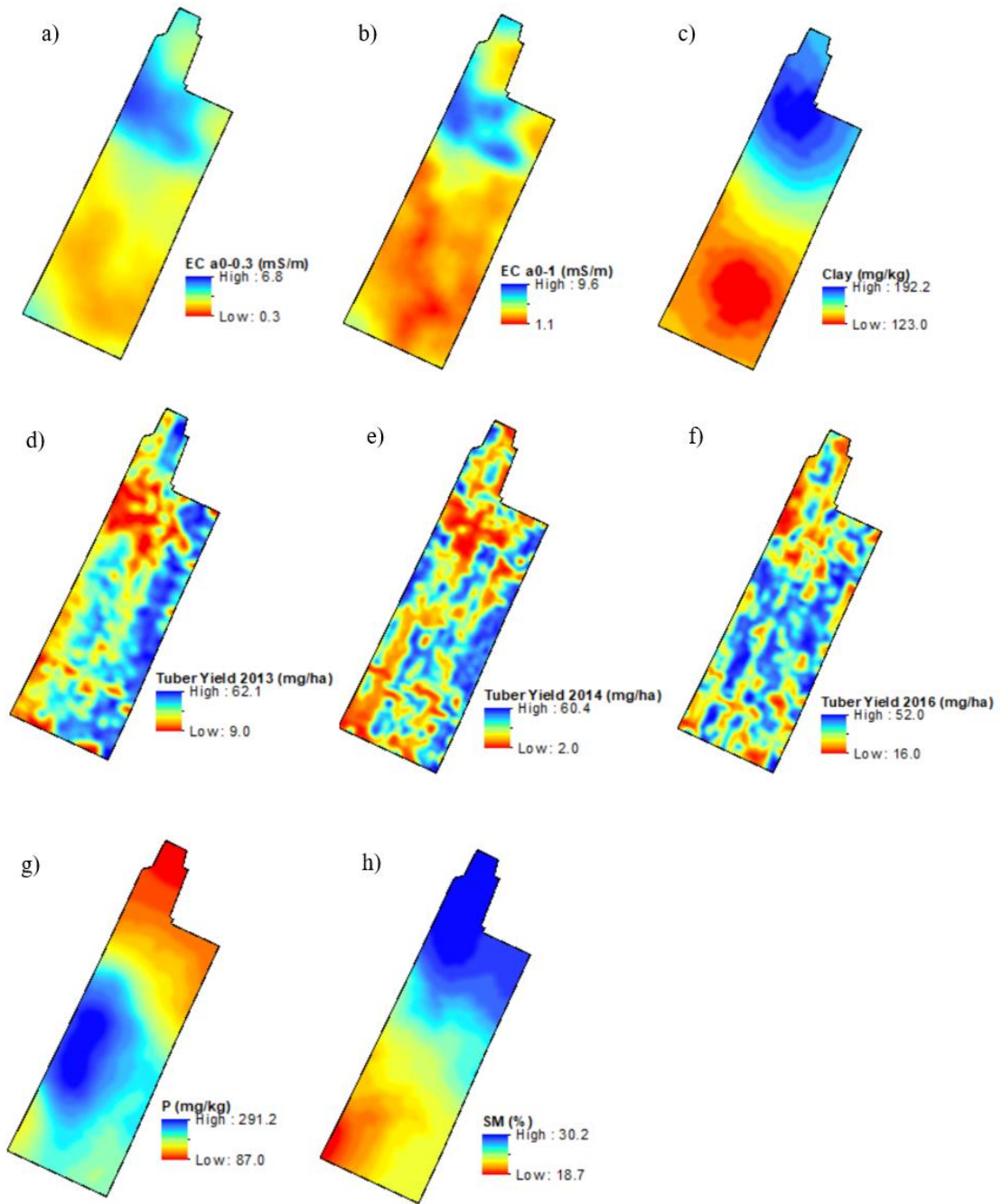


Figure 5.7. Results generated from Perron et al. (2018) for the Saint-André field (47°06'58.6"N 67°47'54.2"W).

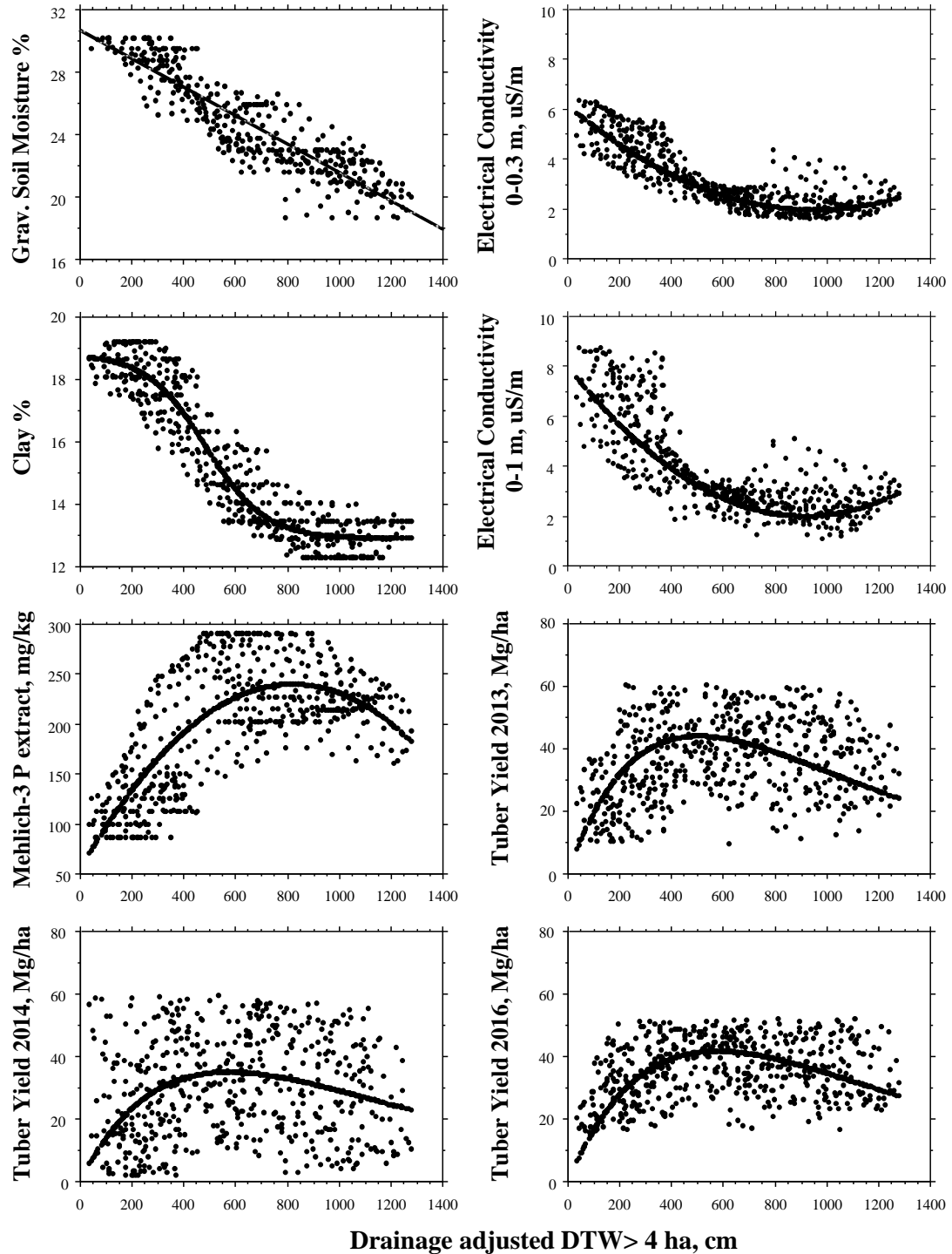


Figure 5.8. Fishnet-extracted data on gravimetric SM, EC ( $EC_{a0-0.3m}$  and  $EC_{a0-1m}$ ), Clay content, Mehlich-3 extracted P, and 2013, 2014, and 2015 tuber yields (Mg/ha) from Perron et al. (2018), with best-fitted drainage-adjusted DTW projections for the Saint-André field.

Table 5.1. Best-fitted trend results with equations for average tuber yield, SM (%), EC (mS/m), Mehlich-3 extracted P, and clay (%), per modified DTW class (0-1, 1-2, 2-3 m, etc.).

Variable	Year	a	b	c	R <sup>2</sup>	RMSE
Tuber Yield	2013	18.0 ±0.8	0.154 ±0.005		0.829	0.30
	2014	14.5 ±0.7			0.338	0.59
	2016	17.4 ±0.8			0.636	0.36
SM %		30.5 ±0.1	-0.95 ± 0.02		0.863	1.27
ECa		5.90 ±0.08	-0.84 ± 0.03	0.046 ± 0.003	0.765	0.6
ECb		7.86 ±0.14	-1.29 ± 0.06	0.074 ± 0.005	0.686	1.1
P		67.6 ±4.9	46.7 ± 2.0	-3.04 ± 0.16	0.662	3.6
Clay		5.2 ±0.3	1.1 ± 0.2	5.0 ± 0.20	0.985	0.10

Tuber yield (Mg/ha) = a DTW exp(-b DTW)

SM (%) = a + b DTW

ECa (mS/m), ECb (mS/m), Melich P (mg/kg) = a + b DTW + c DTW<sup>2</sup>

Clay (%) = a (1-1/(1+exp(-b (DTW -c)))) + d; d = 13.0 ± 1.0

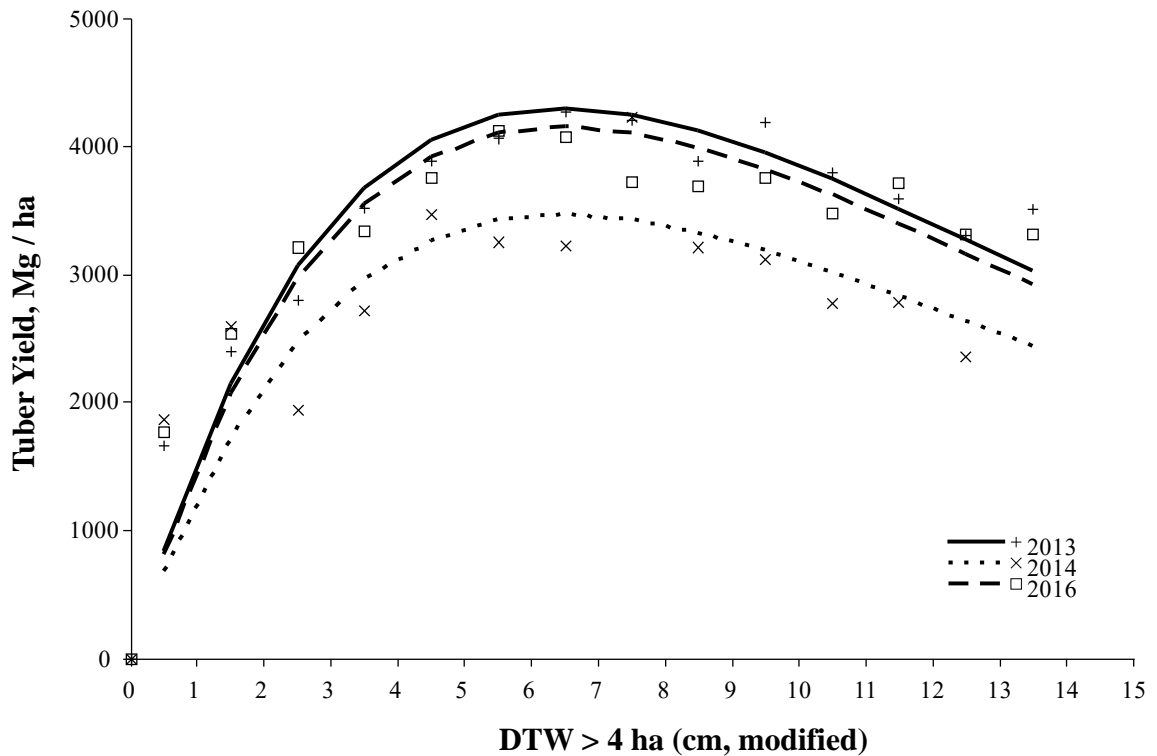


Figure 5.9. Averaged 2013, 2014 and 2015 tuber yields (Mg/ha) per 1 m modified DTW classes on the Saint-André field.

The combined Table 5.1 and Figures 5.10 and 11 results suggest a strong dependency between tuber yields, clay (%), Mehlich-3 extracted P and soil moisture content as these vary across the field from lower to higher elevations. In particular, and as

expected, soil moisture increases with decreasing DTW. On the Saint-André field, clay (%) is also systematically increasing by about 6 % towards the low DTW location. This increase is likely due to an increasing up-to 6 % downhill difference between increasing Silt and decreasing Sand content (see Chapter 6). The electrical conductivity determinations are lowest along the slopes at the DTW = 8 m locations and increase slightly from there to the higher elevations, and strongly increase from there to the lower DTW locations. Part of this is likely related to gravitational water flow by which dissolved ions not only accumulate in the lower locations but is further concentrated there due to wet-soil facilitated evapotranspiration. Along the ridge area, electrical conductivity would also increase due to enhanced wind exposure. Mehlich-3 extracted P also peaks at DTW = 8 m. This could be related to better P retention where the soil is not too dry and not too wet. The drier upslope areas generally tend to be shallower and are eroded therefore may contain lower amounts of P retaining minerals and organic matter. Toward wetter soils, soil pH tends to increase which implies low P retention by Al and Al oxides/ hydroxides.

Tuber yields tend to vary by soil conditions when too wet and when too dry: too dry implies reduced photosynthesis due to reduced evapotranspiration; too wet leads to insufficient root uptake of oxygen due to high biological oxygen demands throughout drainage-challenged soils. According to Figure 5.11, optimal tuber yields occurred where DTW  $\approx$  6 m. Interestingly, 2014 tuber yields in 2014 were on average and across the soil moisture and DTW range about 8 Mg/ha lower than in 2013 and 2016. While this could be related to a sustained difference in wet/dry weather pattern between 2014 versus 2013 or 2016, it could also be due to repeated same-field potato cropping during 2013 to 2014. Potato

cropping without intervening crop rotations engenders the proliferation of crop-harming soil organisms.

While soil moisture content will vary from day to day depending on the preceding and current weather pattern, the results Table 5.1 and Figures 5.10 and 11 suggest that there can also be a close relationship between SM (%) content and the channel-adjusted modified DTW data layer. This correspondence is revealed in Figure 5.12 by overlaying the fishnet extracted tuber yield and soil property data on the channel-modified DTW layer.

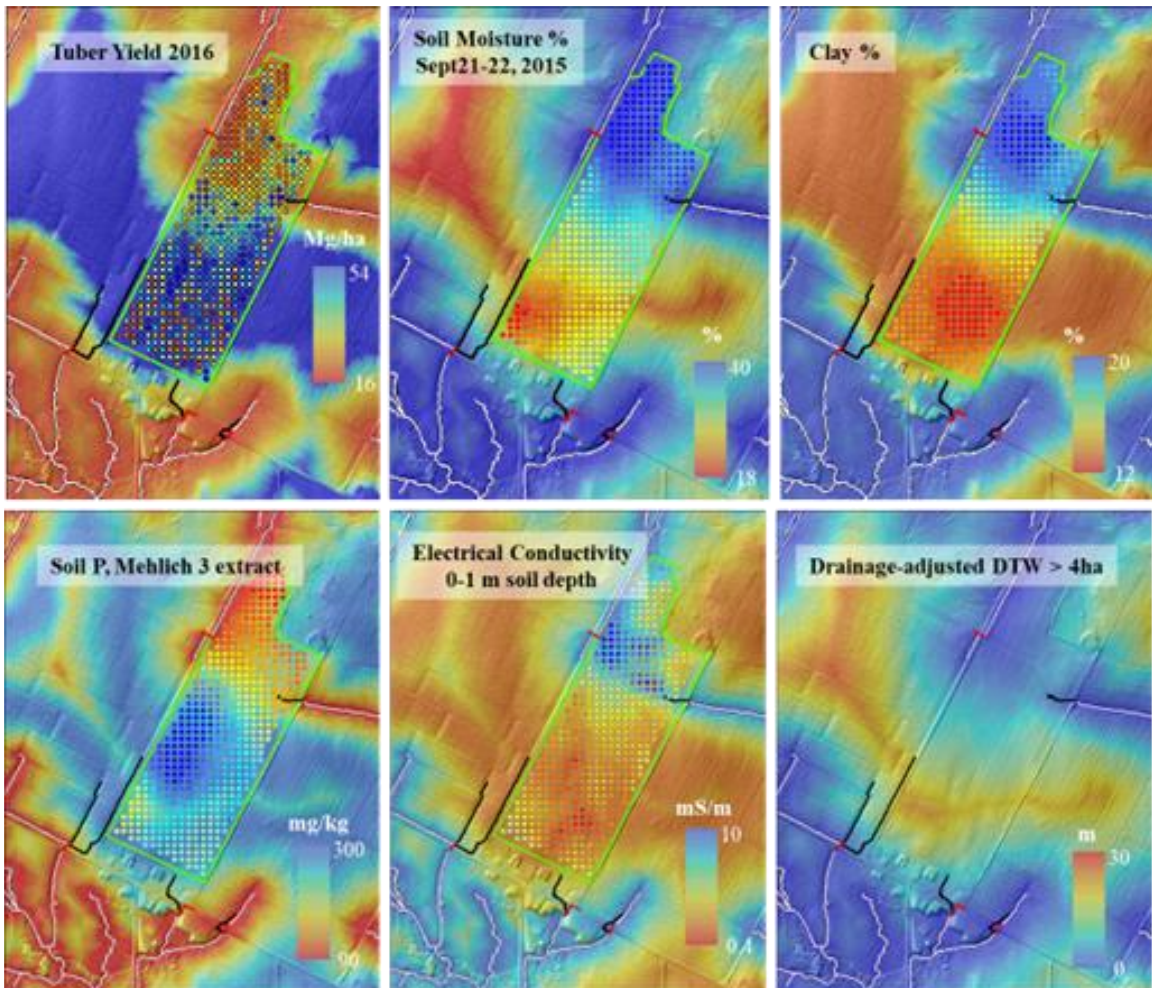


Figure 5.10. Overlays of the fishnet-extracted data on the drainage-adjusted DTW projections for tuber yield (2016), SM, clay, Mehlich-3 extracted P, and EC for the Saint-André field.

This close relationship cannot be expected to occur during dry but not wet or draughty weather conditions, so the time of determining yield-determining soil moisture requires weather related considerations.

### **5.3.2. Centreville Field**

Figure 5.13 shows the reconstructed Perron et al. (2018) data layers for the Centreville field for Tuber Yield 2014, 2016 (Mg/ha), EC 0-0.3 m and 0-1 m, clay (%), and Mehlich-3 extracted Ca and P (mg/kg). The best-fitted regression equations for these layers are presented in Figure 5.14. These plots and equations were generated using the fishnet-extracted values for these properties and for the DTW > 2 ha upslope flow accumulation areas. To illustrate, the > 2 ha and > 4 ha flow channels and DTW patterns are shown in Figure 5.15 on the left. In comparison, the best-fitted 2014 tuber yield raster with (bottom) and without (top) the fishnet-extracted 2014 tuber yields are shown in Figure 5.15 on top right and bottom right. Based on these results, it appears that tuber yields on the Centreville field are also influenced by DTW-influenced soil moisture patterns as they develop across the potato cropping season in response to the changing wet and dry weather conditions. The difference between the Centreville and the Saint-André field are likely related to corresponding changes in texture-related soil-specific water flow and moisture retention. To this effect, the sandy-loam, textured Saint-André field and its flow channels with > 4 ha upslope flow accumulation would be well-drained. In contrast, drainage would be somewhat slower along the loam to clay-loam textured Centreville field thereby prolonging moist soil conditions along the flow channels with >2 ha upslope flow accumulation. Doing a sensitivity analysis pertaining to all the fishnet-extracted soil properties depicted in Figures 5.10 and 5.14 in relation to > 1 > 2 and the > 4 ha upslope

flow accumulation revealed that >2 ha and modified > 4 ha DTW patterns captured the soil property trends across the Centreville and Saint-André fields the best, respectively. This is especially so revealed when analyzing the mean soil property values per 1 m DTW classes (Table 5.2).

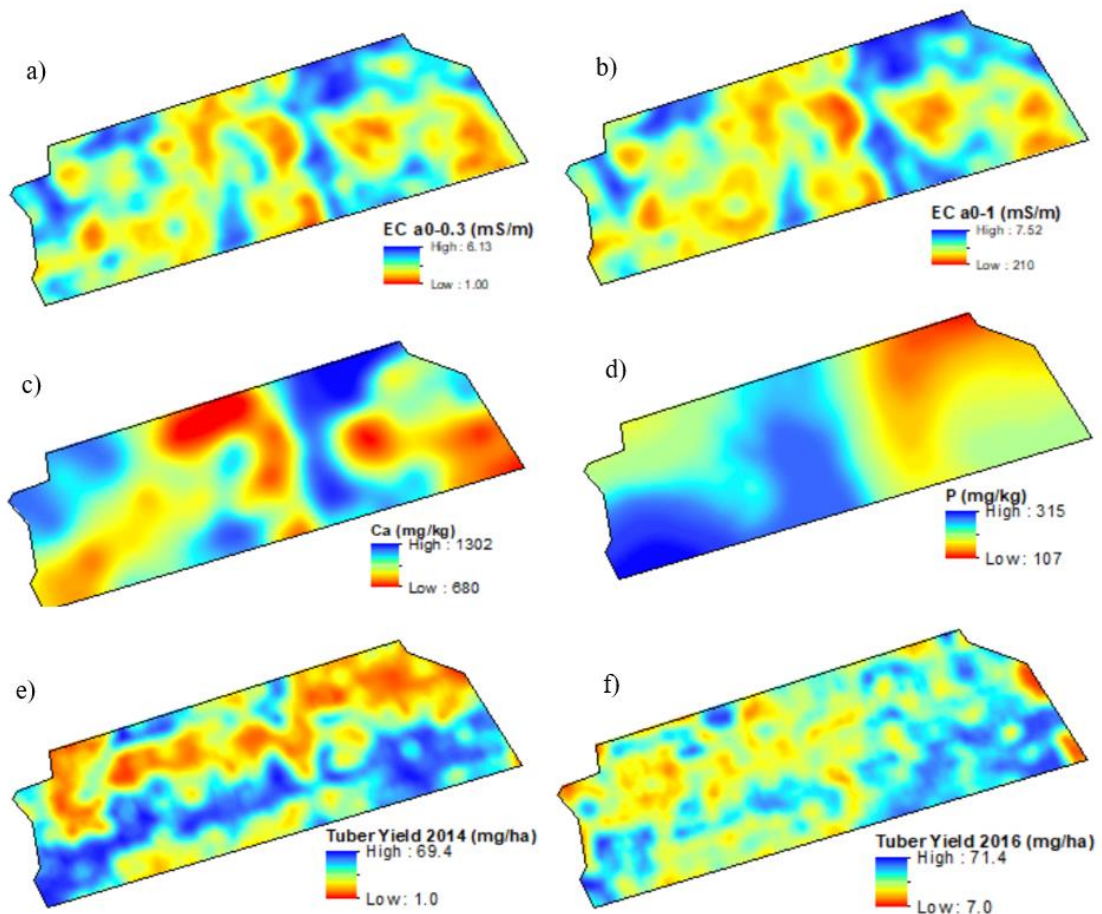


Figure 5.11. Results generated from Perron et al. (2018) for the Centreville field (46°26'22.0"N 67°42'43.2"W).

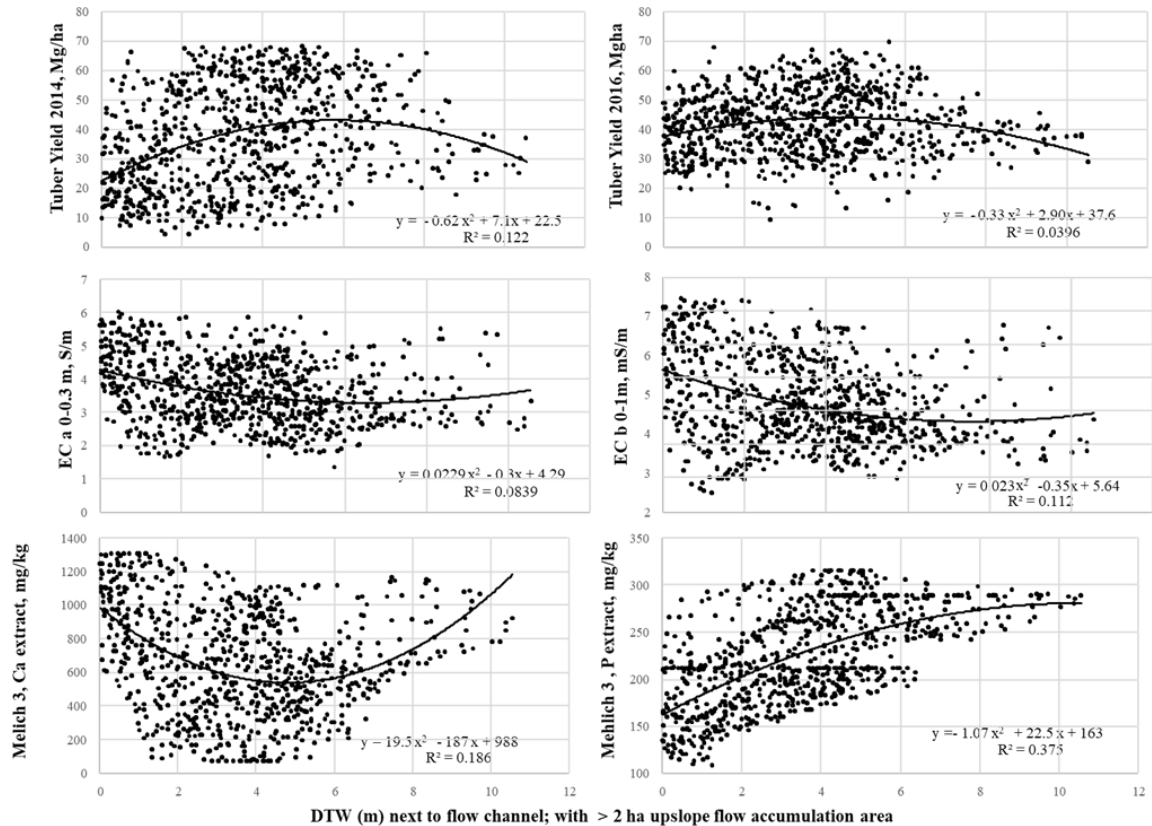


Figure 5.12. Fishnet extract values for 2014 and 2015 tuber yields, EC (EC<sub>a0-0.3m</sub> and EC<sub>a0-1m</sub>), and Mehlich-3 extracted Ca and P for the Centreville field. Also shown are the best-fitted trend lines with their regression equations.

Further in comparison, the overall DTW > 2 ha patterns for EC and P are more variable and less pronounced for the Centreville field than for the Saint-André field. In part, this may be due to (i) the shorter 10.5 m uphill-to-downhill range from drier to wetter along the Centreville field, versus 14 m on the Saint-André field. In addition, the effect of surface erosion would - in principle - be less pronounced on the Centreville soil because of its calcareous parent material, which would facilitate Ca and organic matter binding soil aggregation. However, soil depths would still be shallower on the higher ground locations where extractable Ca and P concentrations are presumably higher because of a higher exposure of the underlying soil parent material. Towards the lower slopes, extractable Ca and P divert from one another with Ca increasing and P decreasing with each maintaining

a high variability range. For Ca, this trend would relate to continued transfer of  $\text{Ca}^{2+}$  ions from uplands to lowlands, followed by retention organic matter and fine textures mineral particles. For P, this trend would relate to increased pH-related P-solubility and subsequent loss of p from the lower slope locations, as also appears to be the case for the Saint- André location.

In all of this, past cropping actions including liming combined fertilizer with P additions would add to the tuber yield, extractable Ca and P and electrical conductivity variations across the Centreville field. This being so, it is noteworthy that clear DTW-related uphill-downhill patterns can be recognized and can therefore be quantified as illustrated in Figure 5.16, which – in turn – facilitates mapping.

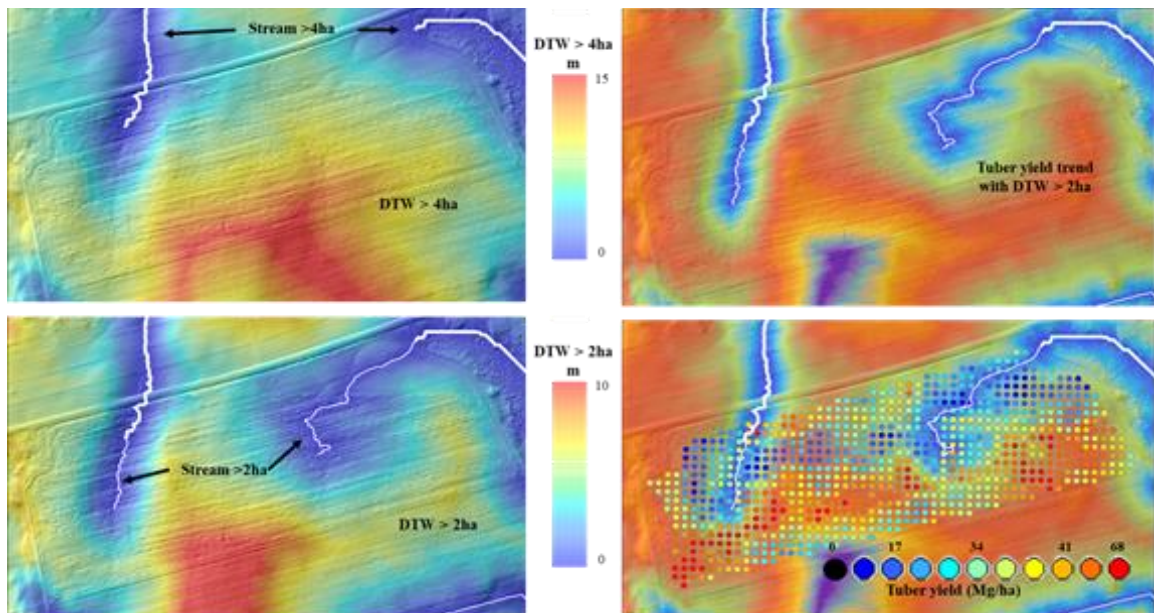
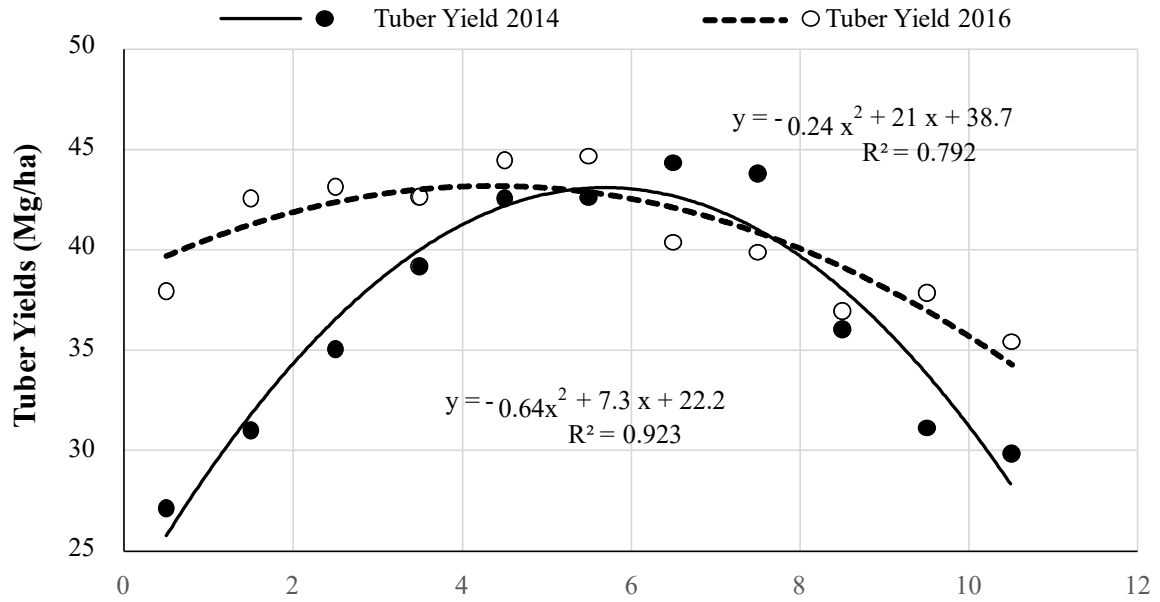


Figure 5.13. Depth-to-water patterns (DTW) along flow channels with > 2 and > 4 ha upslope flow accumulation for the Centreville field (left), compared with the DTW > 2 ha evaluated tuber yield pattern (top right) overlaid with fishnet-extracted tuber yield points (bottom right).



**DTW (m) along flow channels with > 2ha upslope flow accumulation areas**

Figure 5.14. Mean 2014 and 2016 tuber yields per 1- m DTW > 2 ha classes from DTW > 2ha = 0.5 m upwards. Also shown are their best-fitted regression lines and equations. The 2014 versus 2016 differences are likely due to year-by-year variations in seasonal weather and field-specific crop management patterns.

**5.5. Conclusion**

The results of this Chapter show that the LiDAR-DEM flow channels and associated depth-to-water layers can be used to reveal some of the cross-field soil property and tuber yield trends. For best results, however, the flow channels and DTW delineation process needs to be modified. For example, fast drainage across the field would lead to drier uphill soils which – in turn – would imply choosing flow channels with greater upslope flow accumulation areas. Doing so was needed to account for the DTW > 4 and > 2 ha related differences in data variations across the coarse-textured Saint-André field versus the fine-textured Centreville field respectively. In addition, it was necessary for the Saint-André field to eliminate the automatic DTW = 0 m assignment along some of the flow channels with > 4 ha upslope flow accumulation network to get the best possible

emulation of the cross-field data variations, and especially so for the reported soil moisture variations.

While the cross-field data for the Saint-André and Centreville fields are highly variable and remain especially so for tuber yields, they all shared consistent property specific trends across the flow-channel modified DTW ranges. These trends, whether established by property-versus-DTW scatterplots or plotting mean property values versus 1 m DTW classes, refer to the following:

1. Tuber yields would be optimal at DTW = 4 to 6 m with tendencies towards lower values uphill as well as downhill (Figures 5.15, 5.14).
2. Electrical conductivity would be lowest at DTW = 6 m (Figures 5.15, 5.14).
3. Melich 3 extractable P would decrease towards DTW = 0 (Figures 5.15, 5.14).
4. For the Saint-André field there is also a clear trend towards increased clay content towards DTW = 0, but only by 6 % (Figure 5.10). This difference would likely be due to the downslope accumulation of upslope eroded silt which would be greater than upslope eroded sand (Chapter 6).
5. For the Centreville field, there is a clear trend of downslope Ca accumulation (Figure 5.14)

With decreasing DTW, one could expect tuber yields to approach 0, but this would only be the case where DTW = 0 would correspond to very poorly-drained soil locations. In this regard, the Saint-André field would have poorly-drained areas along the likely permanent flow channels with > 4 ha upslope flow accumulation along its norther part. For the Centreville field, such channels only approach at the northwestern and eastern margin. In many cases, soils that would be located at or near DTW = 0 defining flow channels with

> 1, > 2 and > 4 ha upslope flow accumulation areas could be receiving well-aerated and therefore growth promoting seepage flows. Hence, the tuber yield versus DTW = 0 plots in Figures 5.10, 5.14, 5.16 do not converge to 0 when DTW = 0.

## 5.6. Literature Cited

- Furze, S. 2018. *A high-resolution digital soil mapping framework for New Brunswick, Canada* [PhD Thesis, University of New Brunswick].
- GeoNB. n.d. Website: <http://www.snb.ca/geonb1/>.
- Moore, I. D., Gessler, P. E., Nielsen, G. A., & Peterson, G. A. 1993. Soil Attribute Projection Using Terrain Analysis. *Soil Sci. Soc. Am. J.*, 52, 443-452.
- Murphy, P. N. C., Ogilvie, J., & Arp, P. A. 2009. Topographic modelling of soil moisture conditions: A comparison and verification of two models. *European Journal of Soil Science*, 60(1), 94–109.
- Perron, I., Cambouris, A. N., Chokmani, K., Gutierrez, M. F. V., Zebarth, B. J., Moreau, G., Biswas, A., & Adamchuk, V. 2018. *Delineating soil management zones using a proximal soil sensing system in two commercial potato fields in New Brunswick, Canada*. 737(November), 724–737.
- Zebarth, B. J., Drury, C. F., Tremblay, N., & Cambouris, A. N. 2009. Opportunities for improved fertilizer nitrogen management in production of arable crops in eastern Canada: A review. *Canadian Journal of Soil Science*, 89(2), 113–132.
- Zhang, N., Wang, M., & Wang, N. 2002. Precision agriculture - A worldwide overview. *Computers and Electronics in Agriculture*, 36(2–3), 113–132.

# **CHAPTER 6: RE-EXAMINING SOIL VARIATIONS ACROSS A HUMMOCKY FIELD UNDER INTENSIVE POTATO PRODUCTION USING A CARTOGRAPHIC DEPTH-TO-WATER MAPPING PROTOCOL**

## **6.1. Abstract**

This chapter re-examined field-surveyed elevation (5 m grid) and soil property variations (25 m grid) across a hummocky field under intensive potato production using a cartographic depth-to-water (DTW) mapping protocol. This protocol was enabled by NB wide 1 m resolution LiDAR-generated DEM performed in 2017. The soil and the elevation grid surveys were done in 1997. Analyzing the 1997 and 2017 elevation data together revealed small but significant erosion-caused elevation changes across the field, with silt (%) and DTW above streams with > 4 ha upslope flow accumulation areas accounting for upslope and downslope soil losses and gains. The DEM-generated DTW > 4 ha patterns could affect the documented soil physical and chemical distribution patterns across the field, such that sand CF were found to increase with increasing DTW, while silt decreased in the same direction. Soil moisture and nitrate nitrogen (NO<sub>3</sub>-N) also increased with decreasing DTW. Based on these correlations, the DTW > 4 ha pattern then also influenced soil carbon (C), pH, ammonium nitrogen (NH<sub>4</sub>-N), Caesium<sup>137</sup> (Cs<sup>137</sup>), and Mehlich-3 extracted Ca, Mg, K, iron (Fe), manganese (Mn), copper (Cu), and zinc (Zn), at least to some extent. Factor analyzing the data revealed that more than 50 % of the combined data variations were dominated by three factors. These could be interpreted as:

1. A soil loss factor strongly associated with the DTW and soil texture patterns across the field.

2. A soil cropping factor dealing N, P, K, Ca, Mg, and S additions to the soil.
3. A metal-complexing soil OM factor which also accounted for NO<sub>3</sub>-N leaching.

## **6.2. Introduction**

The purpose of this study is to re-analyze selected soil properties for a hummocky farm field in NB. As published by Zebarth et al. (2002). In this publication, the elevations were field surveyed using a 5 m grid spacing. Soil textural, morphological, and chemical properties were determined along a 7 x 17 m grid with 25 m spacing. The re-analysis of these data was facilitated using LiDAR-generated 1 m resolution DEM. Doing so enable a finer hydro-pedological delineation of how the land grades from elevated to the depressed locations, quantifiable by way of the cartographic DTW mapping process (Murphy et al., 2015). The properties so analyzed refer to plough layer depth, soil texture, CF, soil organic carbon (SOC), pH, and soil extractable Ca, Mg, K, S, P, NO<sub>3</sub>-N, NH<sub>4</sub>-N, Fe, Mn, Cu, Zn, and Cs<sup>137</sup>.

## **6.3. Methods**

### **6.3.1. Study Area**

As summarized by Zebarth et al. (2002), the data was obtained from a hummocky 175 x 425 m farm field, approximately one km east of Harland, NB (Figure 6.1; 46°18'23"N 67°30'41"W). The bedrock-controlled surficial deposit (< 2 m) refers to a sedimentary-derived loamy lodgment till with minor calcareous content. The soils that developed in this till refer to an Orthic Humo-Ferric Podzols, and the Carleton (CA) forest soil unit association. Cultivation, which started 120 years ago, transformed the original forest soil and related mound and pit topography underneath northern tolerant hardwoods to a smoothed surface with interrupted soil layer sequences. Across the surveyed field and

beyond, intensified crop management including potato cropping since the 1950 would have induced to slope-dependent soil erosion followed by re-deposition in depressions, estimated to amount to 22 to 53 tons/ha/year. Annual precipitation amounts to 1096 mm, with 796 mm as rainfall 100 mm/month from May to September. The mean monthly May to September temperature is 14.9 °C, with annual mean daily air temperature at 4.0 °C.



Figure 6.1. To the left: NB basemap with AOI (yellow boundary) used for LiDAR-based potato crop suitability mapping and evaluation. To the right: this chapter's study area, an agricultural field located approximately 1 km east of Harland, NB (46°18'23"N 67°30'41"W). Basemap source: GeoNB.

### 6.3.2. Soil Analysis

The surface soil (primarily A-layer) was sampled (augured) and analyzed along the 25 m grid for soil texture (hydrometer method without OM removal), CF content, and SOC concentration (combustion method using a Leco CNS-1000 analyzer). Also determined were soil pH (1:1 water (H<sub>2</sub>O)) and Mehlich-3 extracted Ca, Mg, K, S, P, Fe, Mn, Cu, and Zn (Shiwakoti et al., 2019). The Mehlich-3 extract formulation is composed of 0.2 mole/litre (M) acetic acid (CH<sub>3</sub>COOH), 0.25 M ammonium nitrate (NH<sub>4</sub>NO<sub>3</sub>), 0.015 M

ammonium fluoride ( $\text{NH}_4\text{F}$ ), 0.013 M nitric acid ( $\text{HNO}_3$ ), and 0.001 M ethylenediaminetetraacetic acid (EDTA). Also determined were:

1. 0 to 15 cm depth soil moisture level on July 11, 1997, using time domain reflectometry.
2. Calcium chloride- ( $\text{CaCl}_2$ ) extractable  $\text{NH}_4\text{-N}$  and  $\text{NO}_3\text{-N}$ .
3.  $\text{Cs}^{137}$ , using a Tennelec germanium crystal gamma radiation counter.

All data was received from the Potato Research Centre of Agriculture and Agri-Food Canada in Fredericton, NB.

### **6.3.3. GIS Analysis**

The GIS analysis was conducted in ArcMap 10.7.1. Using the 1 m DEM and Tarboton's D8 algorithm generated the slope, filled, flow direction, flow accumulation, and flow channel rasters (Tarboton, 1997). The latter were classified into flow channel network with 4, 1, 0.25, and 0.1 ha upslope flow accumulations for flow initiation. The slope and reclassified flow-channels raster were used to determine the cartographic cost-distance derived DTW (in cm) so that the 4, 1, 0.25, 0.1 ha DTW classification would respectively represent DTW at the end of summer, following major storm events in summer, and at the intense time of the snow melt season (Figure 6.2). The surveyed point data were subsequently supplemented with their corresponding DEM and DTW extracted values using the *Multipoint Extraction* tool.

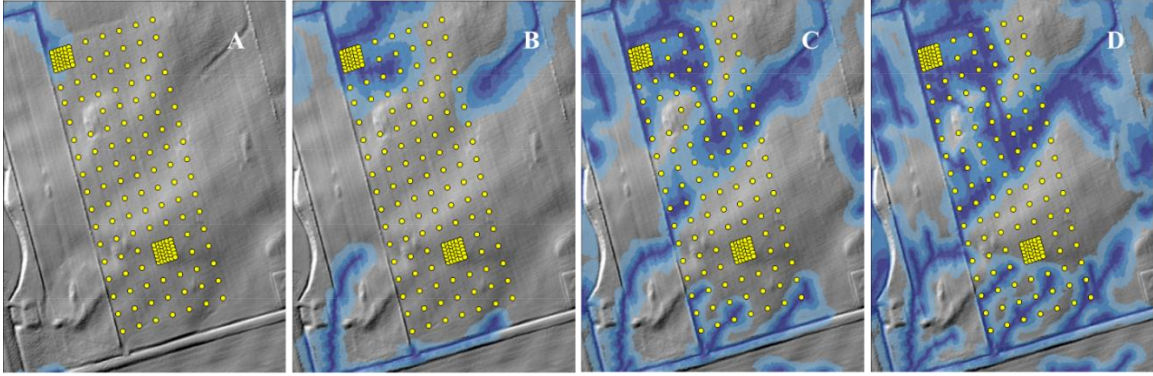


Figure 6.2. Survey grid and cartographic DTW associated from A to D, with the LiDAR and DEM derived flow channels with > 4 ha, 0.25, and 0.1 ha upslope flow accumulation areas overlaid on the hillshaded study area DEM, respectively. DTW grades from < 10 cm (dark blue) to 1 m (light blue) deep.

#### 6.3.4. Statistical Analysis

The combined and GIS generated point data were summarized using basic statistics, multivariate regression analysis, and factor analysis (3 factors, Varimax rotated). The results generated were summarized in the tables and are illustrated using factor plots and actual versus best-fitted scatter plots.

#### 6.4. Results and Discussion

A basic statistical summary of the field-surveyed variables is presented in Table 6.1, by listing the units and the mean, standard deviation, and minimum and maximum values of these variables. The correlations among these vary considerably, as shown in Table 6.2.

Table 6.1. Statistical summary of the field-surveyed variables. Units, mean, standard deviation, and maximum and minimum values of these variables are listed. [AP = plough water depth; CF = coarse fragment; C = carbon; Ca = calcium; Mg = magnesium; K = potassium; P = phosphorus; S = sulfur; Fe = iron; Mn = manganese; Zn = zinc; Cu = copper; Na = sodium; Cs<sup>137</sup> = caesium<sup>137</sup>; NO<sub>3</sub>-N = nitrate nitrogen; NH<sub>4</sub>-N = ammonium nitrate; pH-H<sub>2</sub>O = pH (1:1 water); SM = soil moisture content; DTW > 4 ha = depth-to-water > 4 ha; DEM = digital elevation model].

Variable	Units	Mean	Std. Dev.	Min.	Max.
Ap	m	33.5	4.4	15.0	44.5
CF	cm	34.6	7.7	17.8	53.6
Sand	%	34.5	3.7	26.5	44.0
Silt	%	45.4	2.7	37.7	50.8
Clay	%	20.1	2.1	14.5	24.5
C	%	2.21	0.26	1.40	3.55
Ca	mg/kg	1503.5	239.2	1082.8	2252.2
Mg	mg/kg	188.3	25.4	129.3	260.3
K	mg/kg	176.7	40.7	101.6	281.6
P	mg/kg	327.4	53.4	186.2	470.3
S	mg/kg	81.6	17.7	36.7	141.9
Fe	mg/kg	311.2	34.6	219.2	402.3
Mn	mg/kg	39.7	13.2	19.1	120.4
Zn	mg/kg	3.49	1.15	1.87	10.22
Cu	mg/kg	5.19	1.10	3.10	8.72
Na	mg/kg	40.7	22.4	16.6	107.7
Cs <sup>137</sup>	Bq/m <sup>2</sup>	1690.5	487.5	665.6	3248.5
NO <sub>3</sub> -N	mg/kg	5.47	2.48	1.93	15.85
NH <sub>4</sub> -N	mg/kg	0.48	0.19	0.00	1.01
pH-H <sub>2</sub> O	-	5.40	0.25	4.84	6.08
SM	%	17.4	1.8	13.7	25.7
DTW > 4 ha	cm	631.2	406.5	47.3	1261.9
DEM	M	136.0	2.8	132.0	141.3

Table 6.2. Correlation matrix for the variables listed in Table 6.1. Significant regression coefficients (> -0.300 or < 0.300) are highlighted in gray.

Variables	Ap	CF	Sand	Silt	Clay	C	Ca	Mg	K	P	S	Fe	Mn	Zn	Cu	Na	Cs <sup>137</sup>	NO3-N	NH4-N	pH-H2O	MC	DTW>4ha	DEM		
Ap	1																								
CF	-0.162	1																							
Sand	-0.238	0.785	1																						
Silt	0.289	-0.716	-0.843	1																					
Clay	0.058	-0.498	-0.723	0.237	1																				
C	0.16	-0.193	-0.276	0.363	0.031	1																			
Ca	0.247	-0.182	-0.234	0.265	0.083	0.128	1																		
Mg	0.21	-0.094	-0.191	0.154	0.147	0.178	0.766	1																	
K	0.108	0.368	0.206	-0.159	-0.167	-0.125	0.254	0.34	1																
P	0.08	0.228	0.324	-0.204	-0.324	-0.145	0.423	0.386	0.354	1															
S	-0.019	0.269	0.198	-0.204	-0.096	-0.095	0.095	0.124	0.4	0.263	1														
Fe	0.251	-0.194	-0.21	0.157	0.177	0.084	0.098	0.268	0.005	0.202	0.048	1													
Mn	0.186	0.031	-0.022	-0.024	0.071	-0.232	0.493	0.489	0.229	0.546	0.174	0.45	1												
Zn	0.097	-0.041	-0.068	0.054	0.053	0.118	0.144	0.1	0.024	0.224	0.093	0.23	0.309	1											
Cu	0.357	-0.375	-0.451	0.424	0.27	0.213	0.588	0.545	0.206	0.354	0.005	0.445	0.501	0.439	1										
Na	-0.093	0.284	0.272	-0.246	-0.175	0.078	-0.203	-0.246	-0.164	0.005	-0.207	-0.35	-0.153	0.075	-0.245	1									
Cs <sup>137</sup>	0.543	-0.417	-0.505	0.569	0.181	0.426	0.387	0.389	0.218	0.127	-0.058	0.273	0.188	0.089	0.557	-0.14	1								
NO3-N	0.023	-0.217	-0.316	0.277	0.216	-0.238	0.251	0.047	0.282	-0.052	0.214	-0.261	0.041	-0.055	0.122	-0.14	0.111	1							
NH4-N	-0.069	-0.134	-0.083	0.089	0.036	-0.084	0.023	-0.162	-0.252	-0.031	-0.23	-0.235	-0.018	-0.029	-0.005	0.356	-0.036	0.392	1						
pH-H2O	0.176	0.024	-0.028	0.036	0.004	-0.117	0.617	0.473	0.347	0.21	-0.202	-0.04	0.348	0.011	0.337	-0.07	0.202	0.12	0.014	1					
MC	0.203	-0.264	-0.495	0.422	0.352	0.137	0.355	0.364	0.268	-0.085	0.112	0.184	0.154	0.017	0.38	-0.304	0.406	0.242	-0.097	0.268	1				
DTW>4ha	-0.113	0.705	0.691	-0.61	-0.464	-0.058	-0.222	-0.126	0.115	0.258	-0.032	-0.092	0.088	0.042	-0.299	0.49	-0.309	-0.466	0.019	-0.025	-0.36	1			
DEM	-0.088	0.582	0.619	-0.555	-0.406	0.052	-0.442	-0.268	0.037	0.08	-0.046	-0.006	-0.116	0.04	-0.419	0.514	-0.278	-0.549	-0.078	-0.206	-0.39	0.821	1		

### 6.4.1. Field-Surveyed Versus LiDAR-Registered Elevation

Regressing the field against the LiDAR-elevation data produced a  $R^2$  value of 0.991, and a RMSE of 0.249 m, thereby suggesting a close agreement (Table 6.3, analysis A). Examining the actual field-versus LiDAR-surveyed residuals further with silt % and DTW > 4 ha as additional independent variables increase the  $R^2$  value to 0.995 and decreased the RMSE value to 0.190 m, i.e., an overall reduction of the residual variations by 25 % (Table 6.1, analyses A and B). The regression coefficients so generated indicate that the field was subject to field-internal elevation changes likely due to upslope soil erosion, which in turn increase the silt content along the lower ground locations along the flow channel with > 4 ha upslope flow accumulation. The maximum and minimum elevation differences across the field were 9.6 m in 2002, and 9.3 m at the time of the LiDAR survey which amounts to a 26 cm soil loss in detail. Assuming the soil density to be 1.6 g/cm<sup>3</sup> yields an overall soil displacement value of 3,360 tons/ha.

Table 6.3. Multivariable regressions (A, B, and C) regarding field-surveyed elevation with point-centered LiDAR-DEM, silt %, and DTW > ha as predictor variables.

Variables	Mean	Std. Dev.	Std. Error	Count	Min.	Max.
Surveyed elevation, m	51.9	2.61	0.19	190	47.6	57.2
LiDAR DEM, m	136.0	2.76	0.20	190	132.0	141.3
DTW > 4 ha, m	6.3	4.1	29.5	190	0.47	12.6
Silt, %	45.4	2.65	0.19	190	37.7	50.8
Surveyed Elevation Analysis	Regression Variables	Coefficient	Std. Error	Std. Coeff.	t-Value	p-Value
A: $R^2 = 0.991$ ; RMSE = 0.249 m	Intercept	-76.1	0.892	-76.1	-85.3	<.0001
	LiDAR DEM, m	0.941	0.007	0.995	143.5	<.0001
B: $R^2 = 0.99$ ; RMSE = 0.213 m	Intercept	-84.9	1.302	-84.9	-65.3	<.0001
	LiDAR DEM, m	1.009	0.010	1.07	102.7	<.0001
	DTW > 4 ha, m	-0.056	0.007	-0.087	-8.4	<.0001
C: $R^2 = 0.995$ ; RMSE = 0.190 m	Intercept	-81.7	1.2	-81.7	-65.6	<.0001
	LiDAR DEM, m	1.002	0.009	1.06	113.7	<.0001
	DTW > 4 ha, m	-0.070	0.006	-0.11	-11.2	<.0001
	Silt, %	-0.047	0.007	-0.047	-7.1	<.0001

#### 6.4.2. Regression Analysis: Sand, Silt, Clay, and Coarse Fragment

Plotting sand, silt, clay, and CF % versus DTW > 4 ha showed that sand increased but silt and clay % decreased with increasing DTW > 4 ha (Figure 6.3, left). The decreasing clay % content with increasing DTW > 4 ha relates directly to the upland silt loss, i.e., clay displacement did not occur across the field. Hence, the higher-lying areas were found to be coarser and sandier than the lower less well-drained areas, likely due to natural and recurring cropping-induced upland upland-to-lowland silt-displacing soil erosion. In this regard, Figure 6.3 (right) shows how the surveyed CF % values follow the underlying DTW > 4 ha pattern more closely than the hillshaded elevation pattern. Hence, the coarse-to-fine texture pattern across the field corresponds more closely with DTW > 4 ha than with the overall elevation change.

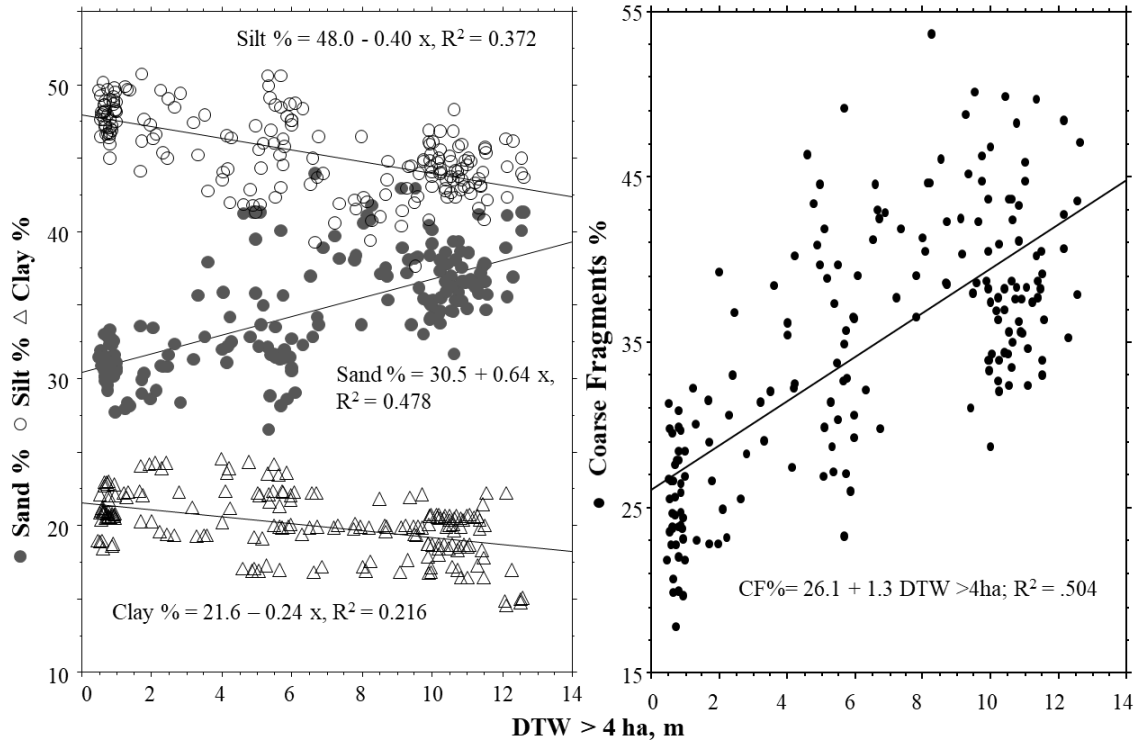


Figure 6.3. Sand, silt, and clay % (left) and very coarse, coarse and medium sand % versus  $DTW_{4ha}$  along the LiDAR-DEM-derived flow channels with > 4 ha upslope flow accumulation areas.

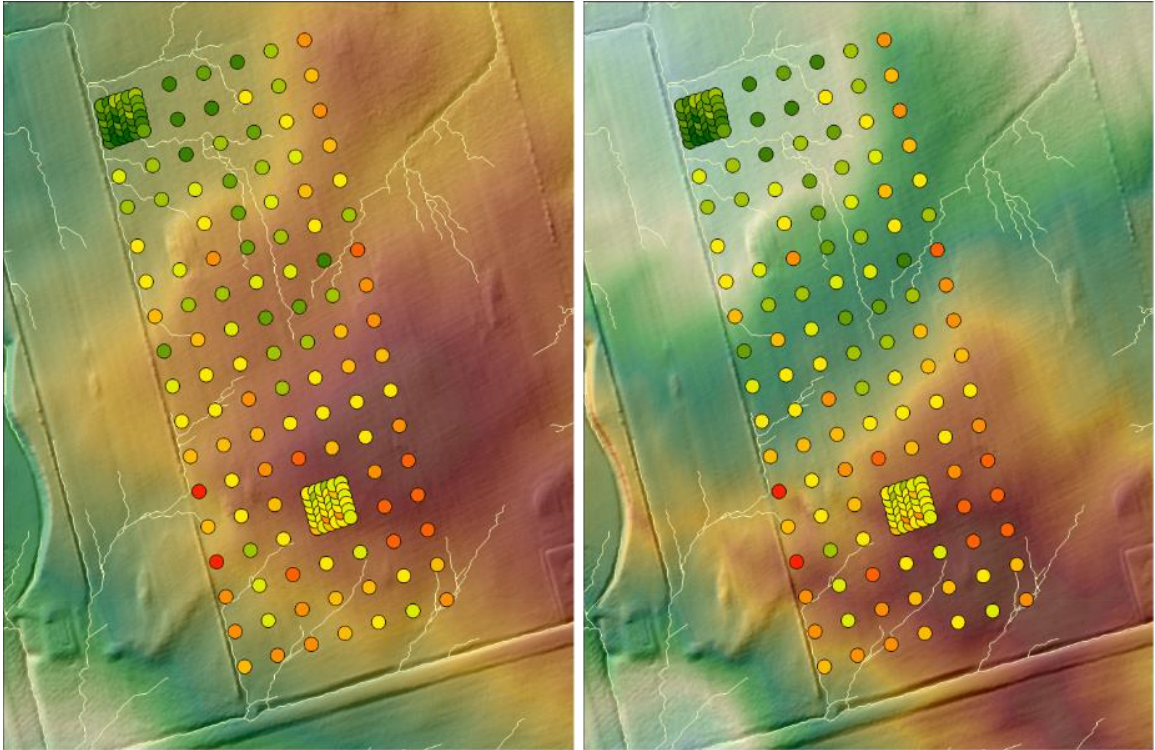


Figure 6.4. Left: surveyed CF % overlaid on the hillshaded LIDAR DEM. Right: surveyed CF % overlaid on the cartographic DTW. Grid colour: red (low CF %) to green (high CF %).

The very coarse (vc), coarse (c), and medium (m) sized fine (f) and very fine (vf) fractions of sand % also increased with increasing DTW > 4 ha, with the trend decreasing towards finer grain size such that  $vc \text{ sand } \% > c \text{ sand } \% > m \text{ sand } \%$  and  $no \text{ DTW } > 4 \text{ ha}$  and  $vf > \text{ sand } \%$  (Figure 6.5, left).

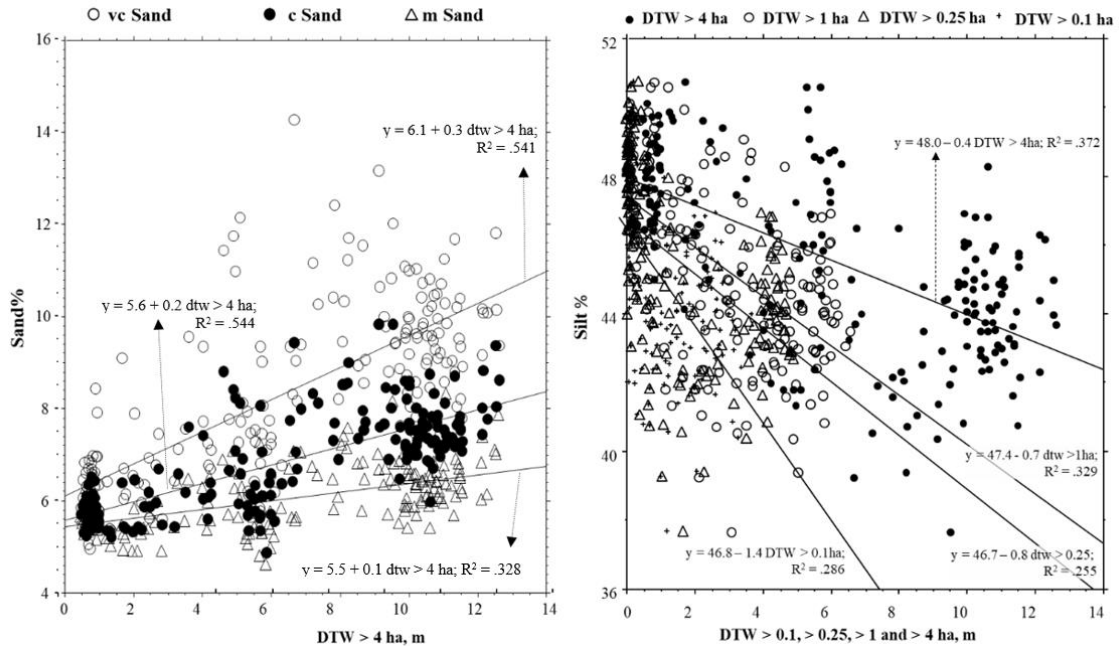


Figure 6.5. Left: decreasing trend from very coarse (vc) to coarse (c) and fine medium (m) sand % fractions versus DTW > 4 ha upslope flow accumulation, with regression equations. Right: silt % versus DTW (m) along the LiDAR-DEM-derived flow channels with DTW > 4 ha, > 1 ha, > 0.25 ha and > 0.1 ha upslope flow accumulation areas, with regression equations.

Testing to which extent the DEM-generated DTW > 4, 1, 0.25, and 0.1 ha pattern influence the textural components led to the regression results entered into Figure 6.5 (right). The corresponding  $R^2$  values decrease in the order: > 0.1 ha:  $R^2 = 0.286$ , > 0.25 ha:  $R^2 = 0.255$ , > 1 ha:  $R^2 = 0.329$ , > 4 ha:  $R^2 = 0.72$ . This means that the field-assessed variations in silt % are best expressed by the slope-affected cost distance between each survey point to its closest > 4 ha downstream location. The smaller the cost distance to the channels so marked, the more soil-eroded silt arrives and settles there due to recurring rains and /or snowmelt induced flooding.

### 6.4.3. Influences of Topography and Other Factors on the Surveyed Soil-Chemical Properties

Factors analyzing the correlation matrix (Table 6.3) of the variables in the Table 6.1 revealed three factors which account for 53 % of the total variance associated with the Table 6.1 entries. The oblique solution pattern for Factor 2 and Factor 3 versus Factor 1 is presented in Figure 6.7. From this, Factor 1 can be interpreted as a soil loss factor, based on the positive association of the DTW > 4 ha variable with the increasing uphill CF and sand content and with the increasing downhill moisture and silt content. Factor 2 can be interpreted as a fertilization factor, with its Mehlich-3 > 0.5 loadings for extractable Ca, Mg, K, P, S, NO<sub>3</sub>-N, and Cu further marked by polygon outline. Note that these loadings also remain within the -0.4 to +0.4 range for Factor 1, i.e., fairly independent of the uphill-downhill soil loss and displacement effect. Factor 3 can be interpreted as a combined organo-metal complexation and leaching factor as reflected by the polygonised > 0.25 Factor 3 loadings for Fe, Zn, Mn, Cu, and Cs137 centered around the soil OM location and the < -25 Factor 3 loadings for NO<sub>3</sub>-N and NH<sub>4</sub>-N in Figure 6.7 (Baken et al., 2011). Factor 3 appears to reflect the ability of soil OM to retain ions prior to Mehlich-3 extraction in the following order: NO<sub>3</sub>-N < NH<sub>4</sub>-N < K ≈ Na ≈ Ca < Mg < Mn ≈ Cs137 < Zn ≈ Cu < Fe. Additionally, there is also an overall upland-to-downhill drift of the positive and negative Factor 3 loadings, likely due to persistent upland soil loss and to uphill-to-downhill flow of silt and NO<sub>3</sub>-N carrying water. The variable for plough water layer depth (Ap) is also associated with soil OM, likely due to higher OM content where the plough layer is deeper.

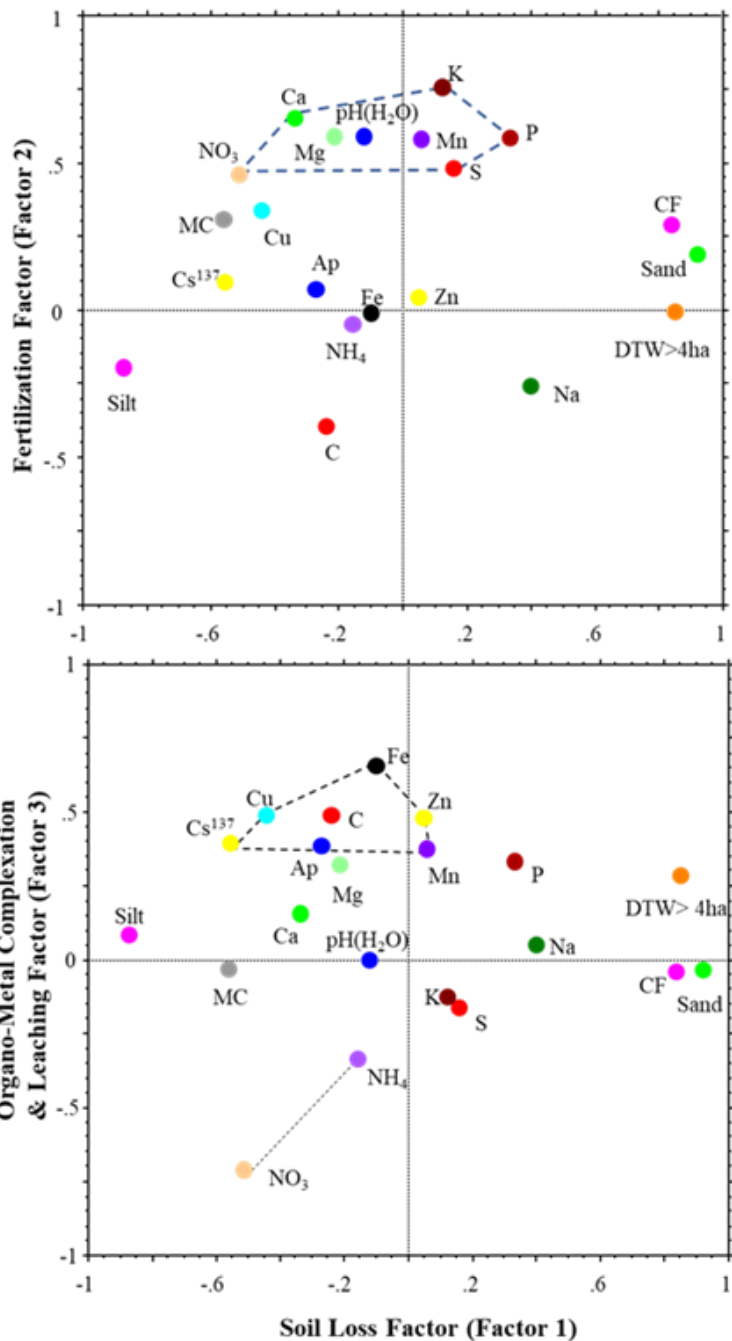


Figure 6.6. Factor analysis: Factor 2 (top) and Factor 3 (bottom) versus Factor 1 plots, with the Factor 2 (Ca, Mg, K, P, S, NO<sub>3</sub>-N) and Factor 3 (Cs<sup>137</sup>, Cu, Fe, Zn, C, Ap) entries polygonised.

Figure 6.7 is used to further illustrate the Factor 1, 2, and 3 association patterns based on by connecting the salient Factor 1, 2, and 3 entries in the Factor 3 versus Factor

2 plot. Doing so leaves the salient Factor 1 entries at center, the salient Factor 2 entries on the right, and the salient positive and negative loadings for Factor 3 in the top and bottom halves of this diagram. In this, the Mn and NO<sub>3</sub>-N entries are shared by Factor 2 and 3. For NO<sub>3</sub>-N, this would be due to NO<sub>3</sub>-N fertilization and low soil NO<sub>3</sub>-N retention. For Mn, this would be due to applying Mn to prevent common scab proliferations (*Streptomyces scabies*; McGregor & Wilson, 1966). Similarly, the positive Factor 3 entry for Cu may be due to foliar Cu applications in order to reduce potato blight infections (*Phytophthora infestans*; Finckh et al., 2006).

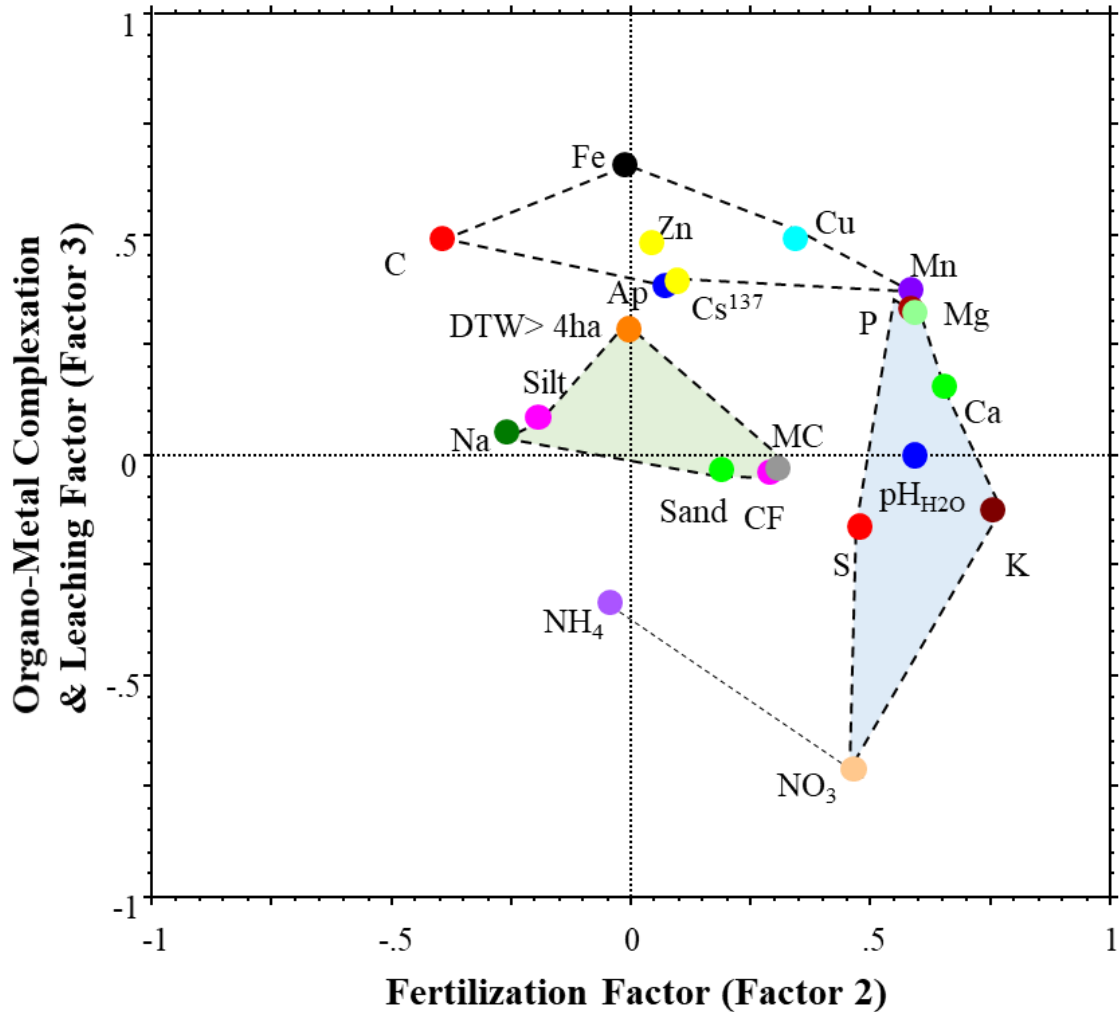


Figure 6.7. Factor 3 versus Factor 2 plot, with the Factor 1 (silt, DTW > 4 ha, SM, sand, Na), Factor 2 (Ca, Mg, K, P, S, NO<sub>3</sub>-N), and Factor 3 (Cs<sup>137</sup>, Cu, Fe, Zn, C, Ap) defining entries polygonised.

The multivariate analysis results presented in Table 6.4 serve to elaborate on the Factor 1, 2, 3 patterns in Figure 6.6 and 6.7 in quantitative terms as follows:

1. The Mehlich-3 extracted Ca and Mg levels are highly correlated (Eq. 6.1) possibly due to their presence in the calcareous soil parent material (Carleton Forest Soil Association) and/or due to periodic Ca/Mg carbonate and phosphate application (Kostic et al., 2015). These applications would also increase soil pH and extractable P (Eq. 6.4 and 6.9). Persistent soil loss along the upper field

locations and related transfer of water-solubilized Ca and Mg enriches extractable Ca and Mg at low DTW > 4 ha field locations (Eq. 6.1 and 6.7).

2. Mehlich-3 extracted P would not only increase with increasing Ca phosphate uptake applications but would also increase Mn and Sand % content (Eq. 6.4; Hopkins et al., 2014). The significant contributions of Mn to P and vice versa (Eq. 6.6) could be due to frequent Mn phosphate applications, designed to control potato scab (McGregor & Wilson, 1966). The increase in extractable P with increasing Sand % could be due to soil erosion due to silt-caused lowering of extractable P concentrations along the lower areas of the field (Fixen & Bruulsema, 2014; Mansfeldt, 2004).
3. The pH levels in soil water would also increase with Ca and K applications but would decrease with elemental S applications (Eq. 6.9; Penn et al., 2018). Ca and K applications increase soil pH through, e.g., calcium oxide (CaO) and potassium oxide (K<sub>2</sub>O) hydration. Elemental S is used (i) to adjust S deficiencies, (ii) to increase soil acidity by lowering soil pH, and (iii) to control the proliferation of bacterial disease-causing agents including scab (Klikocka et al., 2005; Haddad et al., 2016). In this way, Mehlich-3 extracted S also increases with K and Ca soil additions but decrease with increasing pH (Eq. 6.5).
4. The CaCl<sub>2</sub> extractable NO<sub>3</sub>-N levels increase with increasing NH<sub>4</sub>-N, likely due to NH<sub>4</sub>-N and/or urea additions and K-containing NO<sub>3</sub>-N fertilizer (Eq. 6.8). In addition, NO<sub>3</sub>-N as well as K levels decrease significantly with increasing DTW > 4 ha due to flow-induced NO<sub>3</sub>-N and K transfer from the upper to the lower field locations.

5. Likewise,  $\text{CaCl}_2$  extractable  $\text{NH}_4\text{-N}$  increases with extractable  $\text{NO}_3\text{-N}$  but decreases with extractable K (Eq. 6.10). In this, adding  $\text{NH}_4\text{-N}$  containing fertilizer would - in part - lead to (i) K displacement from soil cation exchange sites and (ii) nitrification (Hagin et al., 1990). The  $\text{NH}_4\text{-N}$  increase with increasing DTW > 4 ha (Eq. 6.10) would be related to low denitrification rates on well-aerated upland field locations (Kelling et al., 2011).
6. Mehlich-3 extracted Fe increases with increasing Mehlich-3 extracted Cu and Mn but decreases with increasing  $\text{NO}_3\text{-N}$  and pH (Eq. 6.13; Schwab, 1989). In this and within the existing soil pH range, increasing pH leads to decreasing Fe hydroxide solubility. Decreased Fe extractability with increasing  $\text{NO}_3\text{-N}$  would be due to decreasing Fe retention within low-lying and therefore less aerobic field locations.
7. The variations in Mehlich-3 extracted K are affected by four variables, namely pH,  $\text{NO}_3\text{-N}$ , P, and DTW, with pH,  $\text{NO}_3\text{-N}$  and P likely increasing with K-fertilizer applications while extractable  $\text{NH}_4\text{-N}$  would decrease on account of K induced displacement via cation-exchange (Eq. 6.14).
8. Mehlich-3 extracted Cu, Fe, Mn, Zn, Cs137 are linked to one another via Factor 3, but their quantitative dependencies are element specific. In detail:
  - i. Mehlich-3 extracted Zn is primarily related to Mehlich-3 extractable Cu but weakly so with increasing DTW > 4 ha (Eq. 6.2).
  - ii. Mehlich-3 extracted Mn and Cu are in part quantified by Mehlich-3 extractable Fe (Eq. 6.6 and 6.11), with Cu also increasing with increasing Ca, P, and Sand % content.

iii. Mehlich-3 extracted Cs<sup>137</sup> increases with Mehlich-3 extracted Cu but also increases with increasing soil C, with plough plough depth, and with Silt % (Eq. 6.12). Hence, soil C and Mehlich-3 extracted Cs<sup>137</sup> increase slightly from the upland to the lowland field locations.

The Mehlich-3 extracted Cu, Fe, Mn, Zn fractions as well as Cs<sup>137</sup> are therefore directly or indirectly related to DTW 4 > ha, i.e., directly so for Zn via Eq. 6.2, and indirectly so via increasing NO<sub>3</sub>-N for Fe (Eq. 6.13), increasing Silt % and soil C for Cs<sup>137</sup> (Eq. 6.12), and decreasing Sand % for Cu (Eq. 6.11).

Table 6.4. Multivariate regression results for the variables listed in Table 6.1.

Eq.	Dep. Variable	Intercept		Variable 1		Variable 2		Variable 3		Variable 4		R <sup>2</sup>	RMS E
		Coeff.	Std. Error	Coeff.	Std. Error	Coeff.	Std. Error	Coeff.	Std. Error	Coeff.	Std. Error		
6.1	Mg	66.1	7.6	Ca								0.585	16.4
				0.081	0.005								
6.2	Zn	1.14	0.3	Cu		DTW>4ha						0.232	0.701
				0.364	0.051	0.055	0.013						
6.3	C	0.26	0.28	Silt		NO <sub>3</sub> -N						0.274	0.225
				0.048	0.006	-0.040	0.007						
6.4	P	-73.7	34.4	Ca		Mn		Sand %				0.535	36.5
				0.068	0.013	2.22	0.28	6.2	0.7				
6.5	S	238	25	K		pH-H <sub>2</sub> O		Ca				0.355	14.1
				0.224	0.027	-43.0	5.5	0.024	0.005				
6.6	Mn	-35.1	4.6	Ca		Fe		P				0.523	7.73
				0.015	0.003	0.111	0.017	0.079	0.012				
6.7	Ca	-1727	257	pH-H <sub>2</sub> O		P		DTW>4ha				0.553	160
				513	49	1.76	0.23	-0.182	0.03				
6.8	NO <sub>3</sub> -N	-0.77	0.68	NH <sub>4</sub> -N		DTW>4ha		K				0.585	1.61
				6.67	0.063	-0.323	0.029	0.029	0.003				
6.9	pH-H <sub>2</sub> O	4.6	0.1	Ca		S		K				0.554	0.165
				0.00058	0.00005	-0.0056	0.0007	0.0022	0.0003				
6.10	NH <sub>4</sub> -N	0.47	0.05	K		DTW>4ha		NO <sub>3</sub> -N				0.42	0.149
				-0.0016	0.0003	0.020	0.003	0.042	0.004				
6.11	Cu	0.449	0.07	Ca		Sand		Fe		P		0.6300	0.055
				0.00014	0.00002	-0.0097	0.0013	0.00075	0.00002	0.00046	0.0001		
6.12	Cs <sup>137</sup>	-3394	417	Silt		Ap		C		Cu		0.574	319
				51.4	10.2	36.9	5.8	398	96	122	24		
6.13	Fe	431	44	Cu		Mn		NO <sub>3</sub> -N		pH-H <sub>2</sub> O		0.421	26.6
				12.3	2.1	0.94	0.17	-4.1	0.8	-36.7	8.6		
6.14	K	-109	51	pH		NO <sub>3</sub> -N		P		NH <sub>4</sub> -N		0.42	31.4
				38.9	9.6	7.1	1.0	0.24	0.04	-87.4	12.8		

## 6.5. Conclusion

The data analyses of the variables in Table 6.1 revealed three variation-controlling factors pertaining to topography, crop management and soil-internal nutrient associations. The topographic factor was quantified in terms of point-specific elevation and soil erosion impacts incurred from 1997 to 2016 and relating the uphill-downhill patterns for sand, silt, clay, and CF to the end-of-summer cartographic DTW index. This index refers to the slope-

cost distance between any point along the field and its closest permanent stream locations. The chemical soil properties pertaining to soil C, NO<sub>3</sub>-N, NH<sub>4</sub>-N, Ca, Mg, K, P, S, Fe, Mn, Cu, Zn, Cs<sup>137</sup> were also related to this index directly or indirectly as detailed above, and to Factors 2 and 3 in general. Factor 2 refers to periodic N, Ca, Mg, K, S, and P soil amendments, while Factor 3 represents the general association between heavy-metal micronutrients and soil OM.

In the absence of historical year-to-year field operation records, one-time soil property surveys do not lend themselves for quantifying direct cause-and-effect relationships are related to sequential crop management actions. Nevertheless, the analytical results as described above are consistent with the potato-cropping recommendations as summarized, e.g., by the Government of NB (Government of New Brunswick, 2022). Generally, these recommendations refer to applications involving N, P, K, Ca, Mg, S, Fe, Mn, boron (B), Cu, Zn, molybdenum (Mo), and chloride (Cl). Among these, Ca and Mg containing dolomite is recommended for upward pH adjustments to address the acidifying N and P fertilizer effects and therefore reduce subsequent aluminum (Al) and Mn mobilization (Ondrasek et al., 2021; Holmström et al., 2005). Elemental S is recommended for downward pH adjustments towards  $5.5 \leq \text{pH} \leq 6$  to maintain scab-free soil conditions. Gypsum (CaSO<sub>4</sub>) can be used as Ca and S supplement without affecting soil pH.

Among the micronutrients, only B is generally used as a supplement to reduce brown heart and water core symptoms in the harvested potatoes (Keren & Blingham, 1958). Most of the micronutrients are well supplied by soil OM; however, maintaining soil OM requires replenishment through three-year crop rotation cycles involves carefully chosen

cereal, green manure, and forage sequences, with emphasis to reduce recurring potato-compromising infections referring, e.g., to scab, black-scurf inducing *Rhizoctania* and nematodes (Dhaliwal et al., 2019).

In summary, the results as described and discussed suggest that it is now possible to quantify erosion- and water-flow induced patterns and subsequent changes across fields through high-resolution elevation and soil property surveys that, ideally, would need to be repeated from time to time to further enable field-specific soil-response determinations and evaluations.

## **6.6. Acknowledgments**

The preceding work pertaining to the field survey centered on the Hartland potato field performed on behalf of Agriculture and Agri-food Canada and reported by Zebarth et al. (2002) is very much appreciated. Also, much appreciated is receiving the completed set field survey data as described above, and the GeoNB availability of the 1 m LiDAR surveys for NB.

## 6.7. Literature Cited

- Baken, S., Fien Degryse, F., Verheyen, L., Merckx, R., & Smolders, E. 2011. Metal Complexation Properties of Freshwater Dissolved Organic Matter Are Explained by Its Aromaticity and by Anthropogenic Ligands. *Environmental Science & Technology*, 45, 2584-2590.
- Dhaliwal, S. S., Naresh, R. K., Mandal, A., Singh, R., & Dhaliwal, M. K. 2019. Dynamics and transformations of micronutrients in agricultural soils as influenced by organic matter build-up: A review. *Environmental and Sustainability Indicators*, 1–2, 100007.
- Finckh, M. R., Schulte-Geldermann, E. & Bruns, C. 2006. Challenges to Organic Potato Farming: Disease and Nutrient Management. *Potato Research*, 49, 27–42.
- Fixen, P. E., & Bruulsema, T. W. 2014. Potato Management Challenges Created by Phosphorus Chemistry and Plant Roots. *Am. J. Potato Res.*, 91, 121–131.
- Government of New Brunswick. 2022. Soil Managment. Retrieved from: [https://www2.gnb.ca/content/gnb/en/departments/10/agriculture/content/crops/potatoes/soil\\_management.html](https://www2.gnb.ca/content/gnb/en/departments/10/agriculture/content/crops/potatoes/soil_management.html)
- Haddad, M., Bani Hani, N., Al-tabbal, J., Al-Fraihat, A. 2016. Effect of different potassium nitrate levels on yield and quality of potato tubers. *J. Food, Agric. Environm.* 14, 101 – 107.
- Hagin, J., Olsen, S. R., & Shaviv, A. 1990. Review of interaction of ammonium - nitrate and potassium nutrition of crops. *Journal of Plant Nutrition*, 13(10), 1211-1226.
- Holmström, S. J. M., Van Hees, P. A. W., & Lundström, U. S. 2005. Modelling of aluminium chemistry in soil solution of untreated and dolomite treated podzolic soil. *Geoderma*, 127, 280–292.
- Hopkins, B. G., Horneck, D. A., & MacGuidwin, A. E. 2014. Improving phosphorus use efficiency through potato rhizosphere modification and extension. *Am. J. Potato Res.* 91, 161–174.
- Kelling, K. A., Wolkowski, R. P., & Ruark, M. D. 2011. Potato Response to Nitrogen Form and Nitrification Inhibitors. *Am. J. Pot Res*, 88, 459–469.
- Keren, R., & Bingham, F. T. 1958. *Boron in Water, Soils, and Plants*, 1, 229–276.
- Klikocka, H., Haneklaus, S., Bloem, E., & Schnug, E. 2005. Influence of Sulfur Fertilization on Infection of Potato Tubers with *Rhizoctonia solani* and *Streptomyces scabies*. *Journal of Plant Nutrition*, 28(5), 819-833.
- Kostic, L., Nikolic, N., Samardzic, J. *et al.* 2015. Liming of anthropogenically acidified soil promotes phosphorus acquisition in the rhizosphere of wheat. *Biol Fertil Soils*, 51, 289–298.
- Mansfeldt, T. 2004. Redox potential of bulk soil and soil solution concentration of nitrate, manganese, iron, and sulfate in two Gleysols. *Z. Pflanzenernähr. Bodenk.*, 16, 7-16.

- McGregor, A. J., & Wilson, G. C. S. 1966. The influence of manganese on the development of potato scab. *Plant Soil*, 25, 3–16.
- Ondrasek, G., Kranjčec, F., Filipović, L., Filipović, V., Bubalo Kovačić, M., Badovinac, I. J., Peter, R., Petravić, M., Macan, J., & Rengel, Z. 2021. Biomass bottom ash & dolomite similarly ameliorate an acidic low-nutrient soil, improve phytonutrition and growth, but increase Cd accumulation in radish. *Science of the Total Environment*, 753.
- Penn, C. J., Rutter, E. B., Arnall, D. B., Camberato, J., Williams, M., & Watkins, P. A. 2018. Discussion on Mehlich-3 Phosphorus Extraction from the Perspective of Governing Chemical Reactions and Phases: Impact of Soil pH. *Agriculture*, 8, 106.
- Schwab, A. P. 1989. Manganese-Phosphate Solubility Relationships in an Acid Soil. *Soil Science Society of America Journal*, 53, 1654-1660.
- Shiwakoti, S., Zheljaskov, V. D., Gollany, H. T., Kleber, M., & Xing, B. 2019. Micronutrients decline under long-term tillage and nitrogen fertilization. *Scientific Reports*, 9, 12020.
- Tarboton, D. G. 1997. A new method for the determination of flow directions and upslope areas in grid digital elevation models. *Water Resources Research* 33(2), 309-319.
- Zebarth, B. J., Rees, H., Walsh, J., Chow, L., & Pennock, D. J. 2002. Soil variation within a hummocky podzolic landscape under intensive potato production. *Geoderma*, 110, 19–33.

## **CHAPTER 7: SUMMARIES, CONCLUSIONS, AND RECOMMENDATIONS FOR FUTURE WORK**

### **7.1. Summary**

The objective of this thesis was to produce a LiDAR-based potato crop suitability map, that along the Upper Saint John River Valley in NB at a high 1 m spatial resolution using multi-criteria evaluation. This was done by:

1. Using NB's 1 m resolution DEM for slope, flow channels, and DTW derivation.
2. Updating NB's Forest soil map using NB wetlands and waterbodies maps.
3. Combining soil and topographic criteria into an equation to determine potato crop suitability.
4. Applying results and discussing them in three parts: (i) Grand Falls area, (ii) Florenceville area, and (ii) Woodstock area.

Validation of the produced potato crop suitability map for the AOI was done by:

1. Validating the produced LiDAR-based potato crop suitability map by addressing the extent to which the assessed market value of farmlands and woodlands reflects soil quality across the study area.
2. Validating the produced LiDAR-based potato crop suitability map by addressing the extent to which soil factors (potassium (K) content, calcium content, phosphorus (P) content, potato tuber yield across years, electrical conductivity (EC), clay content, and soil moisture content) reflects soil quality by way of image analysis (Perron et al., 2018).
3. Validating the produced LiDAR-based potato crop suitability map by comparing image analysis results with a DSM for NB (Furze, 2018). More specifically, DSM-

derived layers on SOC content, pH, EC, clay content, PWP, sand content, Db, and FC.

In summary, it was found that:

1. The crop suitability rating as described in Chapter 3 and Chapter 4 is in principle valid across the AOI. The assessment values of farmlands and farm and wood land combinations reflects the soil suitability for potato crop. AOI regression derived equations can, in principle, be used for approximate tax evaluation purposes.
2. In Chapter 5, it is shown that the flow channel network and associated depth-to-water layers (DTW) derived from LiDAR-DEM data at 1 m resolution can be used to quantify and map DTW-related trends pertaining to field surveyed soil property and tuber yield variations, with the latter showing optimal tuber growth at  $4 < \text{DTW} < 6$  m. For achieving best results, adjustments to the automatically generated flow channels and DTW layers may be needed to account for field-specific flow and drainage condition as demonstrated.
3. It is now possible to quantify erosion- and water-flow induced patterns and subsequent changes across fields through high-resolution elevation and soil property surveys that, ideally, would need to be repeated from time to time to further enable field-specific soil-response determinations and evaluations.

## **7.2. Suggestions for Further Work**

Potato crop suitability mapping does not account for GDDs and FFDs since there are ample days to grow potato across NB; however, further work could be done in terms of looking at climate differences across the province. More specifically, further work could be done in terms of looking at topographic pattern changes in precipitation, climate,

temperature, GDDs, and FFDs. Looking at changes in precipitation would inform on soil erosion. Looking at changes in precipitation would, in part, at crop and crop rotations that would minimize soil erosion (Jankauskas & Jankauskiene, 2003). While this project informs on potato crop suitability mapping, this project could technically be applied to other crops and to other provinces. For example, cranberries and rice require DTW-mappable wet soil conditions. When looking at other cold-weather crops in general and applying the potato crop suitability mapping to NB and other provinces, it will be necessary to look at weather- and soil-based factors and related information as provided by each province.

As mentioned in Chapter 4, further work could be done to determine the extent to which potato crop suitability reflects the tax base of individual farmlands and farm and woodland combinations properties since tax assessment is much more technical than just looking at soil quality, property size, and the presence or absence of infrastructure. For example, property location (including nearness to community services, access, etc.), quality of infrastructure construction, etc. are also taken into account by tax assessors (Government of New Brunswick, n.d.).

Furthermore, further work could be done in terms of looking at in-field survey information. In this thesis, it was done for three fields (Saint-André field, Centreville field, and Hartland field). Other fields were not looked at due to a lack of available data.

### **7.3. Practical Applications**

The LiDAR-based potato crop suitability process as described above can, in principle, be used to create new farming opportunities, and/or to explore DEM-mapped within field variations for additional crop-growing potentials, whether these refer to

potatoes or other crops. Technical aspects in this regard refer to, e.g., forest clearing, terracing, improving soil drainage, locating suitable areas for crops with prolonged GDD requirements, and/or delineating in-field soil and crop management zones especially targeted at increasing crop yields while enhancing biodiversity and soil conservation goals at the same time.

#### 7.4. Literature Cited

Government of New Brunswick. n.d. Understanding how properties are valued. Retrieved form: <https://www2.snb.ca/content/snb/en/sites/property-assessment/understanding/valued.html>

Jankauskas, B., & Jankauskiene, G. 2003. Erosion-preventive crop rotations for landscape ecological stability in upland regions of Lithuania. *Agriculture, Ecosystems and Environment*, 95(1), 129–142.

## **Appendix: Comparisons of Published Field-Generated Soil Data with DSM-Generated Data Layers, for the Saint-André Field**

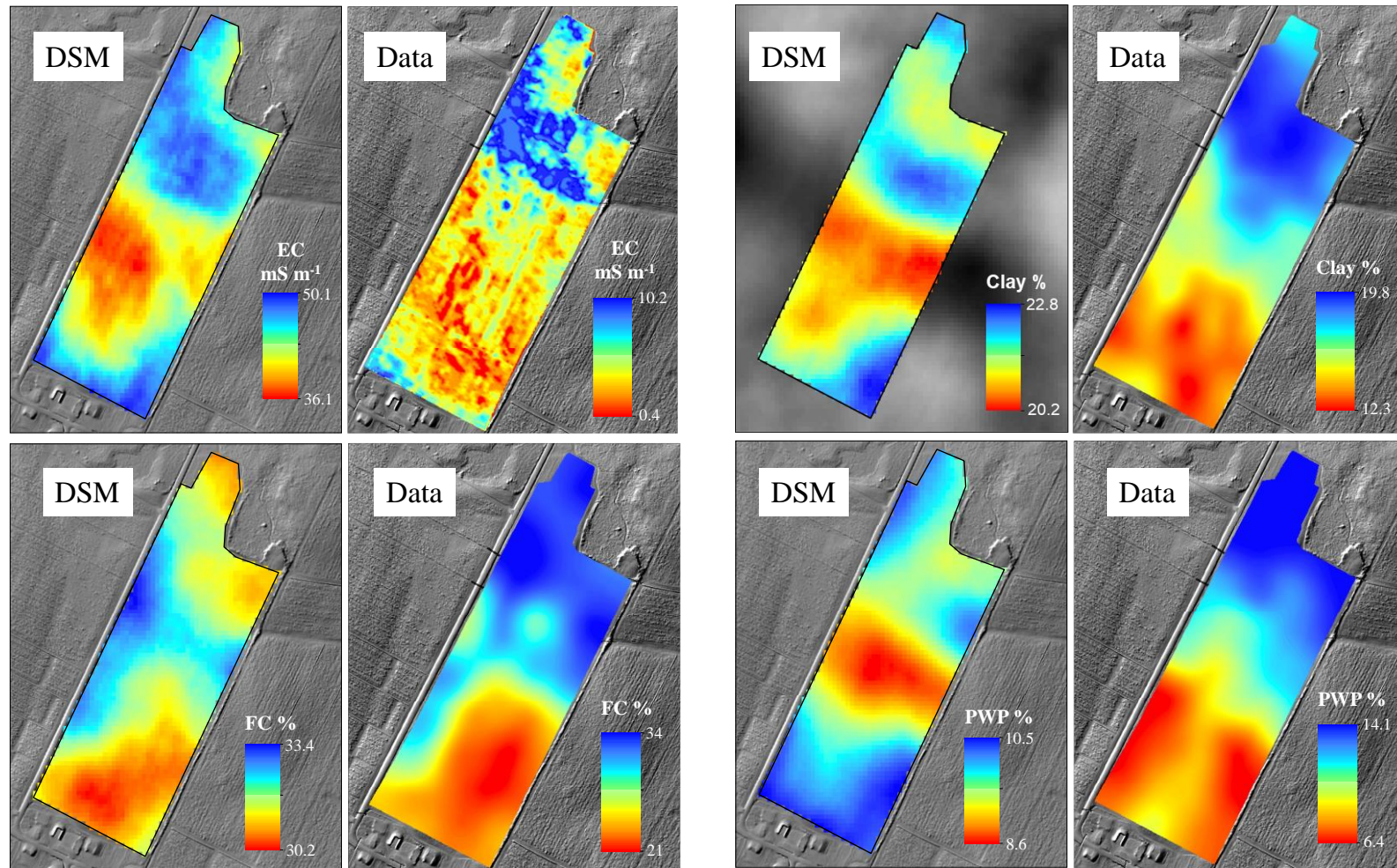
This Appendix informs on a comparison between the field surveyed data for the Saint-André field and the corresponding data layers generated by way of digital soil mapping as developed and described by Furze (2018) using NB-wide LiDAR-DEM elevation data, smoothed and resampled at 10 m resolution. The DSM-generated soil property layers project soil physical and chemical properties from numerous data layers pertaining to, e.g., elevation, DTW, slope, and > 12,000 geochemical survey points across NB. The GIS process of doing so involved random forest regression modelling. Figures A.1 and A.2 show the resulting data layers for SOC (%), pH, EC (mS/m), clay (%), FC (%), PWP (%), and soil Db (g/cm<sup>3</sup>), all in comparison with the surveyed Saint-André field data. This comparison reveals the following the surveyed and DSM generated data layers:

1. **EC (mS/m):** the patterns are similar, but the field data are five times lower than the DSM results; this differences in range is likely not due to forest versus field; also, the DSM-EC pattern was found to be inversely related to DSM-Sand %.
2. **pH:** the field data are categorically higher than the DSM result; this could be due to historical differences in field zonation and liming applications, as shown in Figure A2. The DSM data are based on forest soil conditions which are generally acidic except on calcareous soil formation. Hence, the overall pH survey and DSM patterns would not be compatible nor comparable in principle.
3. **PWP (%) & FC (%):** the field survey results but with a wider range than the DSM results; the patterns so generated not compatible unless modified by calibration.

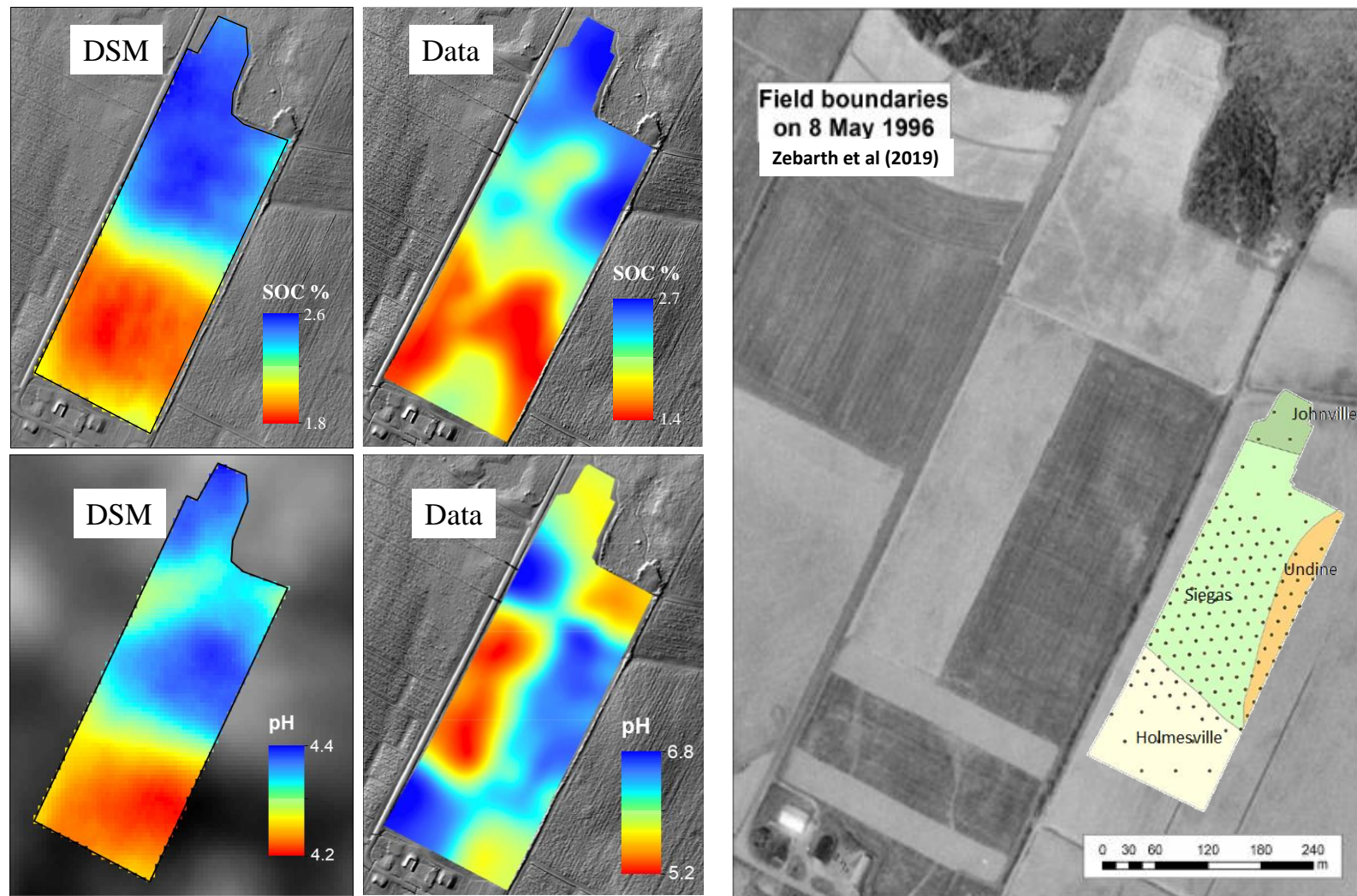
4. **SOC (%):** the DSM and field survey patterns are similar, but the DSM -generated pattern is 10 times higher than field results. This difference unlikely due to forest versus field SOC differences, although field SOCs could be lower than forest SOCs due to ploughing and cropping induced organic matter losses.
5. **Clay (%):** visually, the surveyed results are somewhat compatible with the DSM results. However, the actual numbers are not, varying by 7 percent across the field when surveyed, but only by 0.2 % as DSM modelled.

All of this suggests that more work and fine-tuning is required with respect to digital soil mapping across NB, especially since the results so generated can be compared with detailed in-field survey data. Within this context, it would be good:

1. to pool additional fields with existing soil property GPS-surveys and subject to further LiDAR-DEM based analysis them;
2. to supplement the agricultural field surveys with channel-defined forest cutblock data before and after harvesting;
3. to fine-tune DSM modelling procedures according to the generalizable trends that would emerge from the pooled in-field soil survey information.



Appendix Figure 1. Comparing the Saint-André field data with the DSM generated 0-20 cm deep results for EC (mS/m), clay (%), FC (%), and PWP (%).



Appendix Figure 2. Comparing the Saint-André field data with the DSM generated 0-20 cm deep results for SOC (%) and pH. Also shown: field layout in 1966 and in-field distribution of the NB forest soil associations.

## **CURRICULUM VITAE**

Candidate's Full Name: Kamille Eve Lemieux

Universities Attended: University of New Brunswick 2020-2023  
Master of Science in Forestry

University of New Brunswick 2015-2020  
Bachelor of Science in Biology

Publications: N/A

Conference Presentations: N/A